Department of Process and Environmental Engineering
Fiber and Particle Engineering

FACULTY OF TECHNOLOGY

Alkali-activated soapstone waste - effects of co-binders and fibers on hardened-state properties

Faraz Rahim

Master's Degree Programme in Environmental Engineering

April 2019

Department of Process and Environmental Engineering
Fiber and Particle Engineering

FACULTY OF TECHNOLOGY

Alkali-activated soapstone waste - effects of co-binders and fibers on hardened-state properties

Faraz Rahim

Supervisor(s):
Dr. Zahra Abdollahnejad and Dr. Päivö Kinnunen

Master's Degree Programme in Environmental Engineering

May 2019

ABSTRACT

Degree programme	**Research Group**
Master's Degree Programme in Environmental Engineering	Fiber and Particle Engineering
Author	**Thesis supervisor**
Faraz Rahim Kasimi	Dr. Zahra Abdollahnejad, Dr. Päivö Kinnunen

Thesis title
Alkali-activated soapstone waste - effects of co-binders and fibers on hardened-state properties.

Specialization	**Thesis type**	Submission date	Number of pages
Environmental Engineering	Master's thesis	9th May 2019	88

Abstract

The metamorphic rock (soapstone) has been used since Stone age, even it plays a significant role in the economy of numerous countries. Currently, it is often used for architectural applications such as artefacts, cooking appliances, countertop and slab. Apart, it produces a massive amount of waste powder during the extraction phase and plant processing which is unavoidable. Resulting in a large amount of recyclable material landfilled or released to the environment annually that could be problematic in terms of environmental perspective.

To diminish its adverse impacts and ensure sustainability; it would be beneficial to thrive a new technique to recycle these industrial wastes in construction applications.

Based on previously published results; soapstone ($Mg_3Si_4O_{10}(OH)_2$) is poorly reactive in alkaline-activation owing to its chemical structure and a lack of amorphous components. As a result low mechanical properties which cannot be used for construction applications. Therefore, these types of materials necessitate co-binder, thermal curing at high temperature and high alkalinity to achieve high strength alkali-activated material.

Experimental and statistical investigates were conducted to observe the effects partially replacing of soapstone (talc) with co-binders (i.e., metakaolin, lime, stone wool, and silica fume), and fibers on the hardened-state properties. The variables used in the analyses were the concentration of virgin steel fibers or basalt fibers (dosages = 0.5% and 1%), the proportion of metakaolin, stone wool or silica fume used to replace soapstone (20 wt. %) and lime by 5 wt. %. The effects of employing fibers at two dosages with co-binders in 20 mix compositions were investigated. The designed mixtures were activated by using an alkali solution, which contains NaOH (10M) and sodium silicate (molar ratio of SiO_2/Na_2O = 2.5). The samples were treated by thermal curing at 60 °C for 24 hours, and placed under ambient conditions (24°C and 35% RH).

The findings showed that using co-binders and fibers were different behaviors on the hardened-state properties, however, the metakaolin reinforced mix composition with 0.5% basalt fibers improved compressive strength about 25 MPa after 28 days. This strength enables the use of the proposed binders for construction applications.

Keywords: Soapstone, alkali activation, geopolymer, thermal curing, 28 days curing, mechanical strength, durability.

Library location: University of Oulu, Science and technology library Tellus

FOREWORD

The purpose of this thesis was to investigate and evaluate the effects of using co-binders and fibers on the hardened-state properties of the alkali-activated magnesium aluminosilicate binders from waste soapstone. This work was done at University of Oulu, Fiber and particle engineering laboratory.

I am thankful to Allah (S.W.T) who had given me the strength to complete this research, and my sincere gratefulness goes to my worthy supervisors, Dr Zahra Abdollahnejad and Päivö Kinnunen for their suggestions and supervisions.

Special thanks are also to the laboratory staff for their remarkable help with everything as well as my colleagues.

Finally, I would like to thank my parents, also my siblings and beloveds for their honorable support.

TABLE OF CONTENTS

SYMBOLS AND ABBREVIATIONS

ASTM	American society for testing and materials
AAM	Alkali-activated material
Al	Aluminum
Al_2SiO_5	Aluminosilicate
˚C	Degree in Celsius
CaO	Calcium oxide
CO_2	Carbon dioxide
C-S-H	Calcium Silicate Hydrate
σc	Compressive strength
d	Particle size
DTG	Differential thermogravimetry
EN	European standard
σf	Flexural strength
GHG	Greenhouse gas
GPa	Giga Pascal
kN	Kilonewton
LOI	Loss of ignition
LM	Lime
µm	Micro meter
M	Molarity
MK	Metakaolin
mm	Millimeter
MPa	Mega Pascal

N	Newton
NaOH	Sodium hydroxide
Na_2SiO_3	Sodium silicate
OPC	Ordinary Portland Cement
OH-	Hydroxyl ions
RH	Relative humidity
SCM	Supplementary Cementitious Materials
SF	Silica fume
SFRC	Steel Fiber Reinforced Concrete
SW	Stone wool
TGA	Thermogravimetric analysis
UPV	Ultrasonic Pulse Velocity
WBCSD	World Business Council for Sustainable Development
Wt. %	Weight in percentage
XRF	X-ray fluorescence

1. INTRODUCTION

1.1 Background

A large amount of ordinary Portland cement (OPC) is being manufactured all over the world. It was reported that around 3 billion tons of OPC was produced in 2012. World Business Council for Sustainable Development (WBCSD) reported that OPC demand would reach to 3.7- 4.4 billion tons by 2050. OPC is one of the major sources of releasing CO_2 emission in the atmosphere called greenhouse gases (GHG). Globally, OPC received high demand due to its high mechanical performances although production of one ton of OPC emits one ton of carbon dioxide in the atmosphere; therefore, it should be thought of strive to minimize the adverse environmental impacts. The uses of technologies and any kind of invention that can result in reducing greenhouse gases emission have recently received considerable attention. (Schneider et al., 2011; Benhelal et al., 2013; Imbabi et al., 2012).

Utilization of side streams such as (talc, stone wool, and silica fume, etc…) could play an essential role in terms of reducing the adverse effects of OPC utilization, mainly in the construction area. The world population is growing, and there will be a higher demand regarding construction materials and the materials produced by conventional methods are not adequate to fulfil this demand. (Abdollahnejad et al., 2018; Wickler, 2018; Sivrikaya et al., 2014).

Soapstone has been used for artifacts and architectural applications since many years ago. Soapstone quarries and processing plants produce a massive quantity of waste powder, which is unavoidable. A large amount of recyclable material landfilled or released to the environment annually that could be problematic in terms of environmental perspective.

Soapstone has two main components are SiO_2 (39 wt. %.) and MgO (38 wt. %), however, magnesium aluminosilicate binders are poor reactive in alkali activation due to its chemical structure and a lack of amorphous components. As a result, their mechanical properties are shallow in terms of construction applications. The mechanical performances of these materials could be improved by using co-binders, thermal treatment, and high alkalinity. Also, employing fibers and admixtures in the alkali-activated magnesium aluminosilicate binders could be sufficient to minimize the efflorescence (Abdollahnejad et al., 2018).

1.2 Aim and objectives

The aim of the research is to analyze the effects of co-binders and fibers on the hardened properties of alkali activated magnesium aluminosilicate binders from soapstone waste, to thrive as a substitute to the use of conventional cement (OPC) in the manufacture of concrete.

— Optimization of the mix compositions of alkali activated magnesium binders from soapstone with partial replacement of different co-binders.

— Utilizing two different types and dosages of fibers in order to investigate the effects on hardened-state properties.

— Evaluation of the performance of alkali-activated magnesium binders with respect to the hardened-state properties.

2 LITERATURE REVIEW

2.1 Alkali activated materials

Alkali-activated materials are categorized by two to three-dimensional Si-O-Al structure. They represent a different cementitious material which is capable of delivering ceramic and zeolitic characteristics. However, they do not exist in traditional material (Petermann et al., 2012).

Typically, there are two types of binding systems (calcium silicon and aluminosilicates) which are classified in terms of chemical composition and mechanism of reaction. Their reaction mechanisms are quite different in compare to Ordinary Portland Cement (Gao, 2017).

Fig. 1, presents the two key components of alkali-activated system: a cementitious component and an alkali activator. Alkaline salts or caustic solution are often used as an alkali activator. According to Glukhovsky, activators are classified by six groups in terms of chemical compositions, such as caustic solution, slightly acid, silicates, aluminates, aluminosilicates, and non-siliceous. (Glukhovsky, 1994; 1967). Cementitious components used to produce an alkali-activated cement could be classified into two subgroups, a material with intrinsic hydraulicity (OPC, and metallurgical slags) or pozzolanic materials (silica fume and volcanic ashes). In many cases, pozzolanic materials used as supplementary materials to increase strength, density and decreasing efflorescence (Garcia-Lodeiro et al., 2014; Concrete countertop institute, 2018).

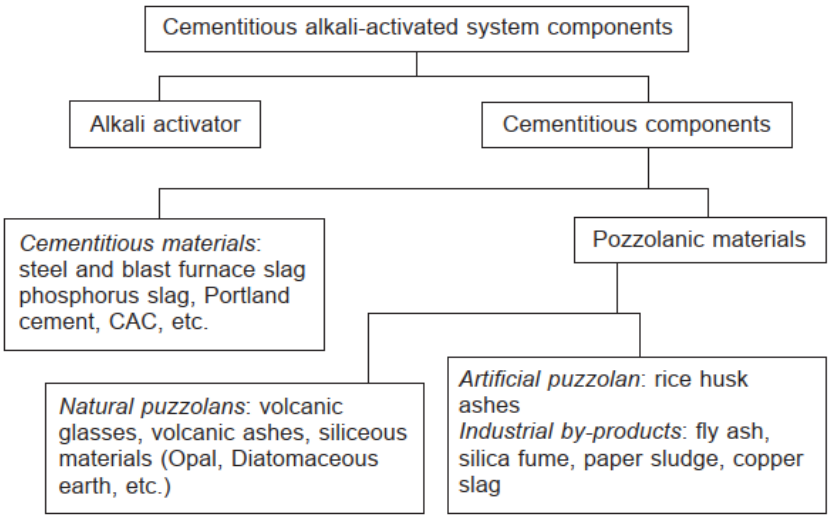

Fig 1. Classification of alkali-activated materials system. (Garcia-Lodeiro et al., 2014).

2.2 Mechanism and Models of geo-polymerization

The activation mechanism for aluminosilicate materials was proposed by Glukhovsky in 1959, it carries out by exothermic process of dissolution. Duxson et al. (2007) proposed another model of the mechanism of geo-polymerization, which has five steps: 1) dissolution; 2) speciation equilibrium; 3) gelation; 4) Reorganization; 5) polymerization and hardening.

In geo-polymerization mechanism has three phases to be achieved geo-polymer. Firstly: the dissolution of solid Al_2SiO_5 occurs, when the alkali activator solution adds. Resulting in the formation of the aluminate and silicate monomers. Secondly: the condensation happens, when these formed monomers merge due to co-distribution of the oxygen molecules to build "oligomers" as well as organize bigger networks. Besides, the water leaves out from the structure that spends in the hydrolysis method. Lastly, when the mix becomes saturate excessively with Al_2SiO gel. (i.e., which is primarily abundant with Al bonds). Where re-arrangement processes go on; silicates disintegrate to the mix, and they establish to the aluminosilicate gel, abundantly. Thus it leads to increase the connectivity, and then geo-polymer gel begins to toughen (Provis et al., 2014; Duxson et al., 2007). These processes are described in Fig 2

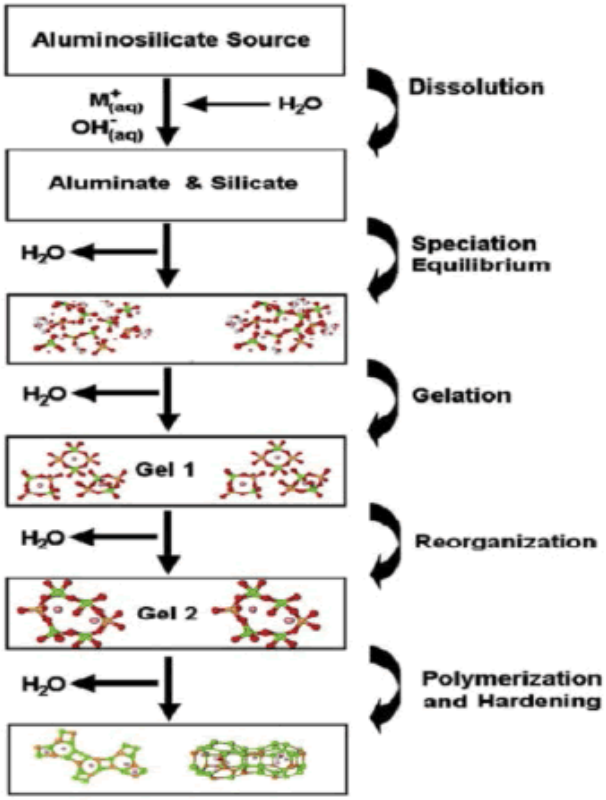

Fig 2. Theoretical model for geopolymerization (Duxson et al., 2007).

By several factors: geo-polymerization activities are managed the dissolution rate; the quantity of reactive phase in the source material, source material the mix's alkalinity, temperature of curing, particle size, the alkalinity of the mix, liquefied silicate's quantity that could be offered by the alkaline solution, and temperature of curing (Adam et., al 2006; Provis et., al 2014).

When an alkali solution reacts with particles resulting in dissolution process starts (Fernandez-Jimenez et al., 2005). And then the reaction products form together inner side and outer side of the domain until the completion of particles of ash or nearly totally consumed (Fig. 3a-c). Simultaneously, precipitations of reaction products take place, when an alkali activator solution enters in the bigger networks and refills the inner space with the reaction product, developing a thick Matrix (Fig. 3b). Consequently, a huge precipitation of reaction products, several portions of minor particles enclose with the products providing crust which avoids the interaction with alkali activator solution (Fig. 3e), resultant an non-reacted fly ash particle. Therefore, various morphologies could co-exist in a same gel: non-reacted fly ash particles, atoms attack by the alkali activator solution, however, which sustain their spherical shape, reaction product and others (Fig. 3d).

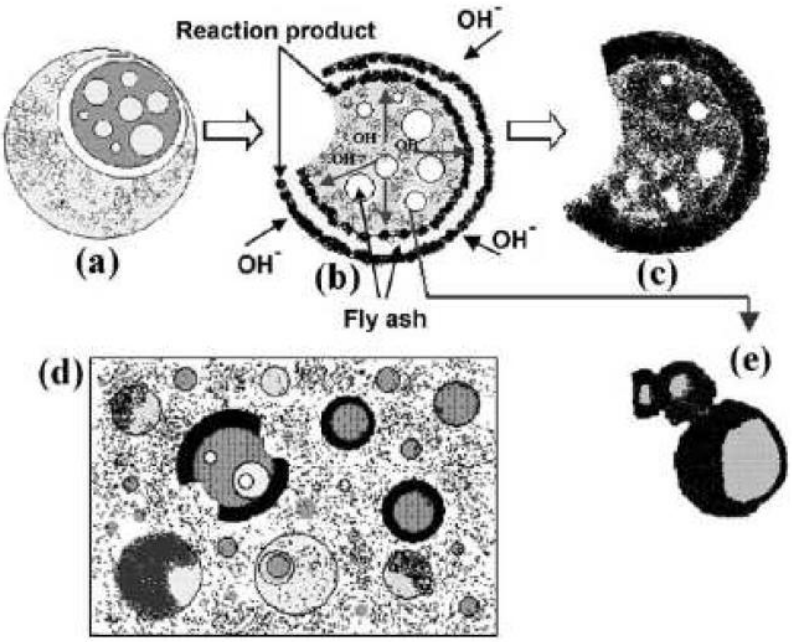

Fig 3. A descriptive model of the geopolymer of fly ash (Fernandez-Jimene et al., 2005)

A reaction structure for the polycondensation process of geo-polymerization from Al−Si material materials was proposed by (Xu, 2002, p. 71).

$$Al{-}Si\ material(s) + MOH(aq) + Na_2SiO_3\ (s\ or\ aq) \quad \textbf{(1.1)}$$

$$Al{-}Si\ material(s) + [Mz\ (AlO_2)_x\ (SiO_2)\ \cdot nMOH \cdot mH_2O] \cdot gel \quad \textbf{(1.2)}$$

$$Al{-}Si\ material(s) + [Ma\ (AlO_2)a\ (SiO_2)b\ \cdot nMOH \cdot mH_2O] \cdot gel \quad \textbf{(1.3)}$$

Geo-polymers with an amorphous structure

In reaction 1 (Equation. 1.1) and 2 (Equation. 1.2), the number of aluminosilicate materials used depends on the size of particle, dissolution of aluminosilicate constituents and the concentration of the alkali activator solution.

The development of $[Mz(AlO_2)_x(SiO_2)y \cdot nMOH \cdot mH_2O]$ gel, which fundamentally depends on the size of dissolution of Al-Si materials, is an essential step in the development of an amorphous structure of geo-polymer (reaction 3). In 2006, Provis had proposed the basic model of reaction processes in the geo-polymerization of metakaolin or fly ash (Al−Si constituents). In fig. 4 shows the model of proposed reaction sequence of geopolymerization

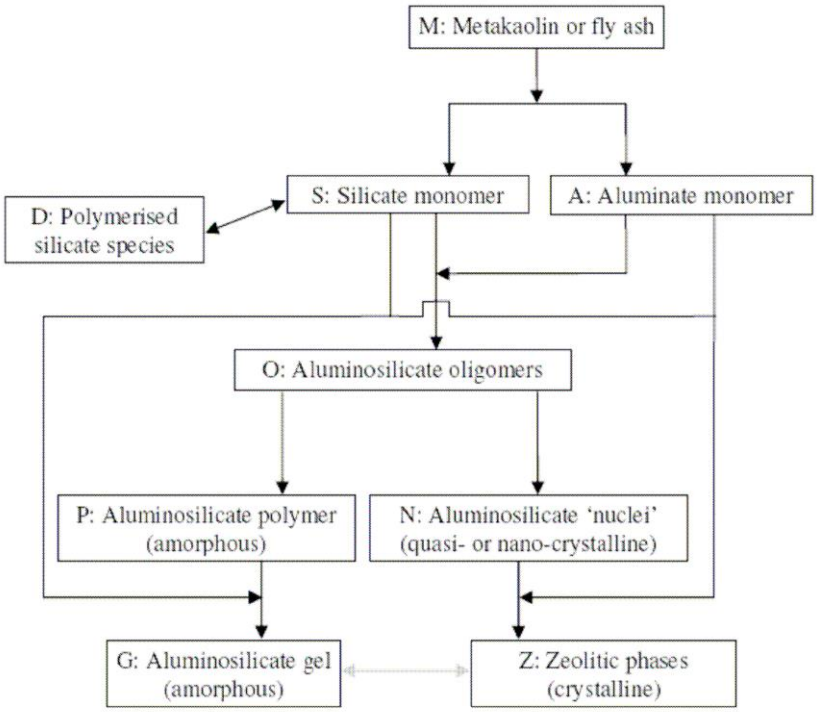

Fig 4. Offered reaction arrangement of geo-polymerization (Provis, 2006, p. 206)

2.3 Geopolymer chemical structure

It is generally defined as the phase of aluminosilicate gel; SiO_4 and AlO_4 tetrahedral are bonded covalently by distribution all oxygen molecules. By co-ordinating alkali cations, resulting in negative charge of the aluminate groups (Kanuchova et al., 2015). To retain the neutrality of the chemical structure; the existence of cations is significant. On the other hand, it is supposed that asides from given a charge-balancing role, the incorporation of cation is important to control the integrity of structure of the final product, the Na+ion affect the brittleness of geo-polymers (Yun-ming et al., 2016).

In 1979, Davidovits formed and applied the term geo-polymer. For the chemical term of geo-polymers based on silico-aluminates, poly (sialate) was proposed. Sialate is stood for silicon-oxo-aluminate. Polysialates are chain and ring polymers with Si4+ and Al3+ in IV-fold coordination with oxygen and range from amorphous to semi-crystalline. The amorphous to semi-crystalline three-dimensional silico-aluminate structures were named geo-polymers of the types as shown in fig. 5 (Davidovits, 2002).

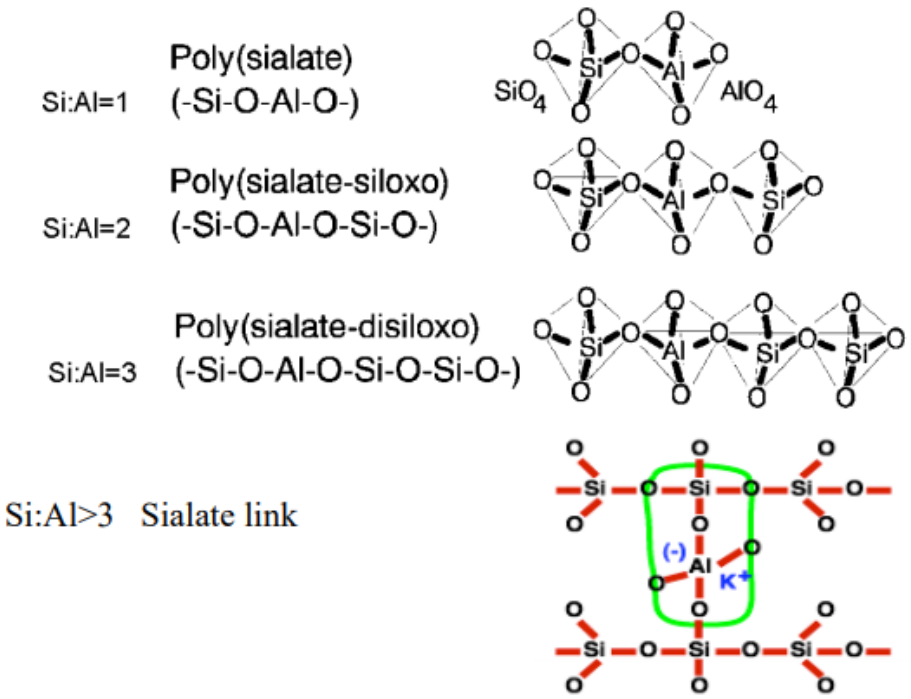

Fig 5. Terminology of geopolymer (Davidovits, 2002).

2.4 Some issues that affect the properties of alkali-activated materials

2.4.1 Alkali activator ratio and pH

Mostly the mechanical properties are influenced by alkali activator ratio. The geo-polymer mixture involves a source material to alkali solution ratio by three resulting in gel formation (Xu et al., 2000). The relationship between porosity and alkali activator ratio; by an increment in alkali activator ratio could decrease in value of porosity, however, could be an increment in mechanical properties of waste catalyst metakaolin based alkali activated composites (Cheng et al., (2015).

The compressive strength of fly ash improved by reducing activator ratio which is partially owing to hydroxide ions which assists in quick dissolution. The usage of highly alkali sodium hydroxide leads to help in dissolving the source material quickly. Likewise, the significance of water in geo-polymerization cannot be overemphasized as it hydrolyses Al3+ and Si4+ ion (Zuhua et al., 2009).

The solution of alkali activator with low silica content such as sodium hydroxide could help to increase the strength of mixture even at a higher ratio of alkali activator (Provis et al., 2009). Although working with nano-silicate metakaolin based composites, it established that variations existed in the compressive strength of the product accordingly by increasing the ratio of alkali activator (Gao et al., 2014). The significance of ratio solid-liquid to geopolymerization mixture and decided that the formation of geopolymer can increase when the ratio of alkali activator is high (Yao et al., 2009).

Using alkali activators without any sodium silicate could be poor influences on mechanical properties. However, it contributes to the main role in the polymerization reaction (P.Torgal et al., 2008).

In geopolymerization, one of the pressing issues is the concentration of alkali activator regardless of the types of activating solution used, by increasing the concentration of alkali activator resulting increasing the rate of reaction (Petermann et al., 2012; Fernandez-Jimenez et al., 1999).

By increasing the molar concentration of sodium hydroxide, consequently, it will be increasing the number of dissolved silicates (Panagiotopoulou et al. 2007). Granizo et al. (2007) reported that by increasing the sodium concentration in the alkali activator; the flexural strength is improved. However, it exceeds to 12M; it reduces the flexural strength because of crystallization formation of faujasite which is caused by extra sodium.

2.4.2 Curing Conditions

Jansen and Christiansen, (2015) reported that by increasing or decreasing temperature; it influences the strength of mix composition.

Many types of research asserted that mechanical strength could be increased while curing at high temperature. However, there is a certain limit if it reaches above; the strength of the mixture will start to reduce (Lemougna et al., 2016).

The suitable curing temperature is 60°C with an extreme being 100 ^{o}C regardless of the mixture. Moreover, curing could either be the higher or irregular one, and some factors must be taken into account during curing; for instances alkali activator ratio, the molar ratio in addition to the resting period (Al Bakria et al., 2011).

Curing at higher temperature improves the fast dissolution of metakaolin thus reducing the time required for setting. Moreover, it is also to be noted that an increase in temperature consistently means that there would be decreasing in polymerization rate of the materials and this will be reflected in alkali-activated mixture properties (Mo et al., 2014).

A large part of moisture which is needed for geopolymerization; it losses while curing of fly ash geopolymer at high temperature thus reduction in the mechanical properties (Chindaprasirt et al., 2007). By increasing the curing temperature above, 60 ^{o}C could not agree to an improvement in compressive strength for fly ash geopolymers. The strength of a geopolymer is also related to the curing time. (Hardjito et al., 2004).

To get maximum strength; using metakaolin based geopolymer should be cured at 75 ^{o}C for 4 hours (Kirschener et al., 2004). To curing rapidly or heated at a higher temperature; it would be affected negatively the properties of the final product (Van Jaarsveld et al., 2002).

Vijai et al., (2010) reported that the hot cured fly ash based aluminosilicate binders were registered higher compressive than ambient curing geopolymer. Also, by comparing cured samples between 7 days and 28 days, the obtained results showed that compressive strength was not improved extensively after seven days.

The curing temperature has an essential influence on the compressive strength of metaklaolin based composite. At room temperature; the compressive strength of metakaolin pastes was prolonged. It could be influenced to improve by increasing curing temperature; however, curing at a moderate temperature below 100 ^{o}C could suitable in

terms of mechanical properties. Curing at a higher temperature and with short curing time influences to good strength as well as robust structured, however curing at a lower temperature with longer time improves the strength (Liew et., al 2013). In fig. 6, shows the effects of curing temperature on the compressive strength.

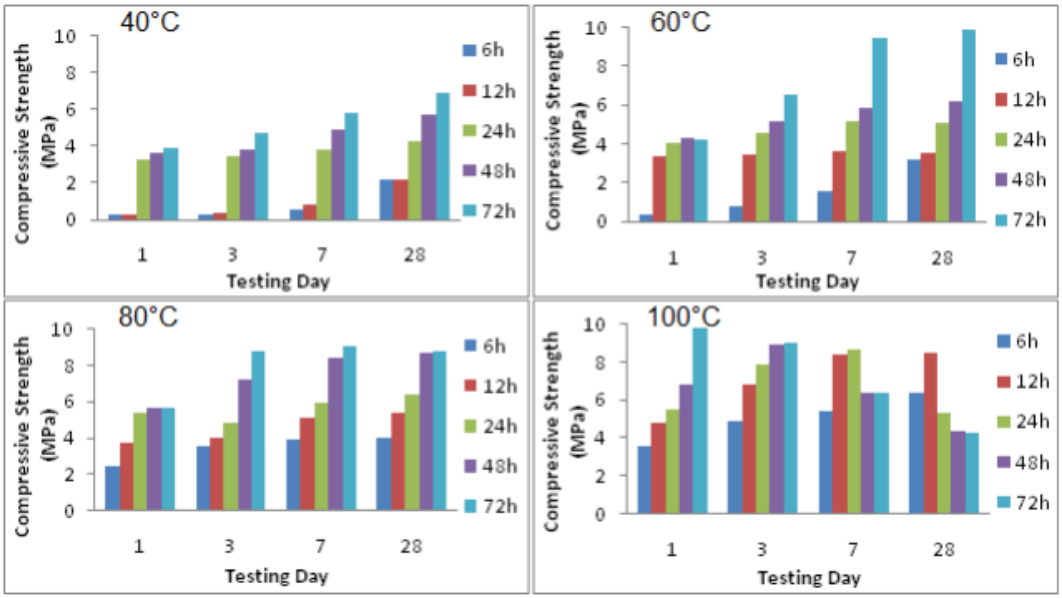

Fig 6. Effects of curing at different temperatures and time on compressive strength (Liew et., al 2013).

Khale et al., (2007) highlighted that to cure the mixture at higher temperature continuously; thus, it leads to a structural failure. Vu et al., (2012) reported that an alteration in the hydration reaction due to the curing temperature, which results in affected the microstructure of the concrete. Taylor (1997) revealed the when the temperature is increased resulting in a fast rate of concrete gel hydration.

Escalante-Garcia and Sharp (1998) reported that by the increase in temperature; the pore size and density of the cement paste could be increased. Due to the quick change in the microstructure distresses the mechanical properties of the concrete in that way makes them weaker. Owing to the rapid absence of water causes the mix composition to squeeze, shrink, and sometimes cracks because of the inadequate geopolymerization process (Cervera et al., 2002).

The curing effect at different temperatures (30 ˚C, 40 ˚C, 50 ˚C, 60 ˚C, 75 ˚C and 90 ˚C) on compressive strength of the metakaolin based alkali activated material, then samples were treated at different temperature at the same duration, however, it was observed different compressive strength values 18 MPa, 14 MPa, 13 MPa were obtained at

temperatures 60 ˚C, 75 ˚C, 90 ˚C respectively, finally they were concluded that the 60 ˚C temperature was good in order to get higher strength and low porosity.

2.4.3 Chemical composition

The ratio of binder amount of the aluminates and silicates in the inclusive mixture has a significant role in influencing on the final product (gel) properties.

To achieve good strength and durability, some molar ratios are suggested by Davidovits (1999) on the basis of his working of zeolite chemistry are: $SiO_2/Na_2O = 1.85$; SiO_2/Al_2O_3 from 3.5–4.5, Na_2O/SiO_2 from 0.2–0.48, Na_2O/Al_2O_3 from 0.8–1.6; and H_2O/Na_2O from 10–25.

The optimal changing ratios provide an indication to the significance of reactive stage of the combining ingredients compared to the molar ratio of the original constituent material, the creative material used has a variable quantity of reactive aluminates and silicates. (Pacheco-Torgal et al., 2008).

2.5 Fiber-reinforced alkali-activated materials

Some studies have been carried out on fiber reinforced geopolymers and the distribution in the mixture effect on the mechanical strength of geopolymers. The significant improvement had been observed in the hardened state properties by adding fibers than plain geopolymer (Silva et al., 2003; Alomayri et al., 2014a, Natali et al., 2011).

The cementitious materials are mainly brittle behavior and fundamentally weak in terms of tensile force while low tensile could be caused by sudden failure due to the propagation of cracks. By using steel fibers as a reinforcement which is quite commonly used to improve the tensile strength of cementitious composites (Neville et al., 2004).

Fiber-reinforcement could be helped to avoid the macro and micro-cracks over a fiber bridging effect; likewise, it alters the post-cracking impact of the material, from an inflexible breakage manner to a flexible way owing to its improved strain energy dissipation ability. Furthermore, different types of fibers have different properties, for instance by using basalt fibers in the mixture could play a significant role to resist the alkali, acidic and salt attack by comparison with glass and aramid fibers. (Samal et al., 2015; Timakul et al., 2016).

By using 2, 3 and 5 wt. % of steel fibers, the flexural strength was recorded 11 MPa and 9 MPa for the mixture of steel and the plain mixture of boroaluminosilicate geopolymers respectively. The maximum and minimum of steel reinforced mixtures on the flexural strength were registered by around 47% and 5% respectively as compared to the plain mix (Nazari et al., 2015).

2.6 Binder

2.6.1 Soapstone

Soapstone is one type of metaphoric rock which contains a large amount of talc, around 50%. Mostly it is used in kilns and other refractory purposes since, its melting point is about 1630 ^{0}C (Indian Mineral, 2012). It is the hydrated layer of magnesium silicate, and the chemical formula is $Mg_3Si_4O_{10}(OH)_2$. It could be used as a raw material in cement, while magnesium interacts with phosphate. Thus, it provides cementitious material. Magnesium oxide-based specimens from talc have given positive outcomes regarding compressive strength and linear shrinkage (Sabouang et al., 2014).

2.6.2 Metakaolin

It is manufactured by heated china clay or mineral kaolin to a temperature around 800 °C. It has good characteristics, such as absorbability, high specific area, and strong coordinative bond (Chen *et al.*, 2016; Concrete society, 2018). This material is being used as supplementary material in the construction field. It is useful in gaining high mechanical strength, toughness, and excellent durability performances, such as high resistance to chemicals. Metakaolin production process releases 80-90% CO_2 emission than OPC (Rovnanik, 2010). Metakaolin becomes cementitious material with high mechanical strength through poly-condensation reaction while it is activated by alkali OH (Granizo et al., 2004).

2.6.3 Lime

It is formed by burning a source of limestone or magnesium limestone between 850 °C, and 1200 °C. Through the following chemical reaction, calcium hydroxide $Ca(OH)_2$ is formed (Ingham, 2013).

$$CaO(s) + H_2O(l) \longrightarrow Ca(OH)_2(s)$$

2.6.4 Stone wool

It is an inorganic fibrous substance that considered as waste which is formed by steam blasting and cooling molten glass. It has many applications such as insulation, and fire protection (Milena et al., 2006). Stone wool occupies large space while landfilled. Landfilling of stone wool is not an eco-friendly method for disposal (Chen et al., 2006). There is an option to tackle this waste by melting, compressing or reprocessing it. It can be used as supplementary cementitious materials (SCM) such as being used as a substitute for OPC in the concrete, to improve the mechanical performances (Ramachandran et al., 2001).

2.6.5 Silica fume (SF)

It is a grey powder with finest non-crystalline silica and produced by smelter processes at a temperature of 2000°C in the silicon-based industries. The particle size is less than 1 micrometer, the bulk density is between 130 to 430 kg/m^3, the specific gravity is 2.2, and the specific surface area is 15000 to 30000 m^2/kg (Holland, 2005).

2.7 Alkali activator

In geopolymerization, a chemical activator is needed that can influence the precipitation and crystallization of the Al and Si constituents in the solution. The alkali hydroxide ions perform as catalysts for the reactivity of the elements, whereas the metal cations help to make a structural element and stabilize the negative framework reinforced by the tetrahedral aluminium network (Petermann et al. 2012).

2.7.1 Sodium Hydroxide

NaOH is mainly used in geopolymerization due to its cost-effectiveness and being reachable, and less viscose. (Vickers et al., 2015). It could be used as a solid or liquid form (National Center, 2018).

2.7.2 Sodium Silicate

Sodium silicate has some familiar names such as “water glass” or “liquid glass”. Sodium silicate used as an activator to activate the aluminosilicates in the binders, and it is available in liquid and solid form (Phoo-ngernkham et al., 2015).

2.8 Fiber

2.8.1 Steel

Steel fibers have two types, such as carbon and stainless steel which are manufactured from virgin steel and recycled steel. Their effectiveness is based on type, length, configuration and diameter. Steel has higher elastic modulus than polypropylene. It is mostly used in concrete to get improvement. Steel fiber reinforced concrete (SFRC) is mainly used in industry for tunnel lining and road paving. Moreover, the primary purpose of the steel fiber is to increase the hardness of concrete. It has excellent characteristics as a composite material such as tensile, shear strength, toughness, and crack resistance. Frost damage could be improved by using steel fibers. It can be distributed in all direction of concrete mix which resulted in blocking the growth of micro-cracks due to evaporation of water from concrete that can result in shrinkage. In addition, these fibers can prevent plasticity and drying shrinkage. SFRC has higher flexural strength and toughness in compare to conventional reinforced concrete (Behbahani et al., 2011; Lau et al., 2006).

2.8.2 Basalt

Basalts fibers could be produced by two methods Junkers and the spinneret. The manufacturing process of basalt fiber takes place at 1400 °C, and in most cases, the diameter of the filament is between 9 to 13μm (Araújo, 2011). Basalt fibers of high strength and high elastic modulus with great shock resistance (Hu and Liu, 2010). Basalt fibers are useful in making the mortar denser, preventing floating and sinking in concrete (Kiisa et al., 2016).

2.9 Sand

Aggregate can play a crucial role in determining the rigidity and stiffness of concretes, and giving concretes their volumetric stability). Based on the CEN-Standard, standard sand should have specific grain size distribution ranges between 0.08 and 2.00 mm (Hajimohammadi et al., 2018; Normen sand, 2019).

3 MATERIALS AND EXPERIMENTAL METHODS

3.1 Materials and mix design

In this thesis, in total twenty mix compositions are prepared and tested. The used materials were soapstone, metakaolin, lime, stone wool, silica fume and various type and content of fibers.

Table 1. Shows the designed mix compositions. The main part of the binder is soapstone from a Finnish company (Tulikivi). Table 2. Depicts the chemical compositions of precursors. Steel and basalt fibers were used in the mixtures, and their specifications are mentioned in Table 3.

Table 1. Mix compositions of soapstone containing different co-binders

Mix	Soapstone (%)	Metakaolin (%)	Lime (%)	Stone wool (%)	Silica fume (%)	Sand (%)	Sodium hydroxide (10M) (%)	Sodium silicate (2.5M) (%)	Steel fiber (%)	Basalt fiber (%)
1	80	20	0	0	0	100	32	68	0	0
2	95	0	5	0	0	100	32	68	0	0
3	80	0	0	20	0	100	32	68	0	0
4	80	0	0	0	20	100	32	68	0	0
5	80	20	0	0	0	100	32	68	1	0
6	95	0	5	0	0	100	32	68	1	0
7	80	0	0	20	0	100	32	68	1	0
8	80	0	0	0	20	100	32	68	1	0
9	80	20	0	0	0	100	32	68	0	1
10	95	0	5	0	0	100	32	68	0	1
11	80	0	0	20	0	100	32	68	0	1
12	80	0	0	0	20	100	32	68	0	1
13	80	20	0	0	0	100	32	68	0.5	0
14	95	0	5	0	0	100	32	68	0.5	0
15	80	0	0	20	0	100	32	68	0.5	0
16	80	0	0	0	20	100	32	68	0.5	0
17	80	20	0	0	0	100	32	68	0	0.5
18	95	0	5	0	0	100	32	68	0	0.5
19	80	0	0	20	0	100	32	68	0	0.5
20	80	0	0	0	20	100	32	68	0	0.5

3.2 Chemical compositions

Table 2, shows the chemical compositions of the used materials which were determined by X-ray fluorescence (XRF).

Table 2. Chemical compositions.

Element/oxide, (wt. %)	Soapstone	Metakaolin	Lime	Stone wool	Silica fume
SiO_2	38.39	53.0	1.69	40.4	93.40
Al_2O_3	1.61	44.5	0.325	15.8	0.75
Fe_2O_3	0.14	0.4	0.384	9.2	1.24
Na_2O	16.59	0.3	-	1.4	0.39
K_2O	0.06	0.1	0.0504	0.4	1.25
P_2O_5	0.03	0.1	0.00788	0.1	-
TiO_2	0.14	1.4	-	0.8	0.02
MgO	37.96	-	2.40	12.6	1.02
SO_3	0.35	-	0.104	-	-
CaO	1.74	-	79.7	17.4	1.39
CrO_3	0.60	-	-	-	-
MnO	0.21	-	1.12	-	-
NiO	0.32	-	-	-	-
Cl	-	-	0.0267	-	-
LOI (525 °C)	21.3	0.3	-	2.4	1.69
LOI (950 °C)	-	0.6	14.212	-	2.31
d_{10} [µm]	2.6	0.6	1.692	0.7	4.7
d_{50} [µm]	24.0	1.3	8.062	6.9	12.53
d_{90} [µm]	124.8	7.5	38.26	33.6	21.85

LOI* = Loss on ignition
d_{10}* = Diameter of particle

3.3 Fiber specifications

The physical and mechanical properties of the two types of used fibers are listed in Table 3 used in the mix compositions. Fig. 7, shows the length of fibers which were used in the designed mix compositions.

Table 3. Physical and mechanical properties of the used fibers.

Fibers	Length (mm)	Diameter (mm)	Density (kg/m^2)	Elastic modulus (GPa)	Tensile strength (MPa)	Elongation at break (%)
Steel	13	0.03	7.88	200	2200	3
Basalt	6	0.018	2.65	100	4500	3.1

a) **b)**

Fig 7. Used fibers: **a)** Steel 12 mm; **b)** Basalt 6 mm

3.4 Alkali activators

The two alkali activators were used which was total around 32%. Table 1. Shows the dosages of alkali activators. The molar ratio of sodium silicate molar ratio is 2.5 (SiO_2/Na_2O=2.5), and sodium hydroxide with a molarity of 10M.

3.5 Aggregate

Standard sand (according to EN 196-1) was used in the designed mix compositions. The grain size distributed between 0.08 and 2.00 mm.

3.6 Preparation of specimens

In the first step of mixing, materials are measured according to Table 1. The dry binder was mixed for 3 minutes with minimum speed. Then alkali activator (NaOH and Na_2SiO_3) were added to the mix composition. After that, it was mixed for a further 3 minutes to get good homogeneity. For reinforced mixtures, fibers were added gradually in the last step after addition of alkali activator.

Fresh concrete filled in the moulds (40x40x160 mm) and placed on the jolting table with the purpose of compaction of concrete according to EN 196-1. The samples were labelled and placed in the oven at 60 °C for 24 hours. After 24 hours, the specimens were demolded and exposed to an ambient conditions (24°C and RH 35%) until the test date. Fig. 8, represents the effects of replacing soapstone with four different co-binders.

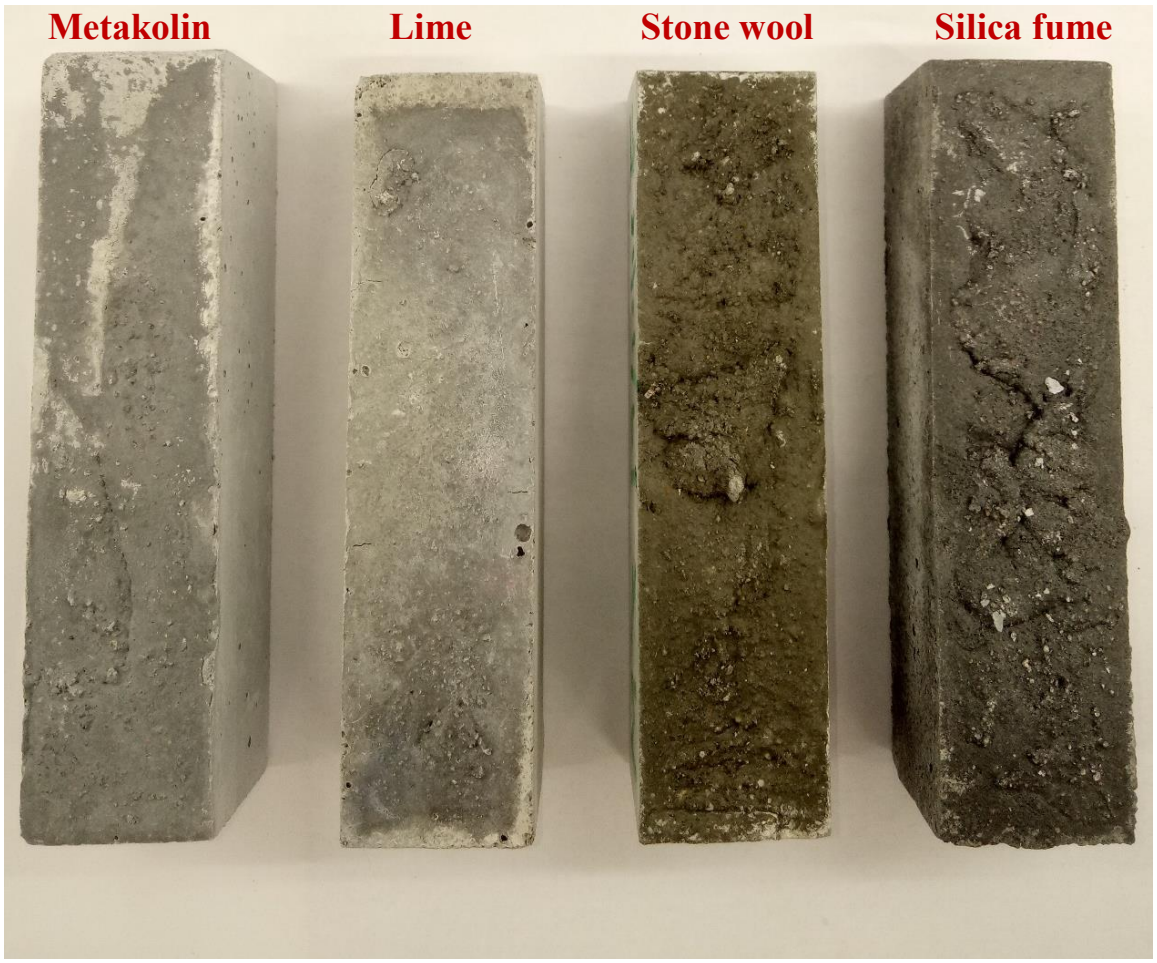

Fig 8. Visual monitoring of the plain mix compositions with four different co-binders.

3.7 Test procedures

3.7.1 Flexural strength

According to the ASTM C78, the flexural test was carried out, and Zwick Z100 material testing machine was used. The flexural load applied on beams at a displacement rate of 0.6 mm/min and 100 kN load cell capacity was used. Fig. 9, shows the flexural strength testing apparatus. The results were obtained from the average of three beams. Flexural strength of the prismatic beams was calculated by using the following equation 2:

$$\sigma_f = 3FL/2bh^2 \qquad (2)$$

Where σf refers to flexural strength, F is the total load, L is the span length, b is the width, and h refers to the height of the specimen.

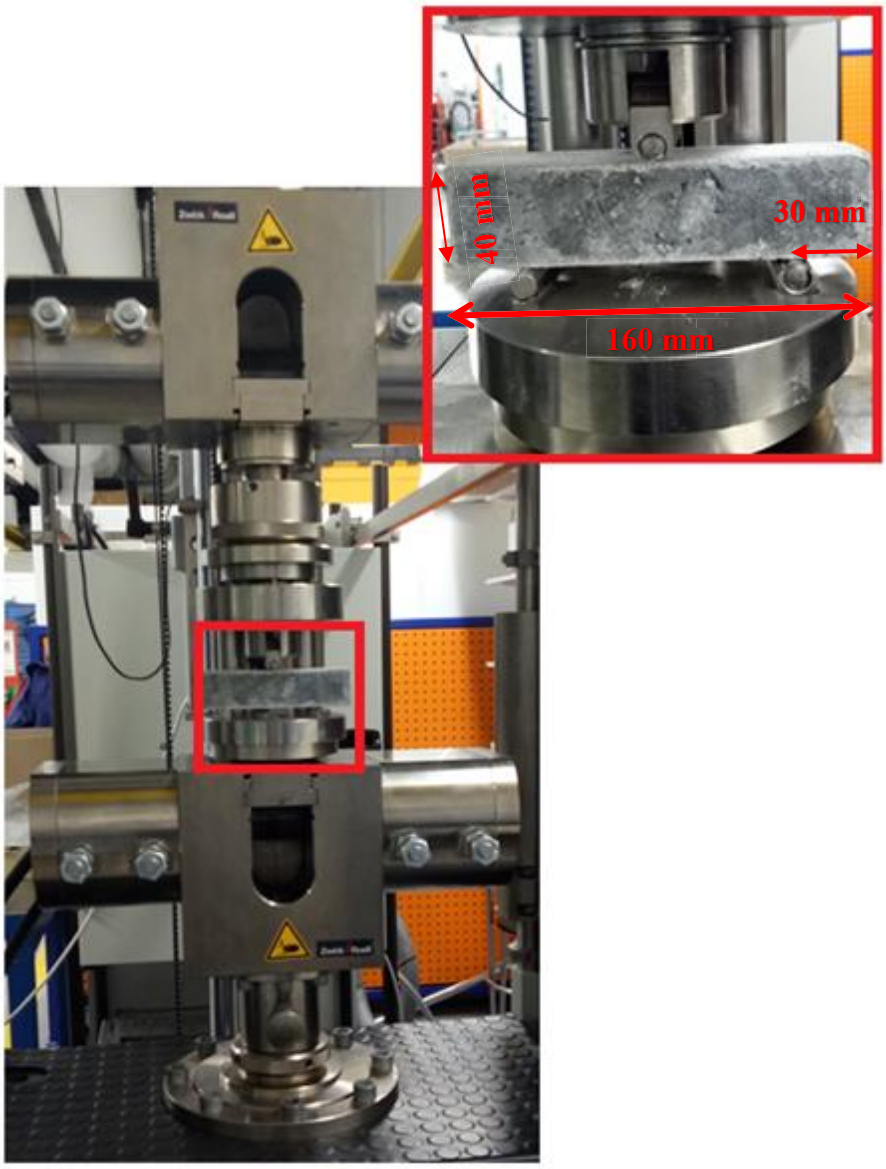

Fig 9. Adopted test setup for flexural test

3.7.2 Compressive Strength

Those split prismatic beams during the flexural test were used for the compressive test according to the ASTM C116-90. The displacement rate was 1.8 mm/min and 100 kN load cell capacity. Fig. 10, shows the adopted test setup for the compressive test. The results were obtained from the average of six tested samples from each composition. The compressive strength was calculated by using equation 3:

$$\sigma c = \frac{F}{A} \qquad (3)$$

Where σ_c denotes the compressive strength (MPa), F is the compressive load (N), and A is the loaded area (mm^2).

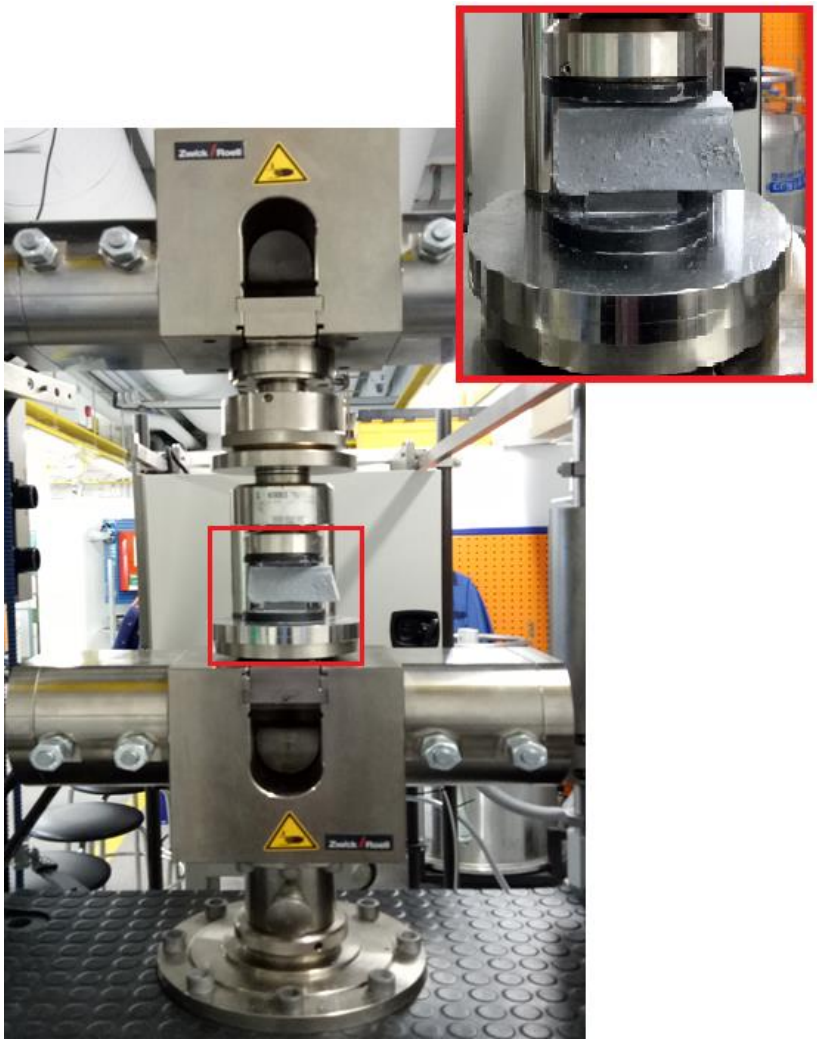

Fig 10. Adopted test setup for the compressive test.

3.7.3 Drying shrinkage

According to the ASTM C157, the specimens (40x40x160 mm) length were measured by mechanical gauge, and the measurement was continued the length change became constant. The measurement started right after de-moulding. The results were obtained from the average of three beams. Fig. 11, shows the used mechanical gauge in this measurement. Drying shrinkage was calculated based equation 4:

$$\Delta l = \frac{ln - l0}{l0} \qquad (4)$$

Where, Δl indicates the shrinkage strain, l_n is the length measurement, l_0 is the initial length of specimen.

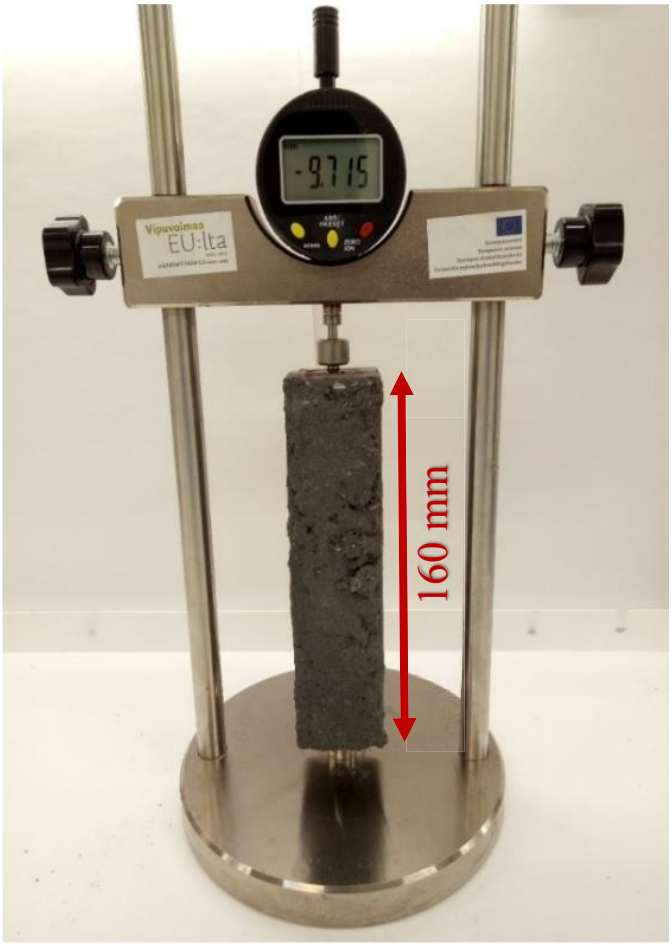

Fig 11. Device used for measuring the length changes.

3.7.4 Water absorption

Based on ASTM C 1585-04, three cubic specimens of each mix (50x50x50 mm) were dried at 100°C for 48 hours, then those samples were placed under water for 48 hours. After that, the samples were removed from the water, and the saturated weight was measured. The results were obtained from the average of three tested samples of each mix composition. Water absorption (W_m) is calculated based on the following equation:

$$\boldsymbol{Wm = \frac{Mw - Md}{Md} X\ 100} \qquad (\mathbf{5})$$

Where, *Wm* denotes the water absorption, M_w stands for saturated mass, and M_d is dry mass.

3.7.5 Apparent porosity

The three cubic specimens of each mix (50x50x50 mm) were immersed into the water, and then weighing buoyancy mass with a basket which was fixed to scale. Fig. 12, shows

the setup for weighing the suspended weight. The Apparent porosity of specimens were calculated by using equation 6:

$$\boldsymbol{Apparent\ porosity} = \frac{\mathbf{Ws - WD}}{\mathbf{Ws - WB}}\ \boldsymbol{X}\ \mathbf{100} \qquad \mathbf{(6)}$$

Where W_s denotes the saturate weight, W_D is the dry weight, and W_B stands for weight buoyancy.

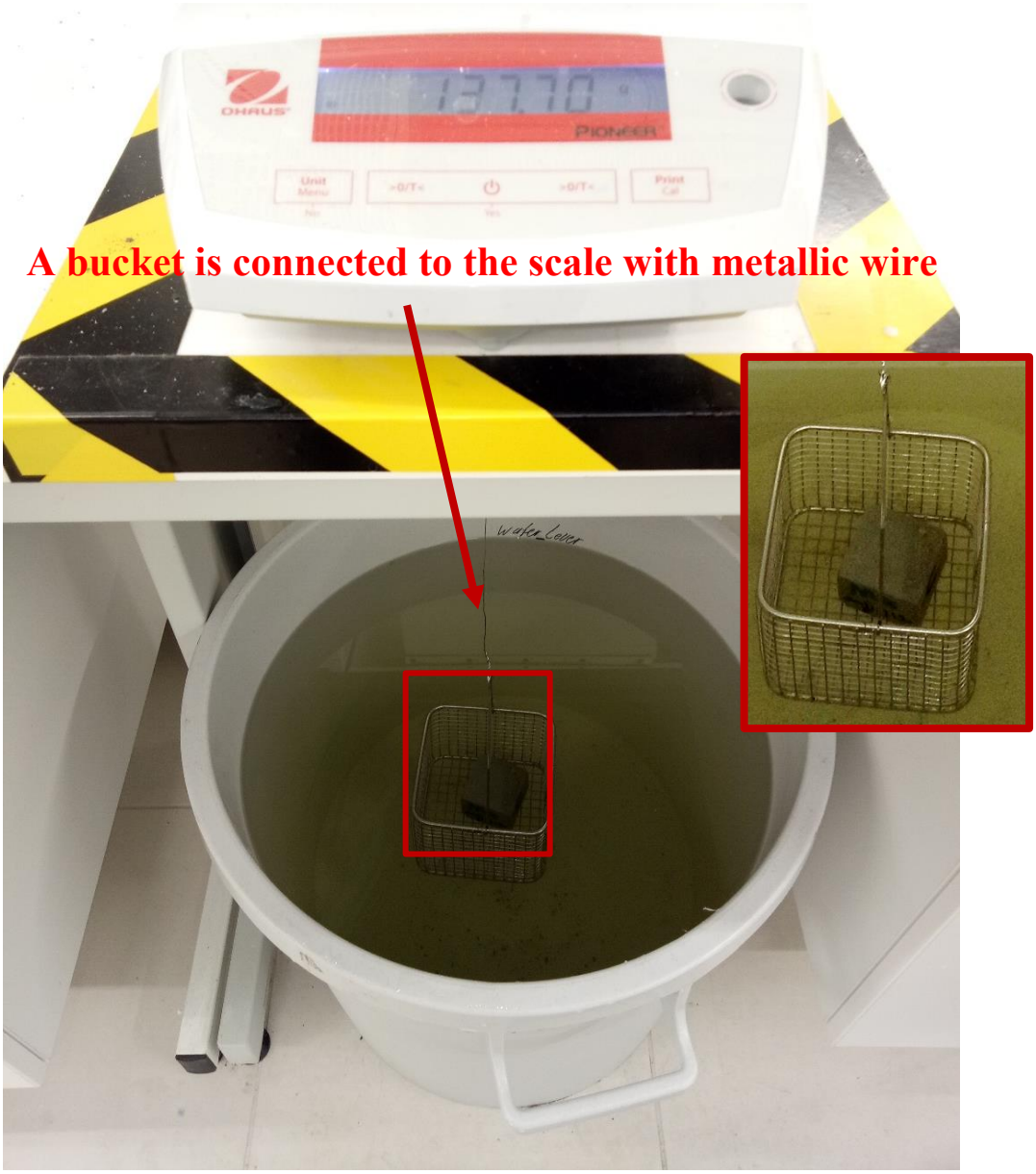

Fig 12. Setup for measuring suspended weight.

3.7.6 Capillary water absorption

The lateral surface of three cubic specimens of each mix composition (50x50x50 mm) were covered by paraffin. The water absorption co-efficient due to capillary action was measured based on BS EN1015-18:2002 recommendation. Fig. 13 shows the set up for

capillary water absorption. The capillary water absorption coefficient were calculated using equation 7:

$$\mathbf{Aw} = \frac{\mathbf{\Delta B}}{\mathbf{A}\sqrt{\mathbf{t}}} \qquad (7)$$

Where, A_w denotes the capillary water absorption coefficient, ΔB is the absorbed mass, A is the surface area, $\sqrt{t}$ is the time ($min^{0.5}$).

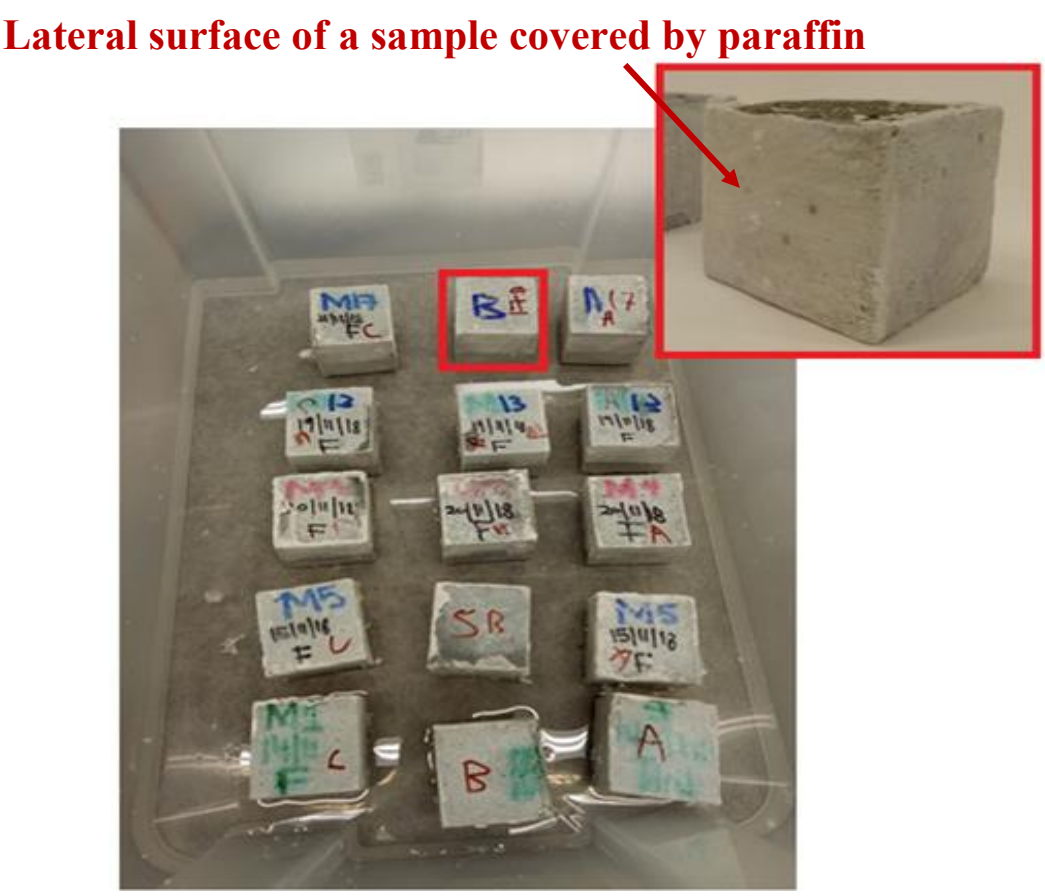

Fig 13. Capillary water absorption.

3.7.7 Acid Resistance

This test was carried out by immersing the sample (50x50x50 mm) in the acidic solution which was 5 % sulfuric acid. Samples were dried at 105 °C for 3 days and weighed. After that samples were immersed in the acid solution.

3.7.8 Ultrasonic pulse velocity (UPV)

The ultrasonic pulse velocity determines the thickness of concrete by a pulse of the ultrasonic wave which passes through the concrete and velocity of the pulse could be

achieved. The velocity passes will indicate the air void or cracks, however higher velocity indicates good quality of concrete. This test is non-destructive and easily carried out on site. Fig. 14, shows the measuring UPV of the sample. Pulse velocity of specimens were calculated by using equation 8:

$$V = \frac{L}{T} \qquad 8$$

Where V refers to pulse velocity (m/s), L is the distance between two transducers (mm), and T denotes transmission time (µsec).

Fig 14. Measuring ultrasonic pulse velocity.

3.7.9 High temperature properties

Three prismatic beams (40x40x160 mm) of each mix were exposed to 800°C for 3 hours. After that samples were left at room temperature to cool down and then flexural and compressive strength were measured. Fig. 15a, shown the samples inside the high-temperature oven and fig. 15b shown the difference after exposure of high temperature

Fig 15. High-temperature exposure: **(a)** Specimens inside the oven; **(b)** After exposure to high temperature.

3.7.10 Carbonation

The three prismatic beams (40x40x160 mm) from each mix composition were used to determine the carbonation resistance of each mix composition. The specimens were placed in the chamber for 7 days, where CO_2 gas was circulated with a concentration of 0.5%, and the relative humidity was 60%. After that flexural and compressive strengths were tested. Fig. 16, shows the carbonation chamber where specimens were treated.

Fig 16. Carbonation Chamber.

3.7.11 Thermogravimetric analysis (TGA)

A Precisa PrepASH 129 analyzer was used to perform the tests. Powders were placed in alumina crucibles and tested at an argon atmosphere and a heating rate of 10 °C/min. Mass loss was recorded with gradual increases in temperature during the test.

3.7.12 Efflorescence assessment

Efflorescence is usually observed in geopolymers which are originated by the fact that alkaline or soluble silicates, those are added during processing which cannot be totally consumed during geopolymerization. It is caused by the transfer of alkaline or earth alkaline ions from pore solution to the sample surface and reacting with atmospheric CO_2 (Abdollahnejad et al., 2018). Efflorescence was observed visually after curing for 28 days in ambient conditions (24°C and RH 35%).

4. RESULTS AND DISCUSSION

4.1 Flexural and compressive strength

The experimental procedure has been designed to evaluate the effects of replacement of soapstone with different co-binders and to investigate how these co-binders will affect the hardened properties of the designed mix compositions. Fig. 17a, indicates that the maximum and minimum flexural strengths were recorded around 11.5 MPa and 1.5 MPa for the mix compositions with metakaolin and lime as a co-binder, respectively. Fig. 17b, indicates the results of compressive strength. The achieved results depicted that the highest compressive strength were recorded around 25 MPa for metakaolin based samples. The maximum and minimum compressive strength were recorded around 25 MPa and 5 MPa, respectively for the mix composition with 5% lime and 20% metakaolin at 28 days respectively.

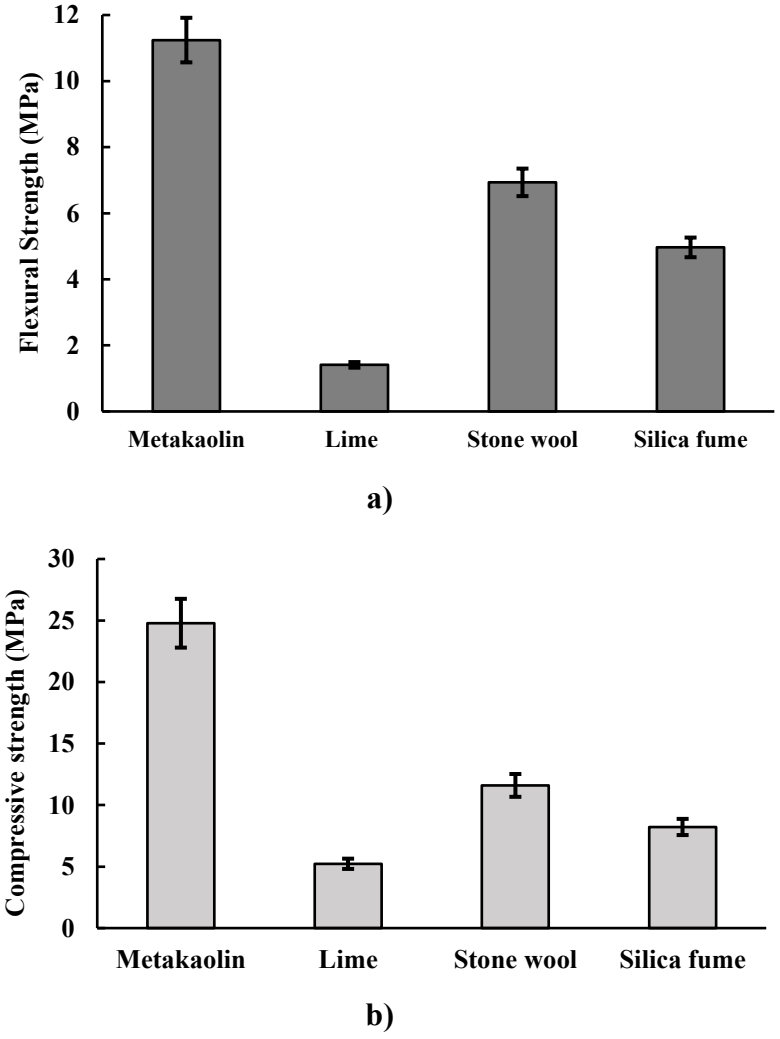

Fig 17. Effects of using replacing co-binders on the: **a)** Flexural strength; **b)** Compressive strength.

There are two different fibers, and two volume fraction (1% and 0.5%) were used in this research in order to investigate; how these fibers and their dosages will effect on the hardened properties of mix compositions. Fig. 18a, illustrates the effects of adding fibers to the mixtures which soapstone was replaced by 20% metakaolin. The results showed that maximum and minimum flexural strength were obtained around 11. 5 MPa and 10 MPa for the mixtures reinforced with 1% and 0.5% steel fibers, respectively. While using 1% steel and 0.5% basalt fibers did not affect the flexural strength in compare to the plain mix composition. Moreover, 1% basalt and 0.5% steel fibers reduced the flexural strengths around 10% and 5% respectively in compare to the reference mix composition. Fig. 18b, shows that the maximum and minimum compressive strength were achieved around 27 MPa and 23.5 MPa for the mixtures reinforced with 0.5% basalt fibers and 0.5% steel fibers, respectively. The compressive strength was improved around 27 MPa as recorded by adding 0.5% basalt fibers. According to the achieved results, the compressive strength was improved and reduced around 4% by adding 1% and 0.5% steel fibers to the mixtures, respectively. Moreover, by employing 1% and 0.5%, basalt fibers were reduced and improved approximately 4% and 10%, respectively by comparison with the plain mixture. It was interesting to find that by reducing the amount of basalt fibers by half, the compressive strength was improved around 10% as compared to the reference sample.

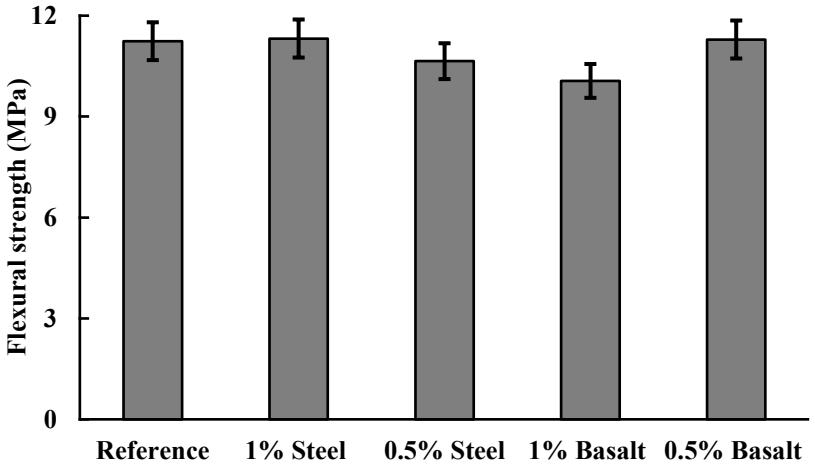

a)

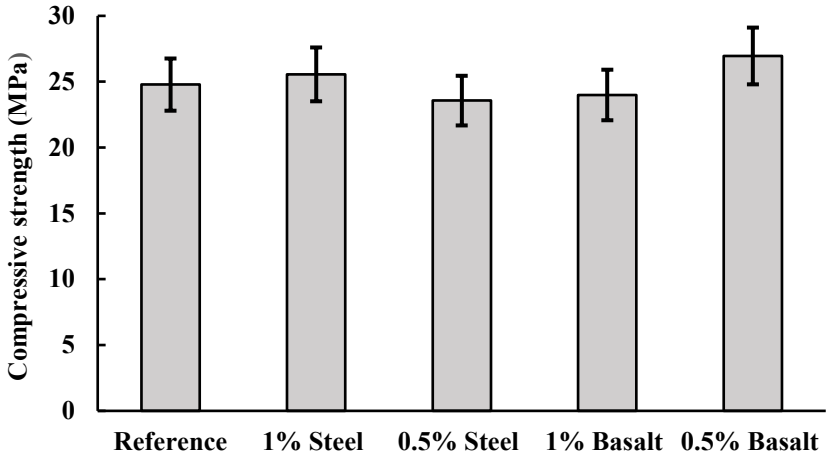

Fig 18. Effects of using different type and dosage of fibers, and replacing 20% of soapstone with metakaolin as a co-binder on the: **a)** Flexural strength; **b)** Compressive strength.

It was tried replacing 20% to 10% of soapstone with lime resulting in mixture had become hardened which was not possible to cast it due to short settling time. Therefore, 5% of soapstone had been replaced with lime. Fig. 19a, represents the effects of adding fibers to the mixtures which soapstone was replaced by 5% lime. The maximum and minimum flexural strength were obtained around 6.5 MPa and 1.5 MPa for the mixture reinforced with 1% basalt fiber and plain mixture, respectively. The results illustrated that the flexural strength was improved up to 250% by employing 1% and 0.5% steel fibers. On the other hand, 1% and 0.5% basalt fibers improved the flexural strength around 500% and 300%, in compare to the plain mixture respectively. Fig. 19b, illustrates that the effects of adding fibers and replacing lime as a co-binder on the compressive strength. The results showed that maximum and minimum compressive strength were obtained around 8.2 MPa and 5.2 MPa for the mixture reinforced with 1% basalt fiber and plain mix compositions, respectively. Compressive strength were improved in mixtures which were reinforced with 1% and 0.5% steel fibers and the increment were around 25% to 38%, respectively. Moreover, employing 1% and 0.5% basalt fibers, the compressive strength were improved around 60% and 45% in compare to the plain mix composition, respectively.

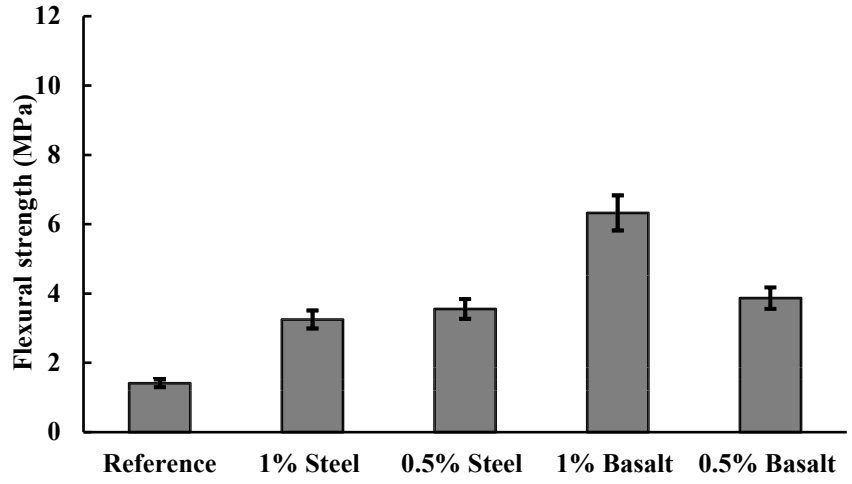

a)

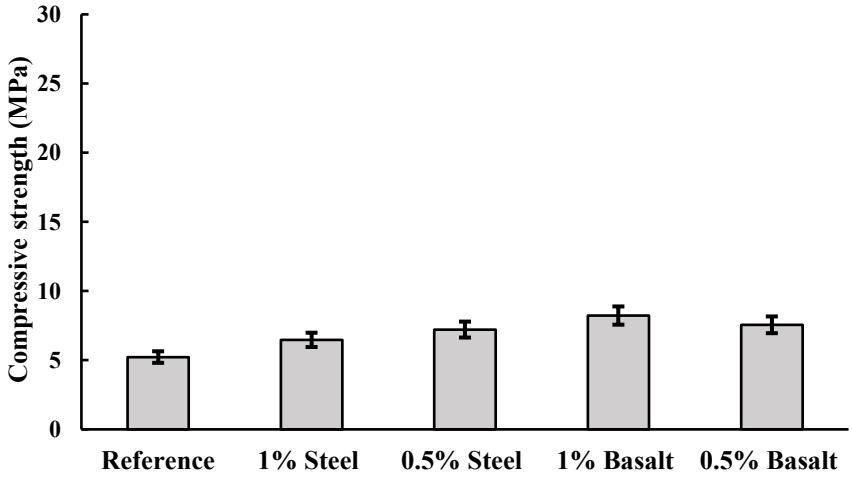

b)

Fig 19. Effects of using different type and dosage of fibers, and replacing 5% of soapstone with lime as a co-binder: **a)** Flexural strength; **b)** Compressive strength.

Fig. 20a, indicates the effects of adding fibers to the mixtures which soapstone was replaced by 20% stone wool. The results showed that maximum and minimum flexural strength were obtained around 8 MPa and 5.5 MPa for the mixtures reinforced with 0.5% and 1% basalt fiber, respectively. It showed that by employing 0.5%, basalt fibers, improved the flexural strength approximately 15% compared to the reference mixture. However, 1% of basalt fibers decreased the flexural strength around 20% in comparison with the reference mixture. Furthermore, addition of 1% and 0.5% of steel fibers resulted in reducing the flexural strength of around 1% and 5%, respectively. According to the obtained results, using 1% and 0.5% steel fibers did not improve the flexural strength; however, in the case of 0.5% basalt fibers, the flexural strength were improved. Fig. 20b,

shows the compressive strength of mix compositions with 20% stone wool as replacement of soapstone. The results showed that maximum and minimum compressive strength were obtained around 12 MPa and 9 MPa for the mixtures reinforced with 0.5% and 1% basalt fibers, respectively. It was revealed that by using 1% and 0.5% steel fibers, the compressive strengths were reduced by around 12%. Besides, 1% and 0.5% basalt fibers were decreased the compressive strength around 20% and 8%, respectively. Moreover, in can be mention that increasing the amount of basalt fibers from 0.5% and 1% led to decrease in the compressive strength.

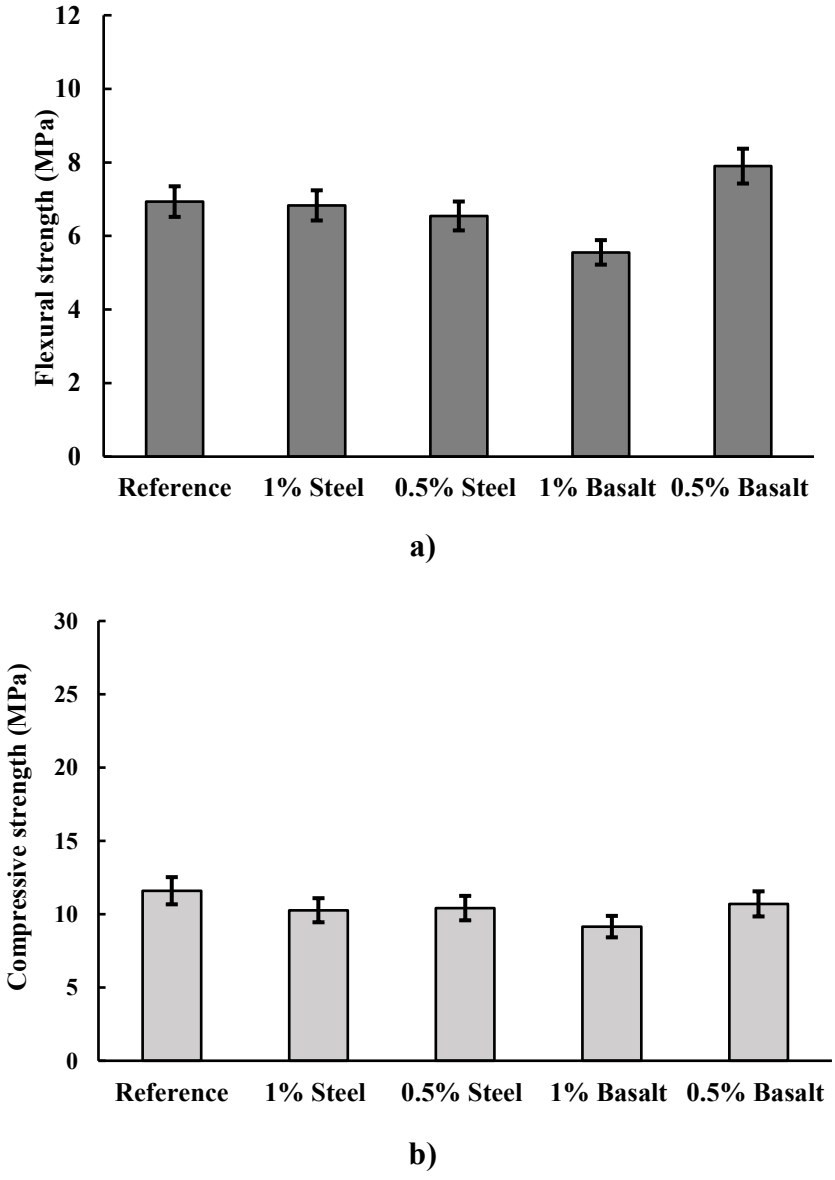

Fig 20. Effects of using different type and dosage of fibers, and replacing 20% of soapstone with stone wool as a co-binder: **a)** Flexural strength; **b)** Compressive strength.

Fig. 21a, shows the effects of adding fibers to the mixtures with 20% silica fume as a replacement of soapstone. The obtained results showed that the maximum and minimum flexural strength were obtained around 9 MPa and 5 MPa for the mixtures reinforced with 1% basalt fibers and plain mix composition, respectively. By employing 1% and 0.5% steel fibers, the flexural strength increased around 40% in compare to the plain mixture. Likewise, 1% and 0.5% Basalt fibers improved the flexural strength around 80% and 40%, respectively. Fig. 21b, shows the effects of addition of fibers on the compressive strength of mixture with 20% silica fume use as a co-binder. The results showed that maximum and minimum compressive strength were obtained around 10 MPa and 8 MPa for the mixtures reinforced with 1% basalt fibers and plain mixture, respectively. By employing 0.5% steel fibers, the compressive strength was improved up to 10% compared to the reference mix composition. However, it was observed that by adding 1% steel fibers, the compressive strength improved by 2%. Moreover, 1% and 0.5% basalt fibers improved the compressive strength around 20% and 15% respectively.

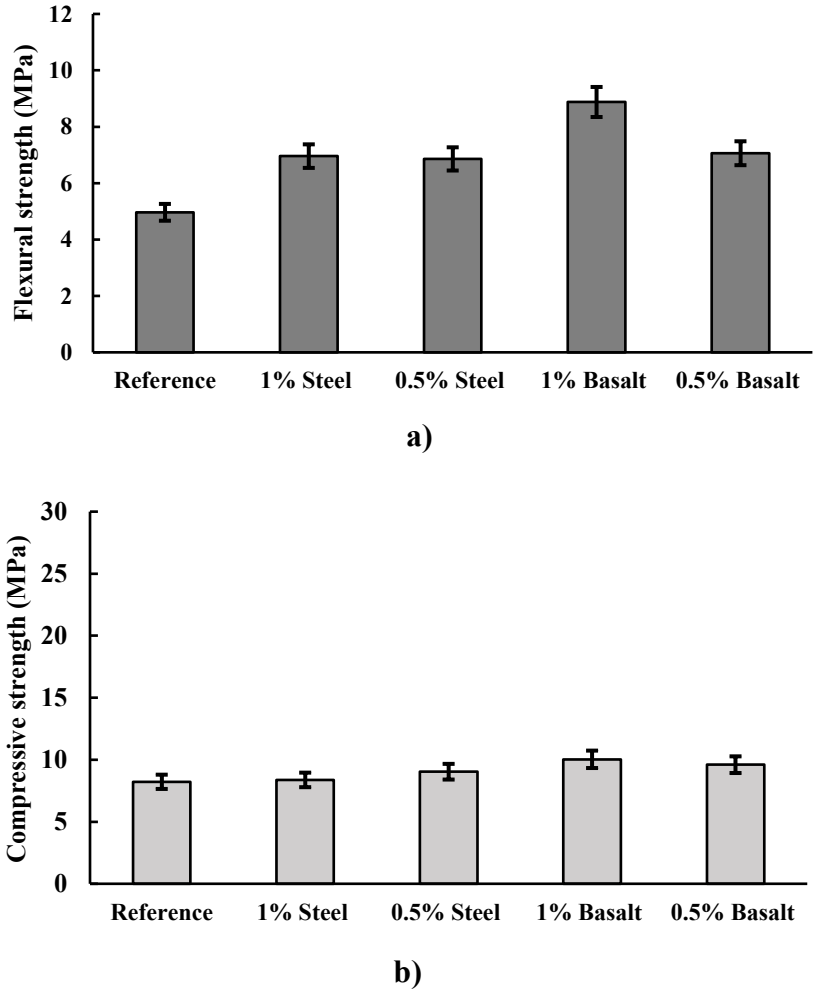

Fig 21. Effects of using different fibers and replacing 20% of soapstone with silica fume as a co-binder on the **a)** Flexural strength; **b)** Compressive strength.

4.2 Drying Shrinkage

Fig. 22, represents the effects of different co-binders when were replaced with soapstone on drying shrinkage rate. It revealed that the drying shrinkage rate of mix composition with 5% lime was increased rapidly in comparison to other used co-binders and reached around -0.20mm in the first 360 hours. The shrinkage rate of mix composition with 20% metakaolin was slightly changed in compare to other used co-binders. Moreover, Gesso et al., 2007 reported that, by using metakaolin as a co-binder, the shrinkage rate could be reduced. Silica and stone wool as co-binders behaved similarly in terms of shrinkage and their rates was been gradually increasing up to a certain point.

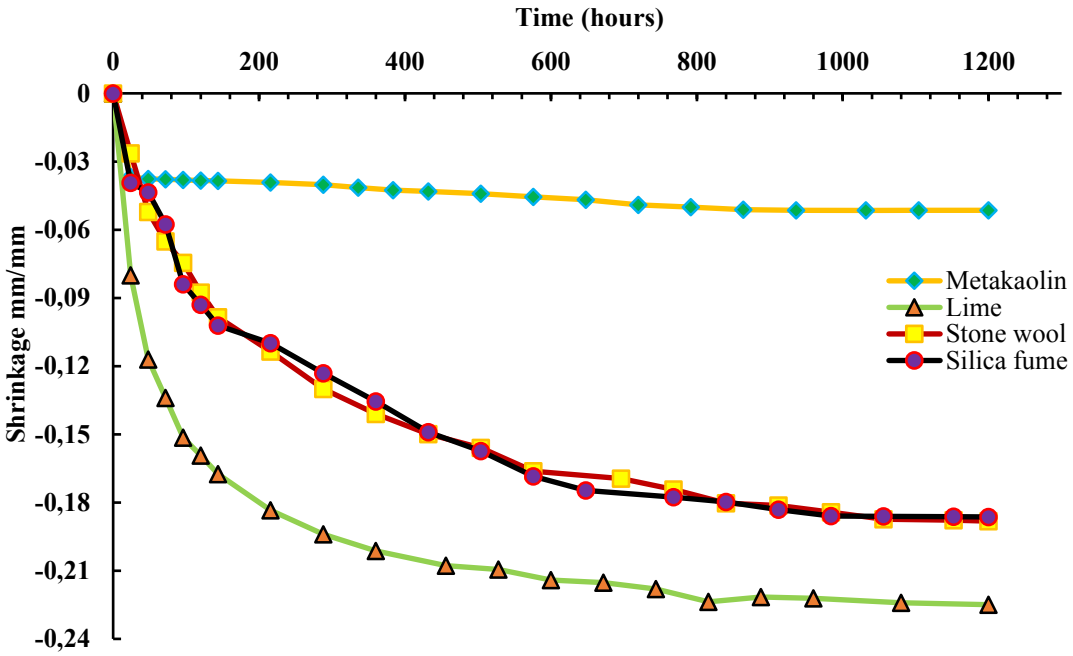

Fig 22. Shrinkage of plain mixtures with metakaolin, lime, stone wool or silica fume used as a co-binder.

Fig. 23, illustrates the results of drying shrinkage of the reinforced mixtures with metakaolin as a co-binder. The obtained values showed that by employing 0.5% and 1% basalt fibers, the drying shrinkage decreased around 70% and 80%, respectively as compared to the reference mixture. Moreover, by employing 1% and 0.5% steel fibers, drying shrinkage rates decreased about 70% in compare to the reference mix composition.

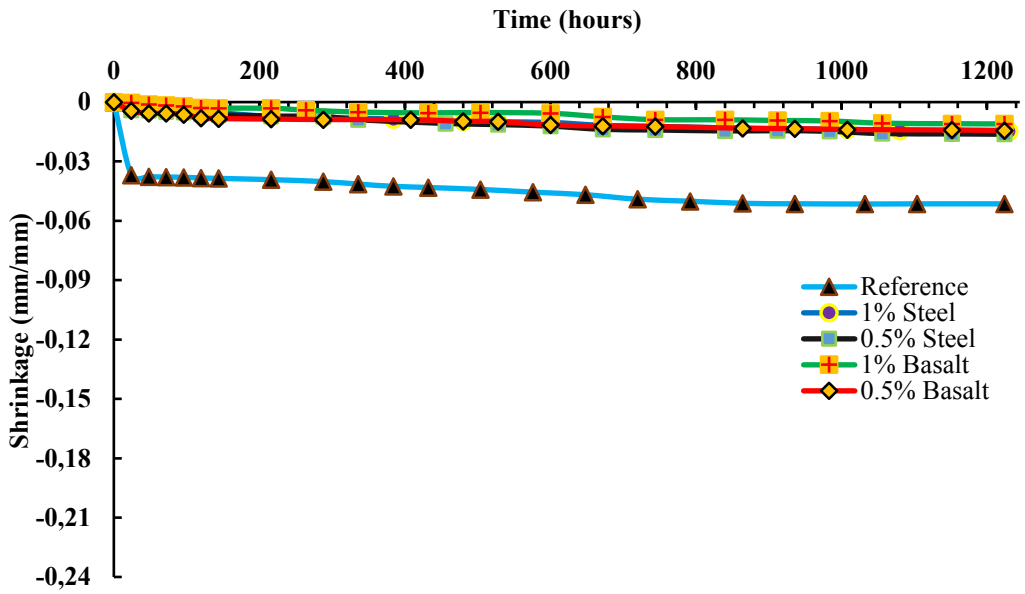

Fig 23. Effects of fibers on the drying shrinkage in the mixture with 20% metakaolin used as a co-binder.

Fig. 24, depicts the results of mixtures with 5% lime as a co-binder. It was recorded that by adding fibers either 1% and 0.5% steel fibers or 1% and 0.5% basalt fibers, the drying shrinkage rate decreased by 55% and 50%, respectively in compared to the reference mixture.

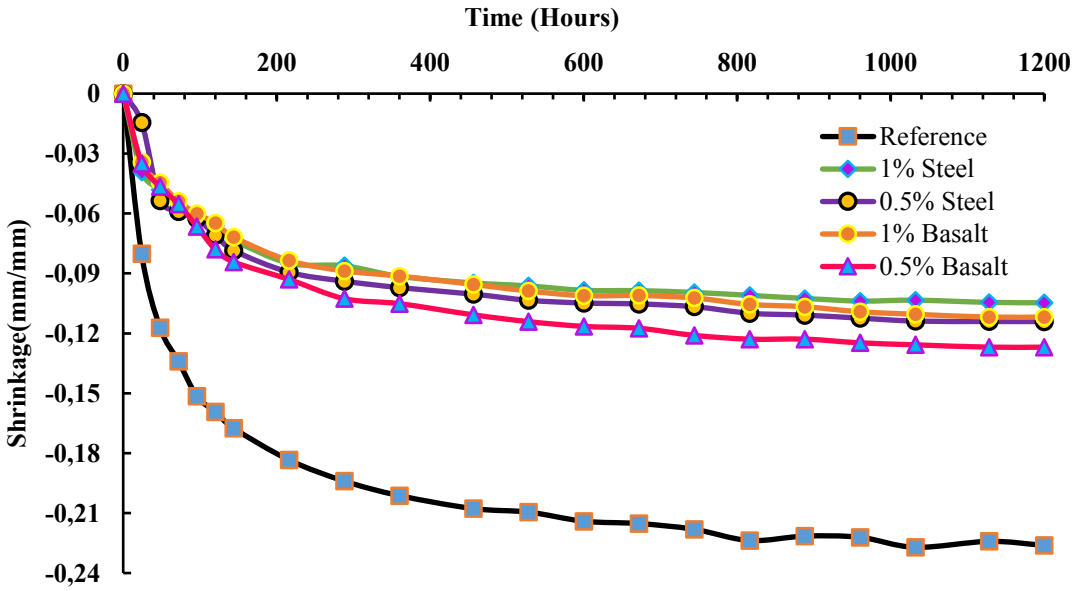

Fig 24. Effects of fibers on the drying shrinkage in the mixture with 5% lime used as a co-binder.

Fig. 25, represents the results of drying shrinkage of mixtures which was soapstone replaced by 20% stone wool. According to the obtained results, the shrinkage rate was

reduced around 31% and 50% by employing 0.5% and 1% steel fibers, respectively in compare to the reference samples. Adding 1% basalt, decreased the drying shrinkage by 40%. Moreover, 0.5% basalt fibers reduced the drying shrinkage rate up to 25%. The obtained results revealed that the higher amount of steel fibers (1%) resulted in the highest resulted reduction in shrinkage rates.

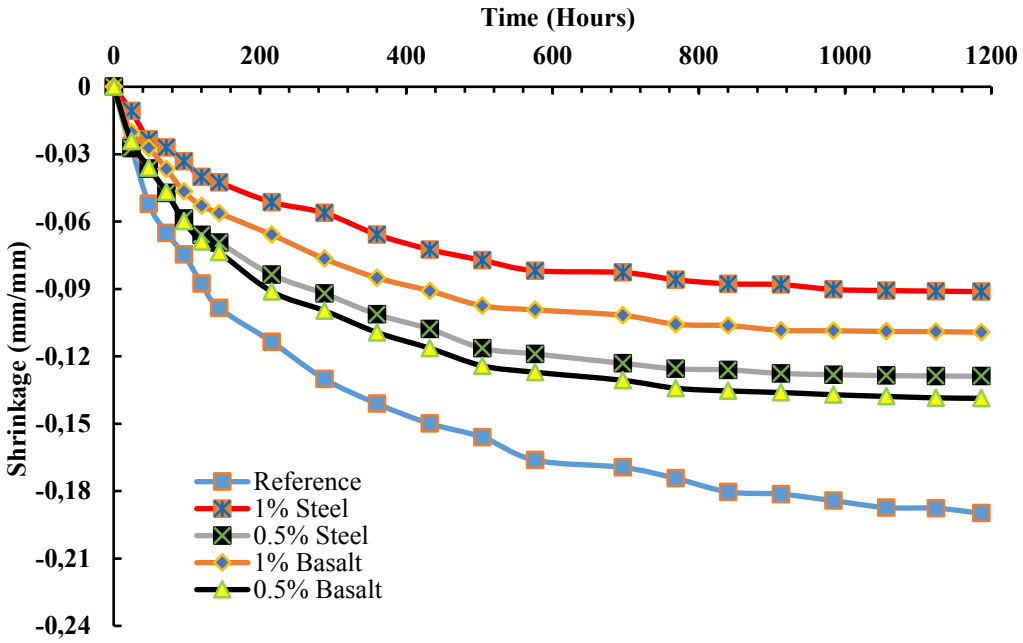

Fig 25. Effects of fibers on the drying shrinkage in the mixture with 20% stone wool used as a co-binder.

Fig. 26, illustrates the results of drying shrinkage measurement for mixtures which soapstone was replaced with silica fume by 20%. The achieved results showed that by adding 0.5% and 1%, steel fibers decreased the drying shrinkage rate around 30% and 45%, respectively as compared to the reference mixture. By employing 0.5% and 1% basalt fibers, the shrinkage rate was reduced around 15% to 30%. Also, it was reported that the higher amount of steel fibers could lead towards the great improvement.

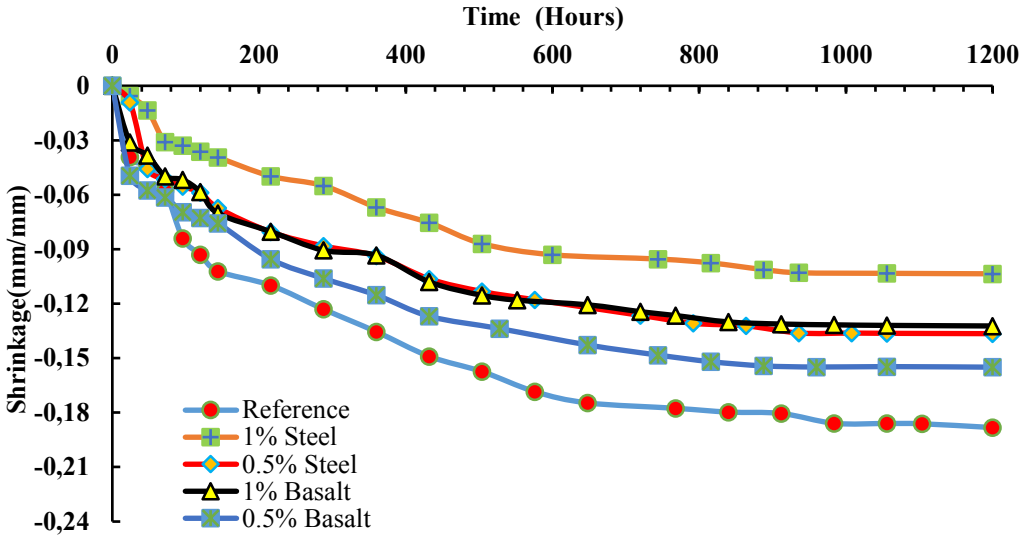

Fig 26. Effects of fibers on the drying shrinkage in the mixture with 20% silica fume used as a co-binder.

4.3 Water absorption

To presented results the effects of using different co-binders on water absorption of soapstone mix compositions. Fig. 27, depicts the results of water absorption by immersion of plain mixtures. According to the obtained results, the metakaolin mixture showed a higher amount of water absorption in compare to two co-binders. Due to the high amount of water absorption in mixture with 5% lime, it was not possible to measure it.

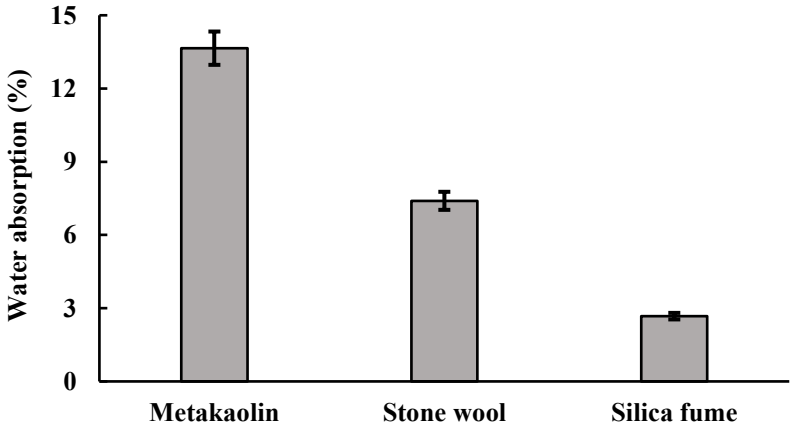

Fig 27. Effects of used co binders on water absorption.

Fig. 28, shows the effects of fibers on the water absorption of reinforced mixtures with 20% metakaolin as a replacement of soapstone. The obtained values showed that fibers reinforced specimens showed reduction in water absorption around 14% in compared to

the plain mixture. However, the amount and types of fibers affected on water absorption about 10%

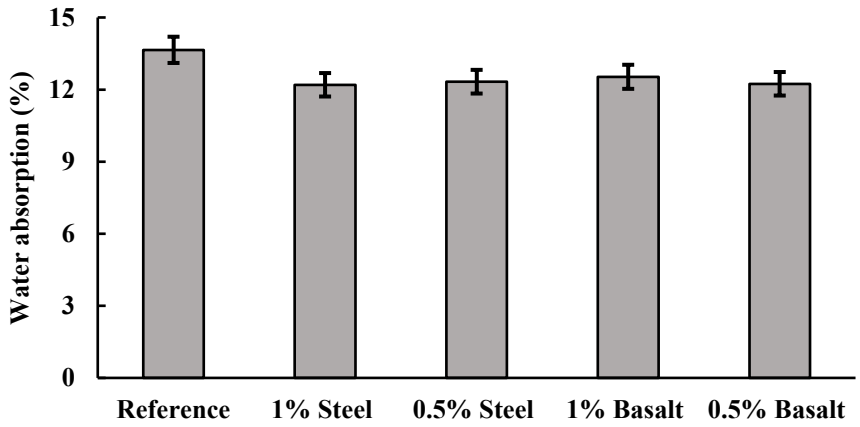

Fig 28. Effects of fibers on the water absorption of mixtures with 20% metakaolin as a co-binder.

Fig. 29, shows mixtures with lime 5% as a co-binder during conducting the water absorption test. This figure shows that within few hours of starting the test, the water absorption was high, and the measurement was not possible for those mix compositions with 5% lime.

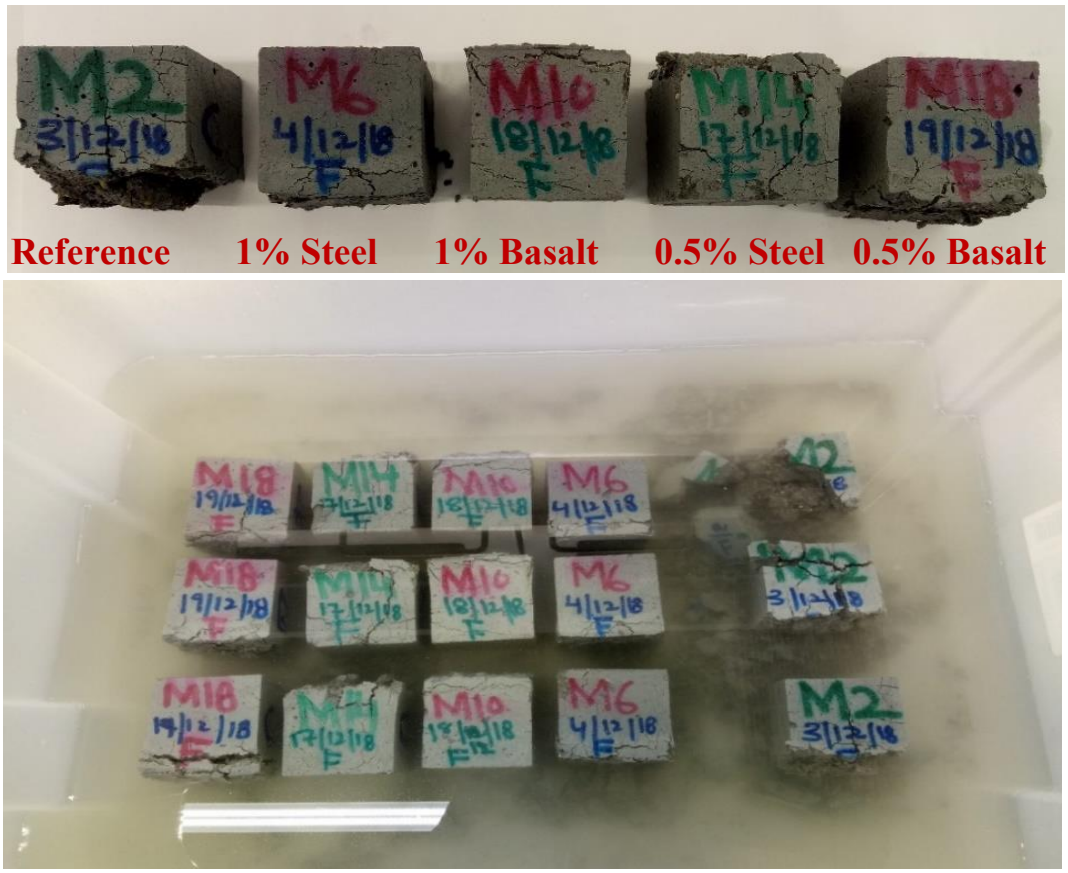

Fig 29. Reinforced mixtures with 5% lime during water absorption test.

Fig. 30, represents the effects of using different fibers on the water absorption of mixtures with 20% stone wool. The obtained values showed that 0.5% and 1% steel fibers increased the water absorption rate around 25%. While, 1% and 0.5% basalt fibers increased the water absorption around 45% and 25%, respectively in compare to reference mix composition. Besides, it was found that by adding (1%) basalt fibers absorption increased in compared to the mixture with (0.5%) basalt fibers.

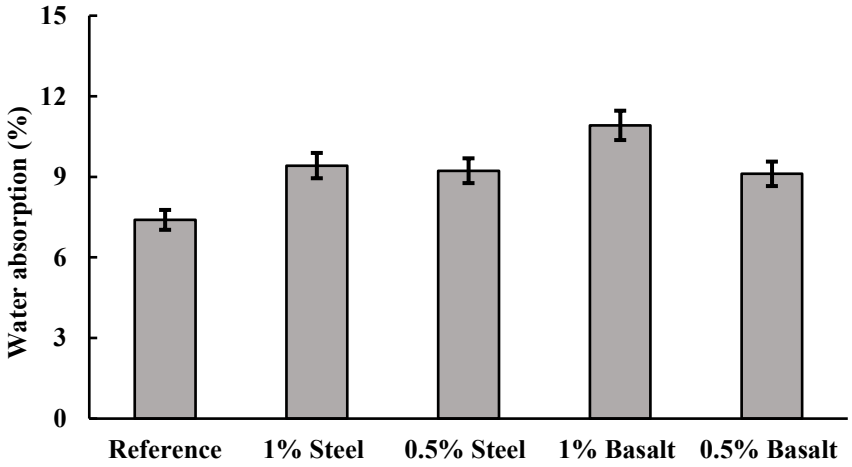

Fig 30. Effects of fibers on the water absorption of mixtures with 20% stone wool as a co-binder.

Fig. 31, represents the effects of using different fibers on water absorption results of the mixtures with 20% silica fume. The achieved results showed that 1% and 0.5% basalt fibers increased the water absorption by 38% and 35% respectively as compared to the reference mixture. Although, Steel fibers did not affect the water absorption in a compare to the reference mixture water absorption.

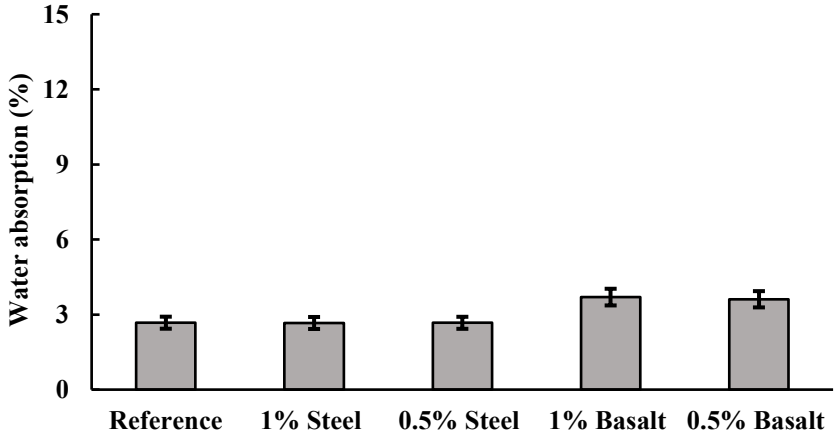

Fig 31. Effects of fibers on the water absorption of mixtures with 20% silica fume as a co-binder.

4.4 Apparent porosity

This part is assigned to investigate the effects of using different co-binders on apparent porosity. Fig. 32, shows the apparent porosity of plain mix compositions. The results for mixture with metakaolin and stone wool plain mixtures were recorded around 25% and 15% respectively, whereas silica fume result was recorded 6% which was lowest apparent porosity in compare to the mixtures with metakaolin or stone wool.

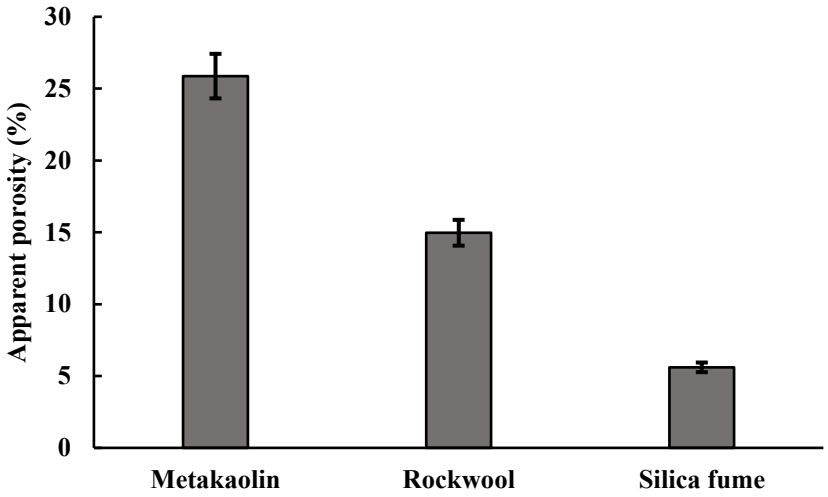

Fig 32. Apparent porosity of plain mixtures.

Fig. 33, shows that the effects of different fibers on the apparent porosity of the mix compositions with 20% metakaolin. The apparent porosity of reinforced mixtures were reduced around 10% in comparison to the reference mixture. The results showed that type and amount of fibers did not affect the results.

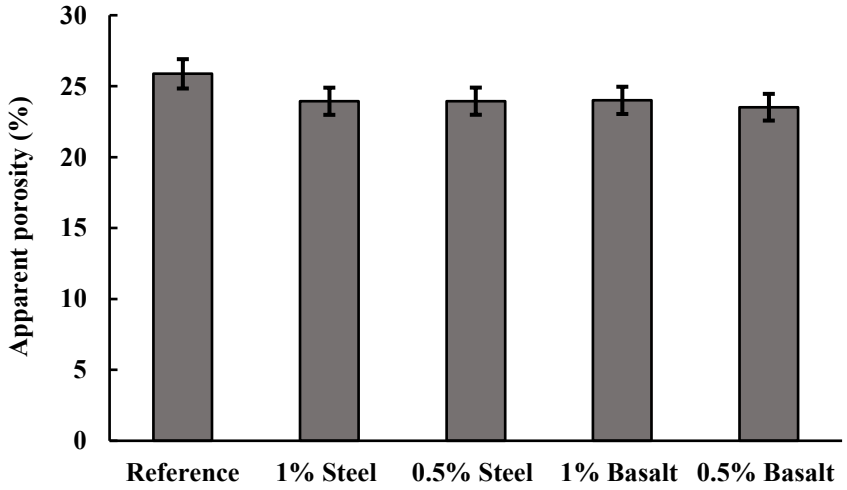

Fig 33. Apparent porosity of fibers reinforced mixtures with 20% metakaolin.

Fig. 34, depicts the results of apparent porosity of reinforced mix compositions with 20% stone wool as a co-binder. According to the achieved values, 0.5% and 1% steel fibers increased the apparent porosity by 27% as compared to the reference mix composition. Moreover, 1% basalt fibers increased the apparent porosity of about 40%. In addition, 0.5% basalt fibers increased the apparent porosity by 21% as compared to the reference mixture. The attained results reveal that fibers reinforced mixtures have higher apparent porosity in compare to the plain mixture.

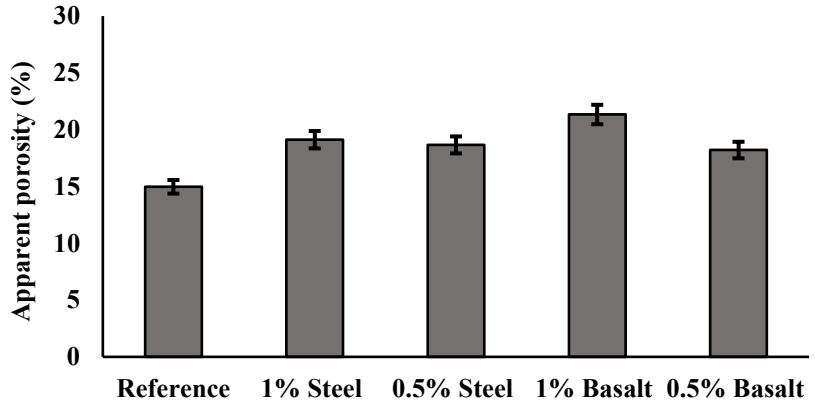

Fig 34. Apparent porosity of fibers reinforced mixtures with 20% stone wool.

Fig. 35, shows the effects of different fibers on the apparent porosity of mixture with 20% silica fume. In 1% and 0.5% steel mixtures, the apparent porosity decreased around 10% in compare to the reference mixture. However, 1% and 0.5% basalt increased the apparent porosity by 30% and 25% as compared to the plain mix composition, respectively.

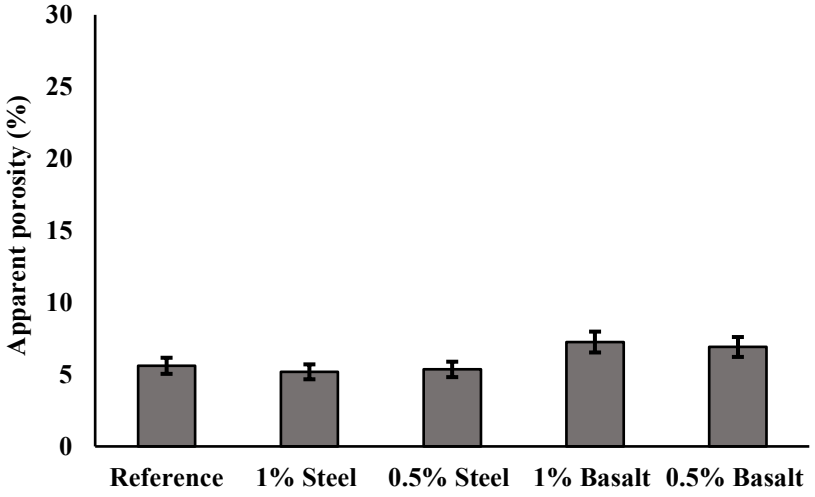

Fig 35. Apparent porosity of fibers reinforced mixtures with 20% silica fume.

4.5 Capillary water absorption

The following results presented the effects of using different co-binders on water absorption by the capillary. Fig. 36a, illustrates the cumulative mass of water of plain mix compositions. It showed that metakaolin plain samples showed higher cumulative mass of water around 11 kg/m^2. The stone wool was 5 kg/m^2 and silica fume around 2.20 kg/m^2. According to the achieved results, silica fume had lower cumulative mass of water about 2.20 kg/m^2. Fig. 36b, represents the capillary co-efficient of plain mixtures. The capillary co-efficient of metakaolin mixture was the highest and silica fume had the lowest of capillary water absorption co-efficient.

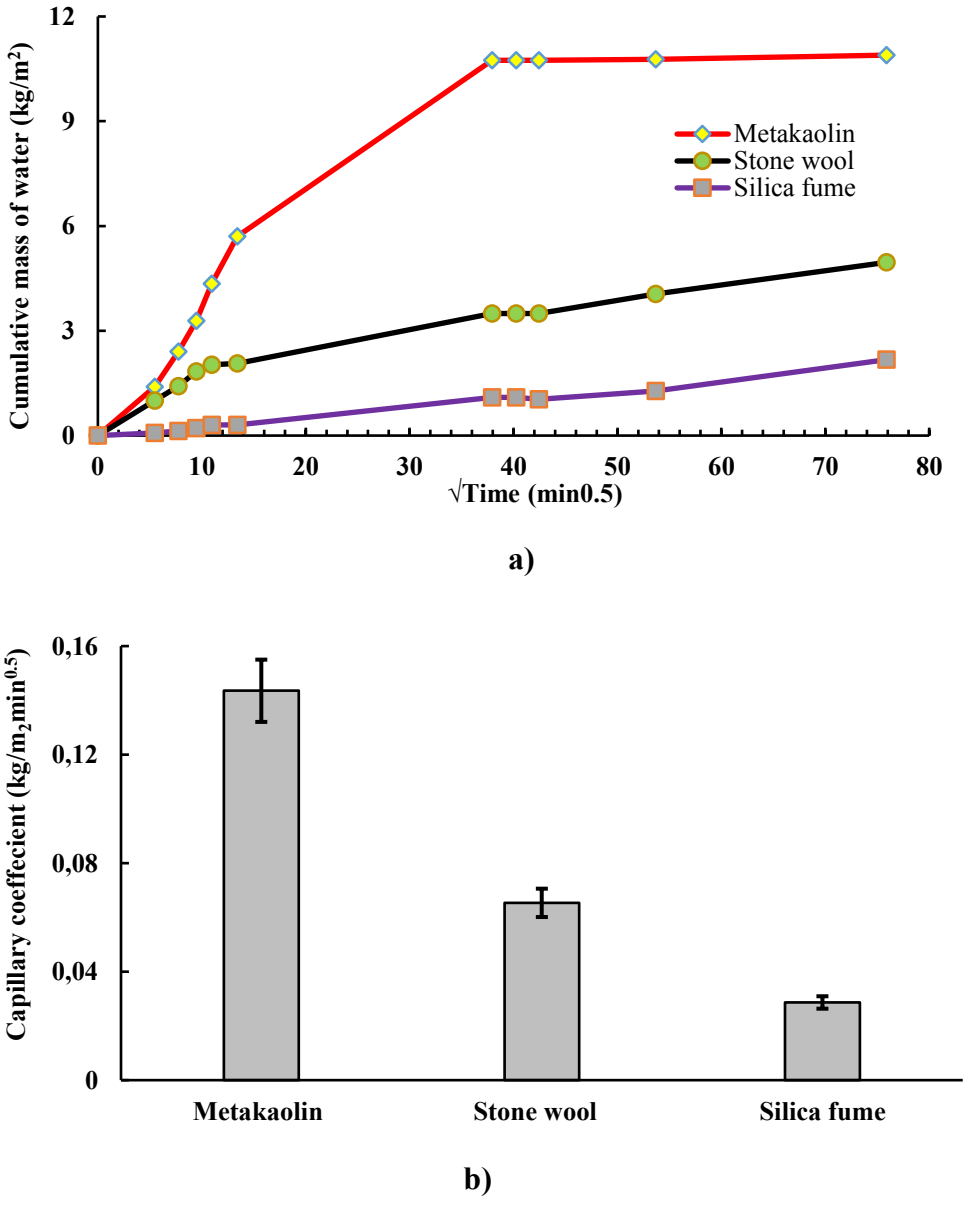

Fig 36. a) Cumulative mass of water in the plain mixtures; **b)** Water absorption capillary coefficient of plain mixtures.

Fig. 37a, illustrates the results of capillary water absorption by using different fibers in the metakaolin mix compositions. It was observed that addition of fibers did not affect the capillary water absorption remarkably. Fig. 37b, represents the capillary co-efficient of metakaolin mixtures. The minimum and maximum co-efficient were recorded around 0.139 kg/m^{2}H$^{0.5}$ and 0.144 kg/m^{2}H$^{0.5}$ for the 1% and 0.5% basalt fiber respectively.

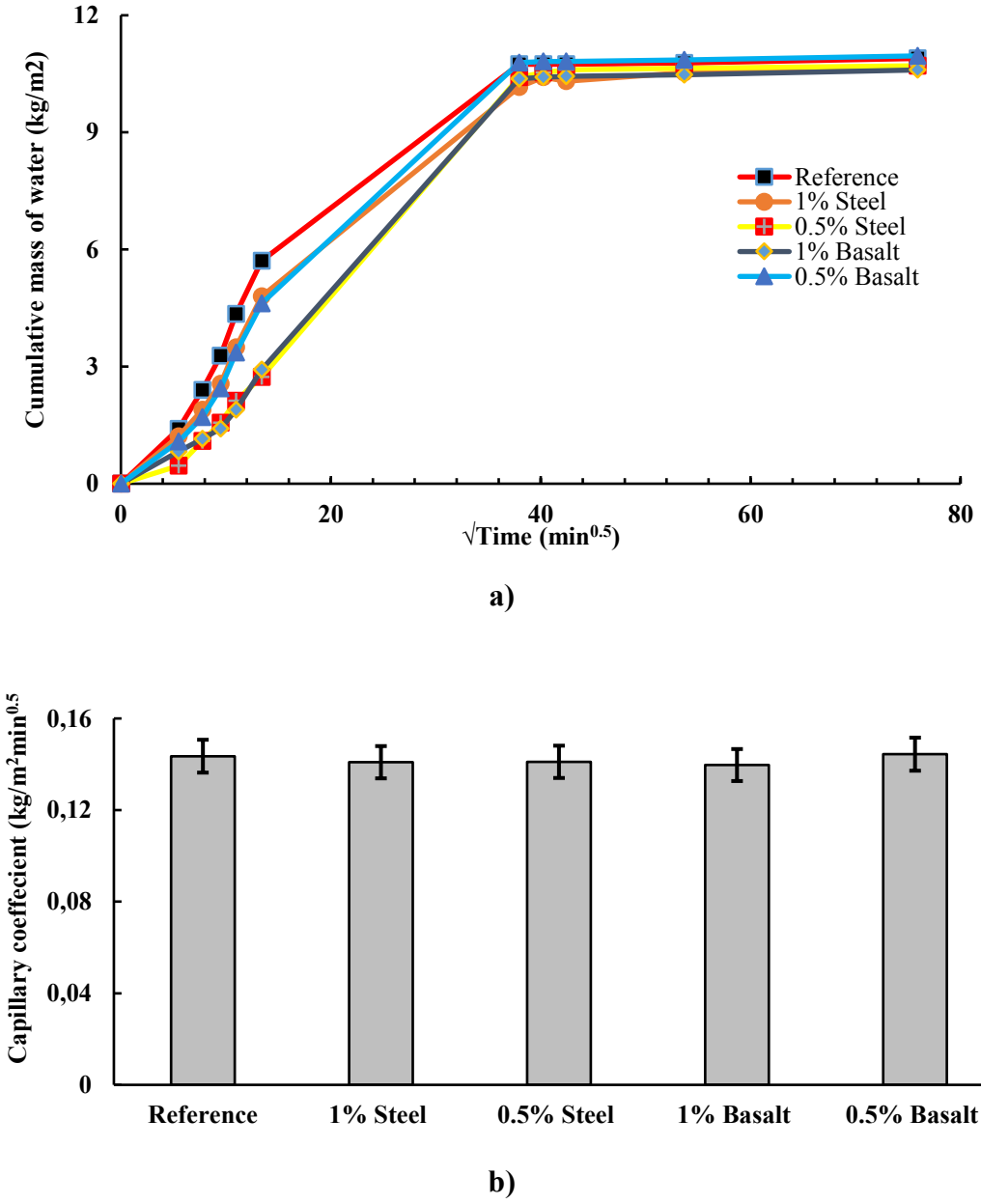

Fig 37. a) Cumulative mass of water in the fiber reinforced mixtures 20% metakaolin; **b)** Capillary coefficient of fibers reinforced mixtures with 20% metakaolin.

Fig. 38, shows the capillary water absorption test on mix compositions with 5% lime. Due to high water absorption by capillary, the samples destroyed while the test was running and no results obtained for these mix compositions.

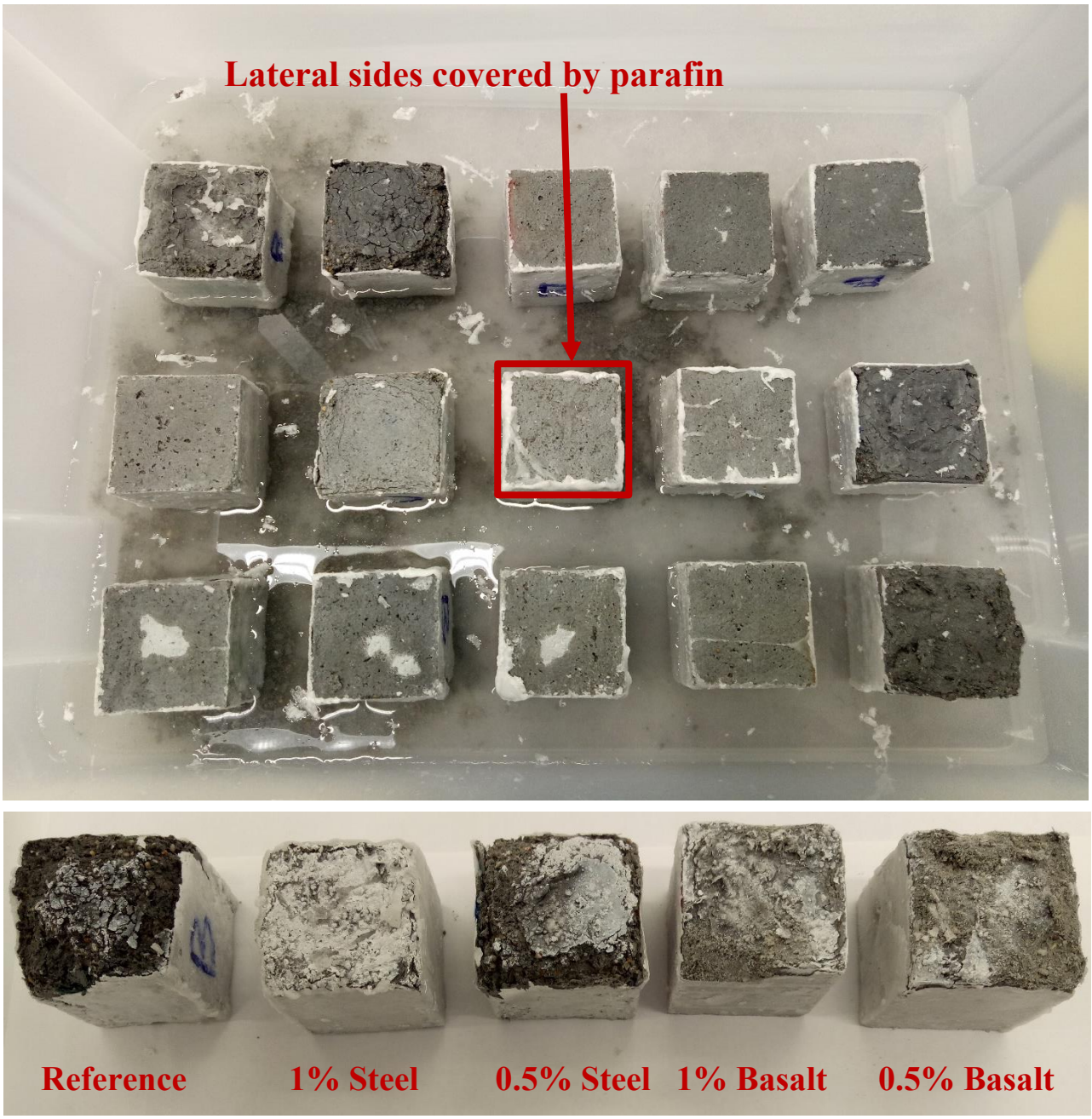

Fig 38. Capillary water absorption of fiber reinforced mix compositions with 5% lime.

Fig. 39a, depicts the cumulative mass of water in mixtures with 20% stone wool. The achieved results showed that 0.5% and 1% basalt fiber increased the water absorption co-efficient by around 45% and 15% as compared to the plain mix composition, respectively. Moreover, 1% and 0.5% steel fiber reinforced mixtures were absorbed water around 25% compared to reference mixture and confirmed that the dosages of steel fibers did not affect the water absorption. Fig. 39b, illustrates the capillary co-efficient results. The minimum and maximum capillary co-efficient were recorded around 0.05 $kg/m^2H^{0.5}$ and 0.09 $kg/m^2H^{0.5}$ for the plain and 0.5% basalt fiber mixture, respectively.

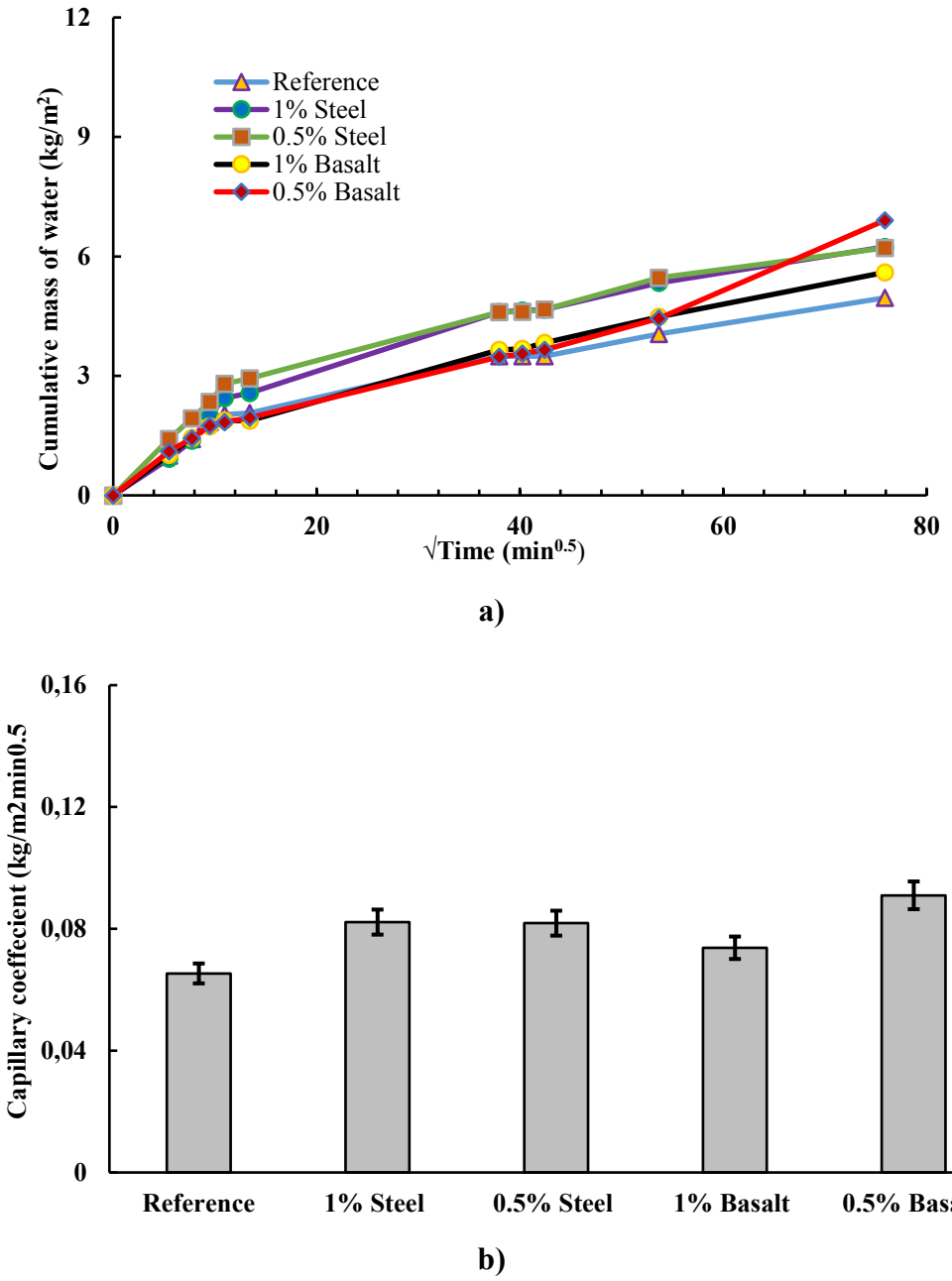

Fig 39. a) Cumulative mass of water in the fiber reinforced mixtures with 20% stone wool; **b)** Capillary coefficient of fibers reinforced mixtures 20% stone wool.

Fig. 40a, depicts the results of fibers reinforced mixtures with 20% silica fume. The attained values showed that 1% steel fibers increased the capillary water absorption around 45% (1.9 kg/m^2). On the other hand, 0.5% steel fibers caused reduction around 15% (1.0 kg/m^2) in comparison to reference mixture. Moreover, by adding 1% and 0.5% basalt fibers, capillary water absorption increased by about 30% and 45% respectively, as compared to the reference mix composition. Fig. 40b, represents the capillary co-

efficient results, which the minimum and maximum co-efficient were recorded around 0.025 kg/m^{2}H$^{0.5}$ and 0.040 kg/m^{2}H$^{0.5}$ for the 0.5% and 1% steel fibers, respectively.

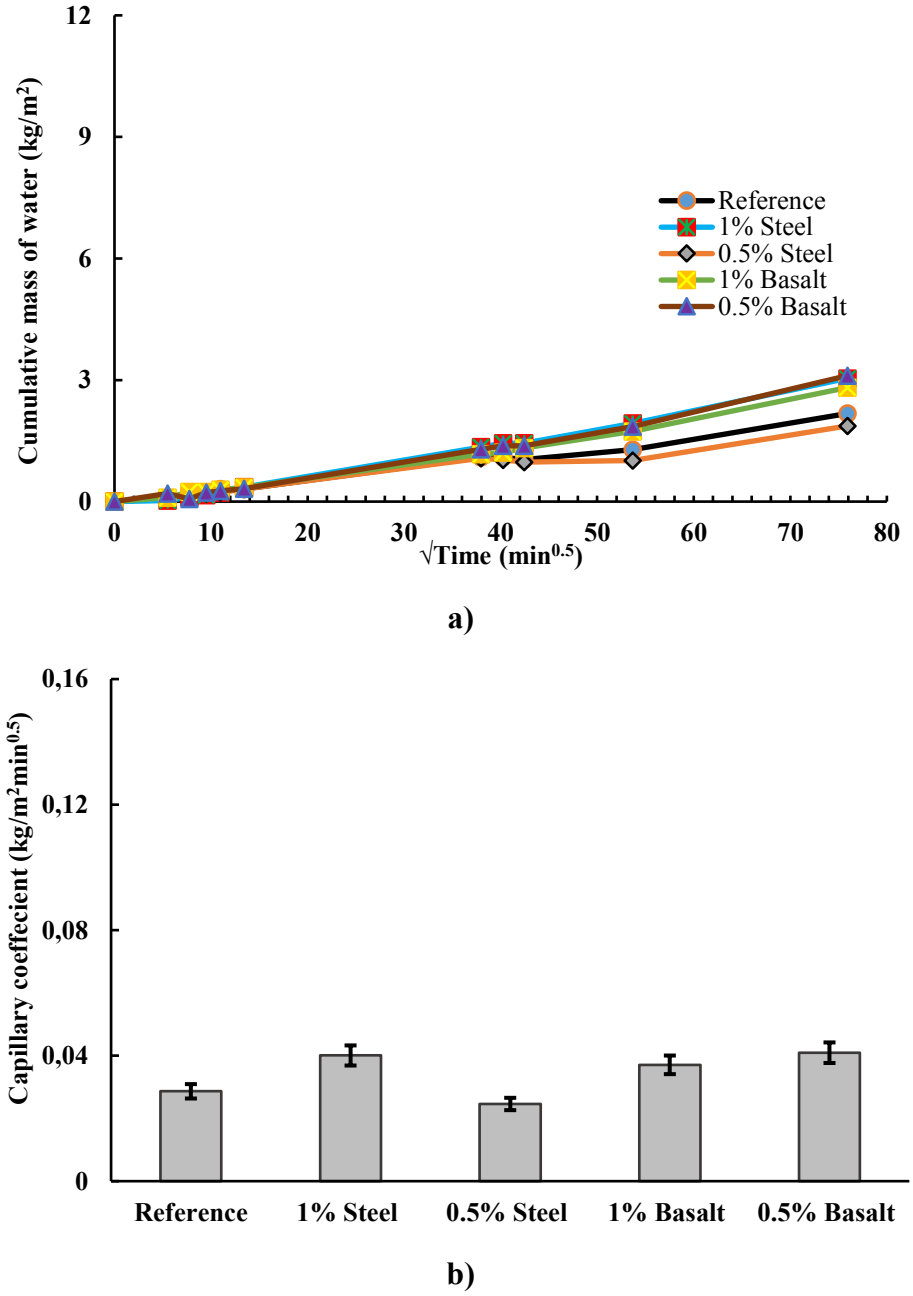

Fig 40. a) Cumulative mass of water in the fiber reinforced mixtures with 20% silica fume; Capillary coefficient of fibers reinforced mixtures 20% silica fume.

4.6 Acid Resistance

The designed mix compositions were submerged in the acidic solution for 7 days in order to investigate the effects of the co-binder on acid resistance. Fig. 41, shows the mass loss for different co-binders which were replacement of soapstone in a total binder. The

obtained values showed that the lime mixtures were dissolved in the acidic solution within few hours. Metakaolin, stone wool and silica fume lost their mass by around 3%, 0.5%, and 0.6%, respectively.

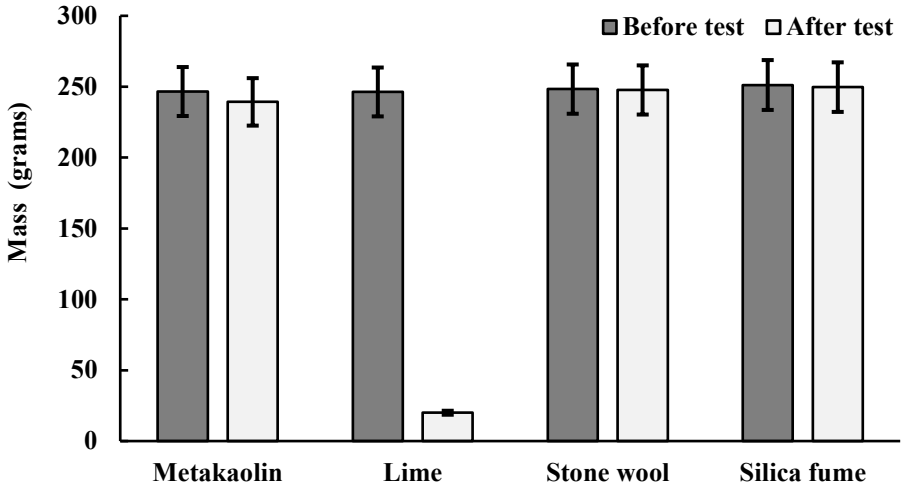

Fig 41. Effect of plain mixtures on acid test.

Fig. 42a, shows the weight loss which was caused due to acid exposure. The plain sample showed 3% weight loss. By employing 1% and 0.5% steel fibers, the mixtures lost their mass around 10% and 35% respectively. In addition, mixtures reinforced with 1% and 0.5% basalt fibers showed only 2% mass loss after 7 days of exposure of acid.

Fig. 42b, shows fibers reinforced samples with 20% metakaolin after the acid test. The plain and reinforced samples with steel fibers decomposed due to acid exposure, conversely, basalt reinforced mixtures were slightly lost their mass, while their structures were stable.

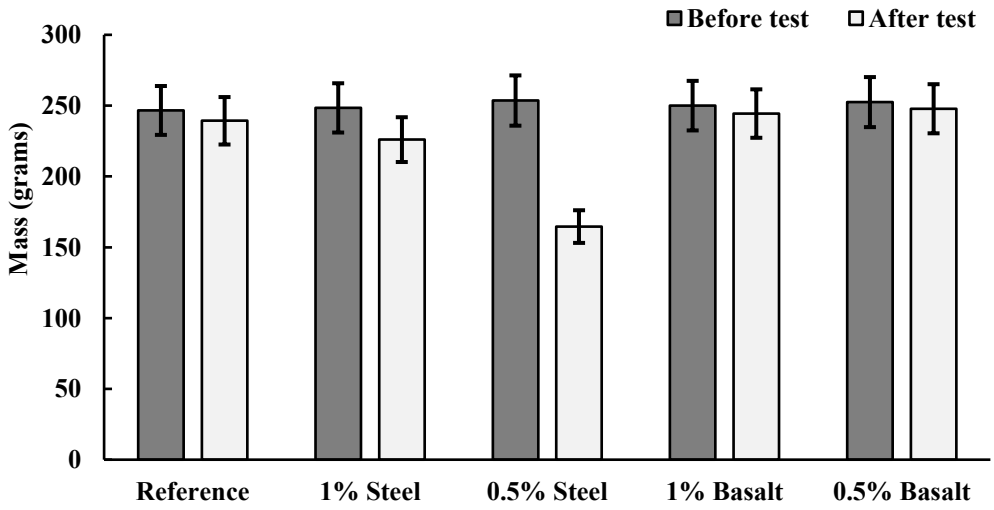

a)

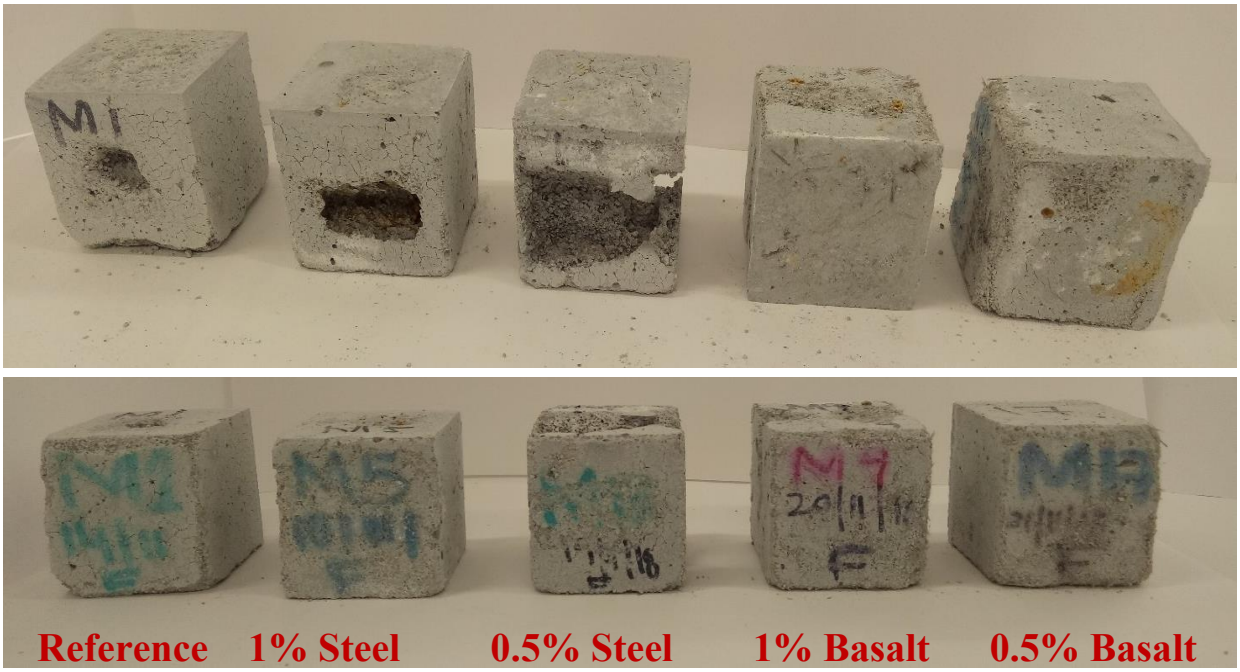

b)

Fig 42. **a)** Acid test results for reinforced mix compositions with 20% metakaolin; **b)** After exposure to acid

Fig. 43a, represents the mass loss of lime mixtures due to acid exposure. The reference specimen was totally dissolved during the test. Mix composition reinforced with 1% steel fibers mass loss was around 25%, and mixture with 0.5% steel fibers mass loss was around 100%. Moreover, by adding 1% and 0.5% basalt fibers, mix compositions lost their mass by approximately 5% and 10%, respectively.

Fig. 43b, represents the visual look the reinforced mixtures with 5% lime, Reference mixture and reinforced mix composition with 0.5% steel fibers were totally dissolved in the acidic solution.

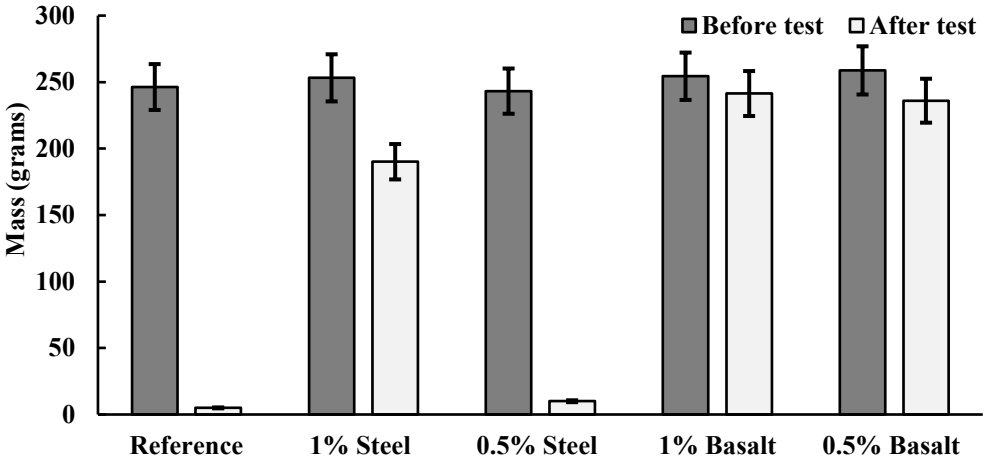

a)

b)

Fig 43. a) Acid test results for reinforced mix compositions with 5% lime**; b)** After exposure to acid.

Fig. 44a, represents the mass loss of mixtures with 20% stone wool due to acid attack. The reference mixture mass loss was approximately 0.2%. Reinforced mixtures with 1% and 0.5% steel fibers lost their mass by 3.5%. Moreover, by adding 0.5% and 1% basalt fibers mixtures lost the mass around 3%. Fig. 44b, shows the samples after the acid test.

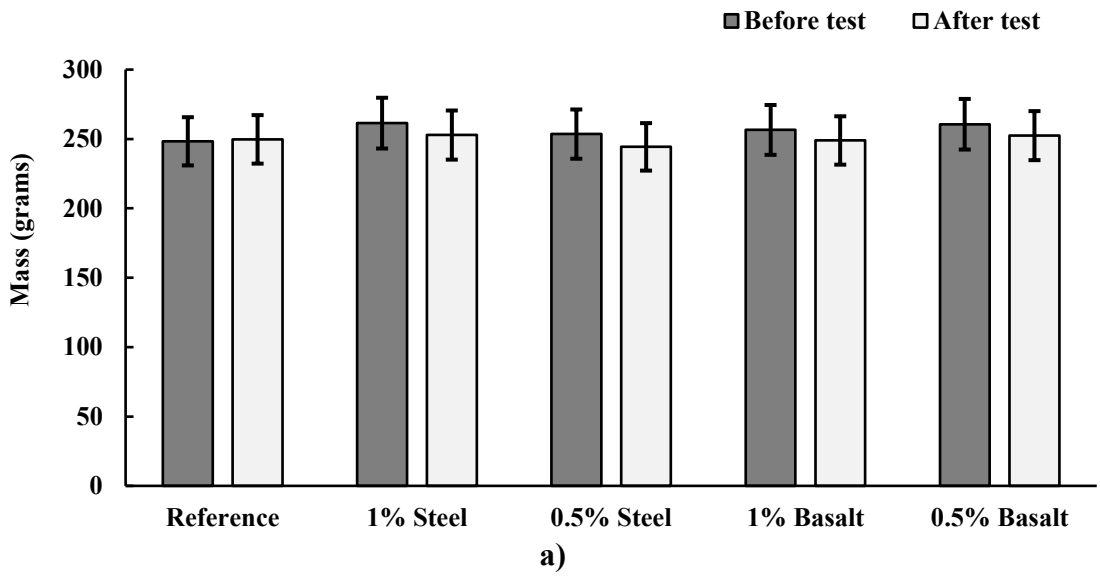

a)

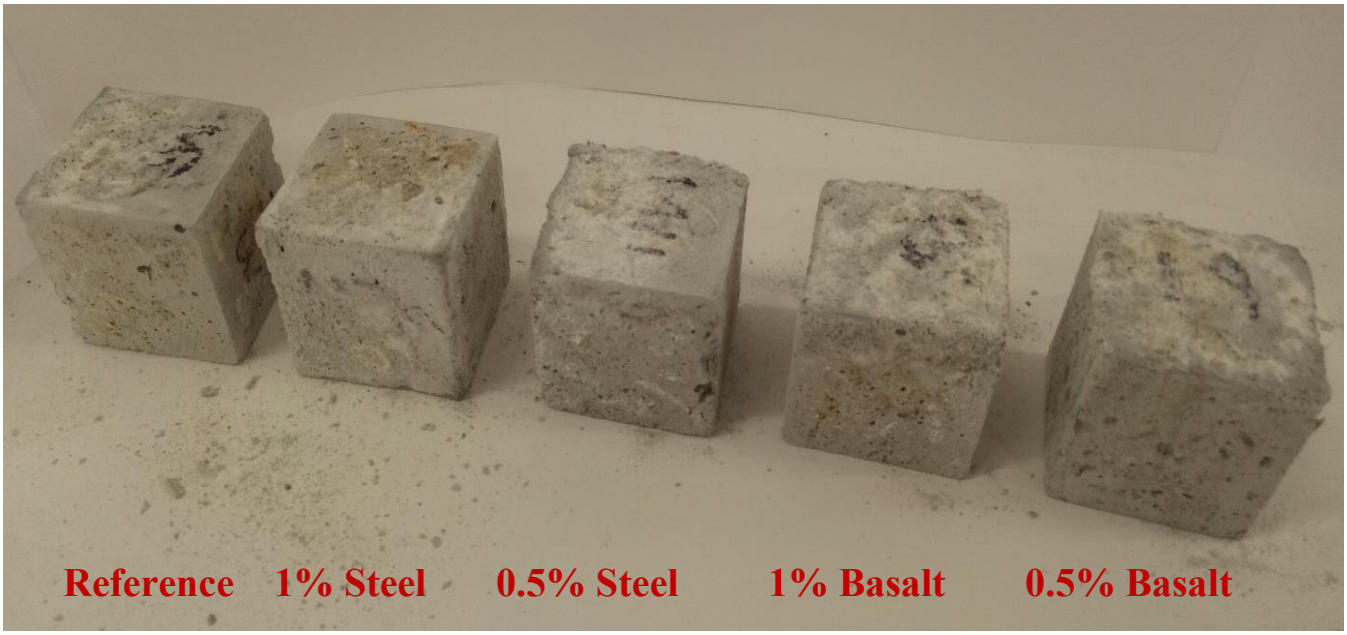

b)

Fig 44. a) Acid test results for reinforced mix compositions with 20% stone wool; **b)** After exposure to acid.

Fig. 45a, represents the mass loss of reinforced mix compositions with 20% silica fume due to acid attack. The reference specimen lost its mass by approximately 0.5%. By employing 1% and 0.5% steel fibers, the mass loss was around 0.2% and 0.05% respectively. While by employing 1% and 0.5% basalt fibers the mass loss reduced to around 0.03% and 0.08%. Fig. 45b shows the tested specimens after acid test.

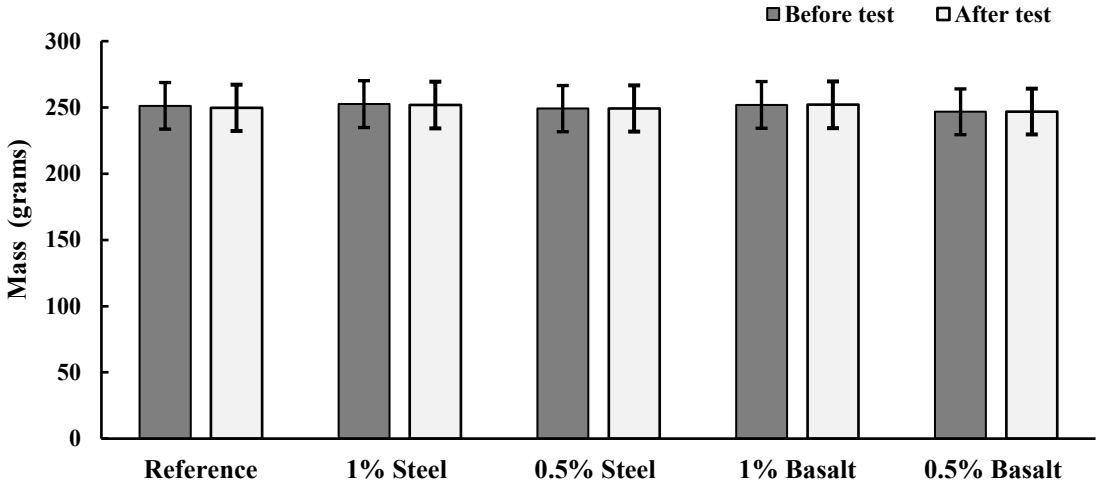

a)

b)

Fig 45. a) Acid test results for reinforced mix compositions with 20% silica fume; **b**) After exposure of acid solution.

4.7 Ultrasonic pulse velocity (UPV)

To presented results showed the effects of using different co-binders on UPV which were partial replaced with soapstone mix compositions. Fig. 46, depicts the results of UPV test of plain mixtures. According to obtained results, the maximum and minimum UPV were recorded around 3540 m/s and 1950 m/s respectively for the mix composition with 20% silica fume and 5% lime.

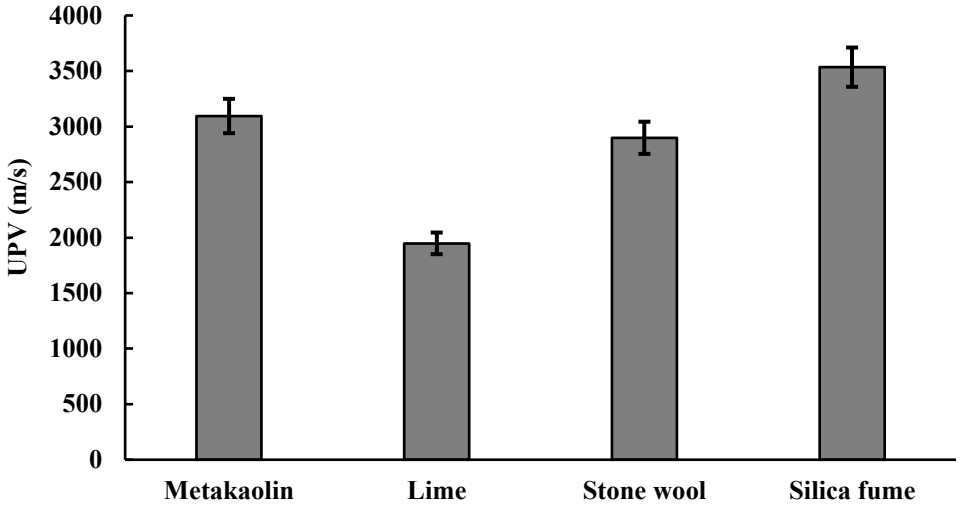

Fig 46. Effects of Plain used co-binders on mixtures on the water absorption.

Fig. 47, shows the effects of using different fibers on the UPV of mixture with 20% metakaolin. The achieved results showed that reinforced mixtures, UPV higher up to 5% as compared to the plain mixture.

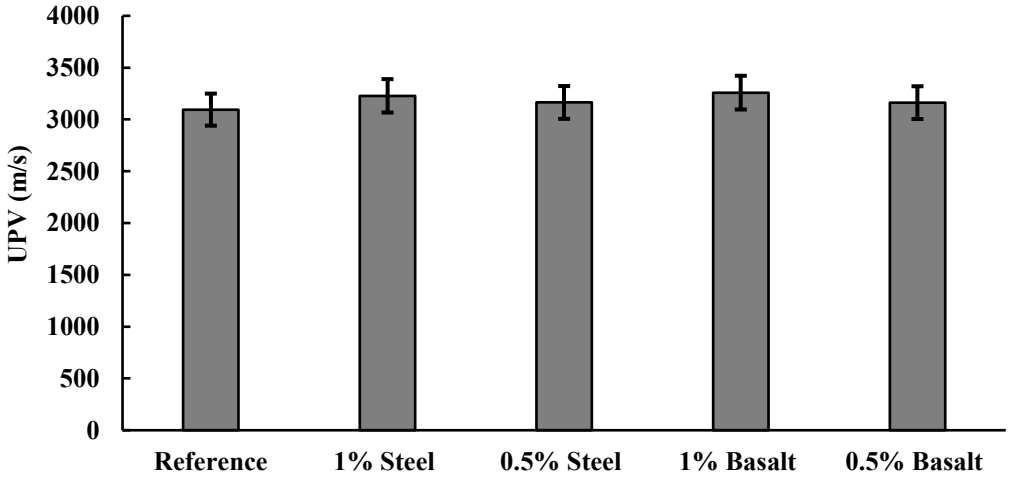

Fig 47. Effects of fibers on the UPV of mixtures with 20% metakaolin as a co-binder.

Fig. 48, shows the effects of using different fibers on the UPV of the mixture with 5% lime. The obtained results showed that mixtures reinforced with 1% and 0.5% basalt fibers were higher around 17% and 23%, respectively as compared to plain mix composition. In addition, mixtures reinforced with 1% and 0.5% steel fibers were around 3% higher UPV as compared to reference mix composition. While, Mastali et al., (2019)

reported that by adding fibers to the mixtures could be led to increase or decrease air voids, for that reason, the UPV could reduce.

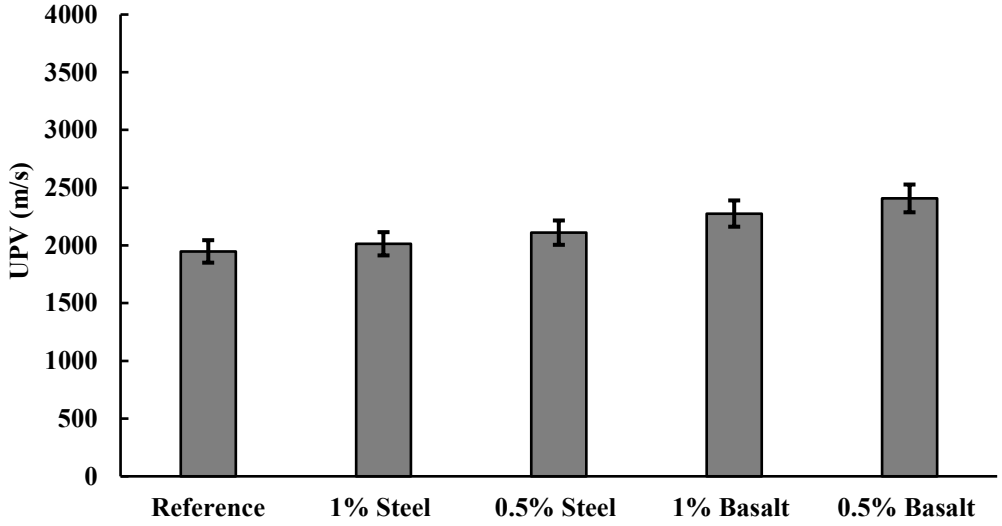

Fig 48. Effects of fibers on the UPV of mixtures with 20% metakaolin as a co-binder.

Fig. 49, shows the effects of using different fibers on the UPV of mixture with 20% stone wool. The obtained results showed that mixtures reinforced with 1% and 0.5% steel fibers were recorded lower UPV by 15% and 12% respectively. Moreover, mixtures reinforced with 1% and 0.5% basalt fibers were recorded 15% and 5% respectively.

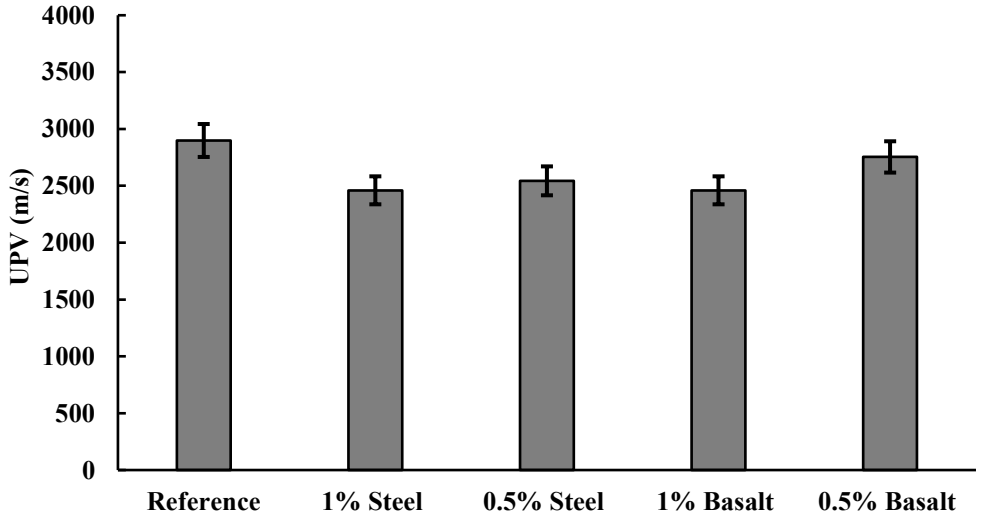

Fig 49. Effects of fibers on the UPV of mixtures with 20% stone wool as a co-binder.

Fig. 50, shows the effects of using different fibers on the UPV of mixture with 20% silica fume. The obtained results showed that mixtures reinforced with 1% and 0.5% steel fibers

were recorded lower UPV around 1%. Moreover, mixtures reinforced with 1% and 0.5% basalt fibers were recorded by 4%.

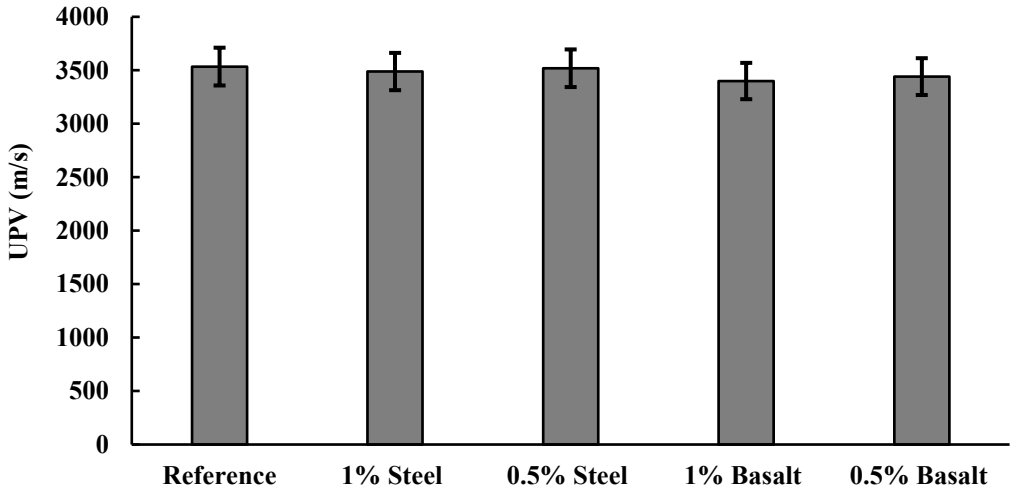

Fig 50. Effects of fibers on the UPV of mixtures with 20% silica fume as a co-binder.

4.8 High temperature properties

To analyze the resistance of designed mix compositions and the effects of different co-binders which were used as a partial replaced of soapstone. In fig. 51a, shows the results of tested samples after samples after exposing to high temperature for 3 hours in 800 ^{o}C which was compared with un-heated mix compositions. The maximum and minimum compressive strength were recorded around 10.5 MPa and 1.5 MPa for the silica fume and lime mix compositions, respectively. The obtained results show that metakaolin mixtures flexural strength reduced around 35% in compared with un-heated mixtures. However, the flexural strength of lime, stone wool and silica mixtures were increased around 5%, 35%, and 200%, respectively. Fig. 51b, shows that the maximum and minimum compressive strength were recorded about 20 MPa and 5.5 MPa for the stone wool and silica fume mixtures, respectively. The attained results showed that, metakaolin based mixture, the flexural strength reduced around 20% compared to un-heated mixture. While, lime and stone wool increased by 20% and 70% respectively, however, silica based mixtures the compressive strength decreased around 35%, in comparison with un-heated mixture.

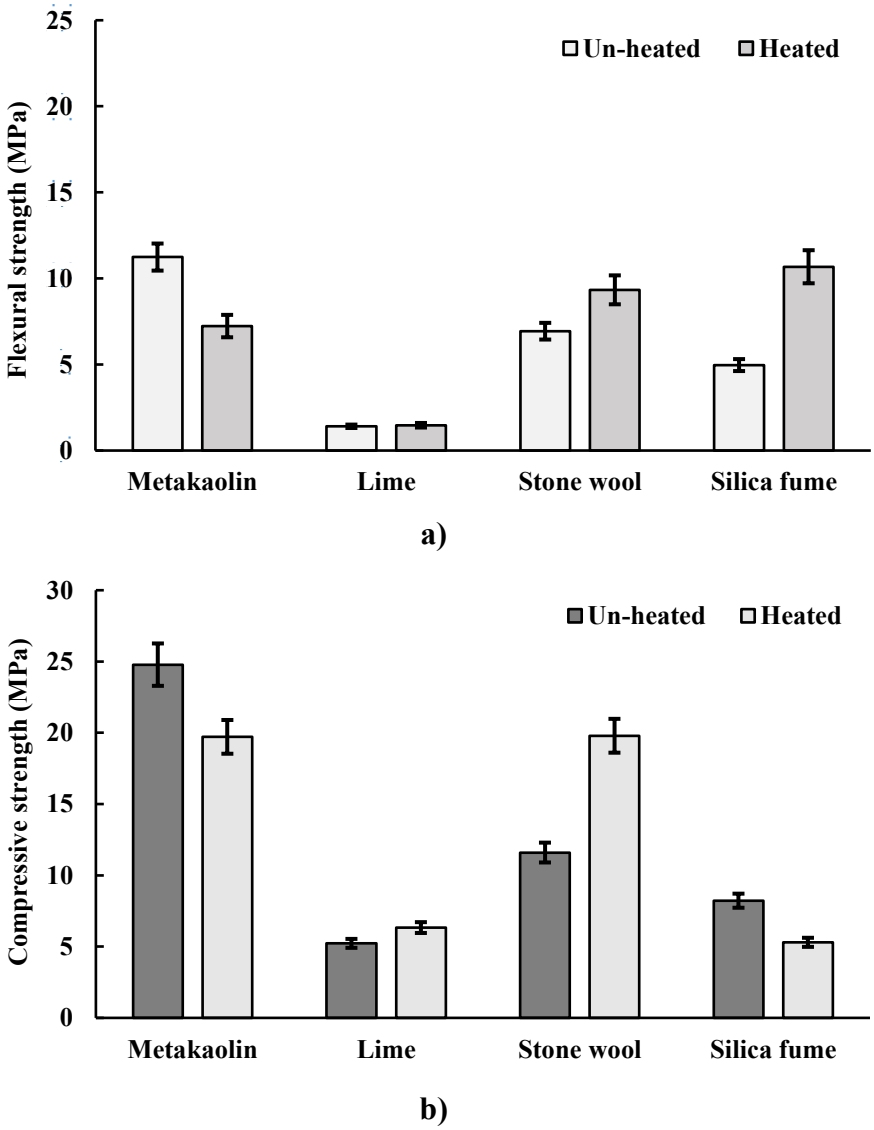

Fig 51. Effects of high temperature on the co-binders: **a)** Flexural strength; **b)** compressive strength after 3 h in 800 ^{o}C.

Fig. 52a, illustrates the effects of high temperature on the flexural strength of the reinforced metakaolin mixtures. The maximum and minimum flexural strength were recorded 9.3 MPa and 7.2 MPa for the mixture reinforced with 1% steel fiber and plain mix composition, respectively. According to the achieved results, the flexural strength were reduced by about 20% by adding 0.5% and 1% steel fibers respectively as compared with un-heated mixtures. Moreover, employing 1% and 0.5%, basalt fibers decreased the compressive strength around 20% respectively. According to the results that fibers types and dosages were not influenced the compressive strength after being exposed to high temperature. Fig. 52b, illustrates the effects of high temperature on the compressive strength of reinforced metakaolin mixtures. The maximum and minimum compressive strength were recorded 20.6 MPa and 15.7 MPa for the mixture reinforced with 1% basalt

fibers and with 0.5% steel, respectively. By adding 1% and 0.5% steel fibers, the compressive strength were reduced by 20% and 35% respectively by comparison with un-heated mix compositions. However, by employed 1% and 0.5% basalt fibers strength were decreased by approximately 25%.

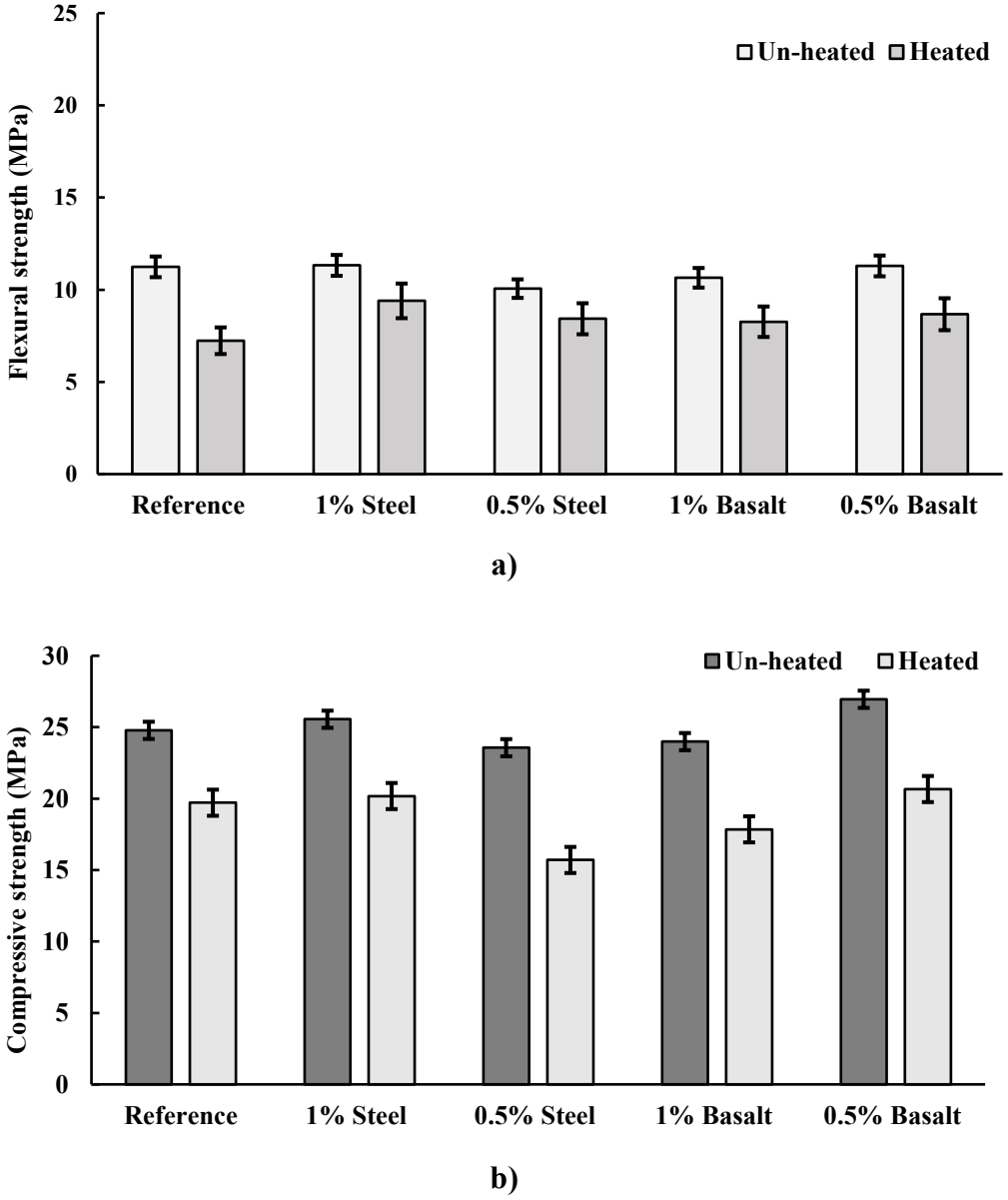

Fig 52. Effects of replacing 20% of soapstone with metakaolin, using various type and dosage of fibers on the exposure to elevated temperature: **a)** Flexural strength; **b)** compressive strength after 3 h in 800 ^{o}C.

Fig. 53a, represents the effects of high temperature on the flexural strength of reinforced lime mixtures. The maximum and minimum flexural strength were recorded 4.7 MPa and 1.4 MPa for the sample reinforced with 1% basalt fibers and plain mix composition, respectively. The results showed that by adding 1% and 0.5%, steel fibers reduced the flexural strength around 5% and 7% respectively. While 1% basalt fibers were decreased

the flexural strength after exposing to high temperature by 25% in compared to un-heated mixture. However, 0.5% basalt fibers increased the strength of around 20% by comparison with un-heated mixture. Fig. 53b, depicts the effects of high temperature on compressive strength of reinforced lime mix compositions. The maximum and minimum compressive strength were recorded 9.4 MPa and 6.3 MPa for the mix composition with 0.5% basalt fibers and plain mix composition, respectively. By adding 1% and 0.5% steel fibers compressive strength increased around 5% compared to un-heated mixtures. Moreover, adding 1% and 0.5% basalt improved the compressive strength by 10% and 25%, respectively in a compare to the un-heated mixtures. Interestingly, it was found that using less basalt fibers led to high temperature after exposing to high temeperature.

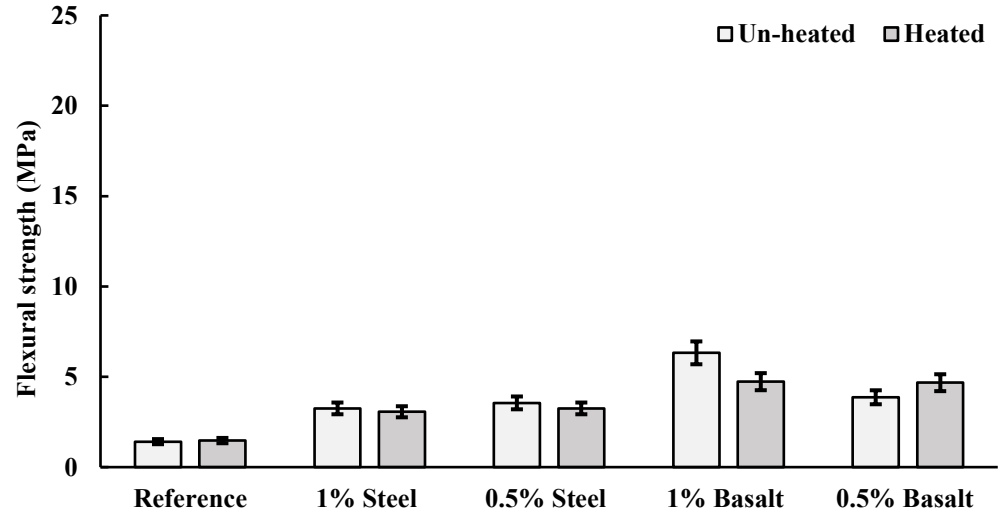

a)

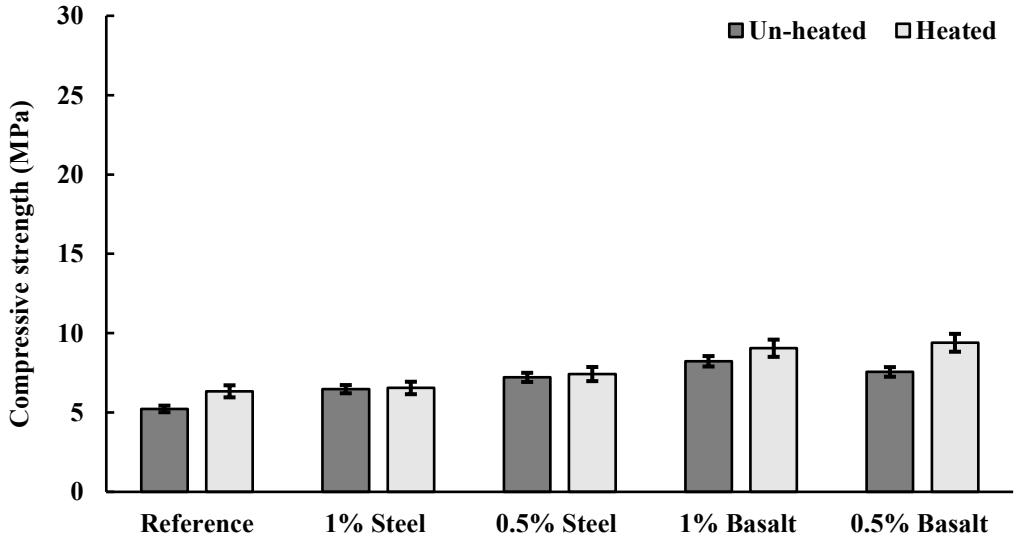

b)

Fig 53. Effects of replacing 5% of soapstone with lime, using various type and dosage of fibers on the exposure to elevated temperature: **a)** Flexural strength; **b)** compressive strength after 3 h in 800 ºC.

Fig. 54a, shows the effects of high temperature on flexural strength of reinforced stone wool samples. The obtained results represented that, the maximum and minimum flexural strength were recorded 10 MPa and 9 MPa for the mixture reinforced with 1% and 0.5% steel fibers, respectively. By adding 1% and 0.5% basalt fibers, flexural strength were increased around 65% and 25% respectively. Moreover, by employing 0.5% and 1% steel fibers 35% and 50% increment were registered, respectively. It showed that increasing basalt fibers from 0.5% to 1% resulted in improving the strength of samples after exposing to high temperature.

Fig. 54b, illustrates the effects of high temperature on the compressive strength of reinforced stone wool samples. The obtained results showed that the maximum and minimum compressive strength were recorded 22.7 MPa and 19.2 MPa for the mixture reinforced with 0.5% basalt fibers and 1% steel fibers, respectively. By adding 1% and 0.5% steel fibers compressive strength increased around 90% and 200%, respectively compared to un-heated mixtures. In addition, using 1% and 0.5% basalt fibers led to higher strength around 200% higher than un-heated mix compositions. It was interesting to find that, using a low amount of steel fibers and high amount of basalt fibers resulted in higher compressive strength improvement.

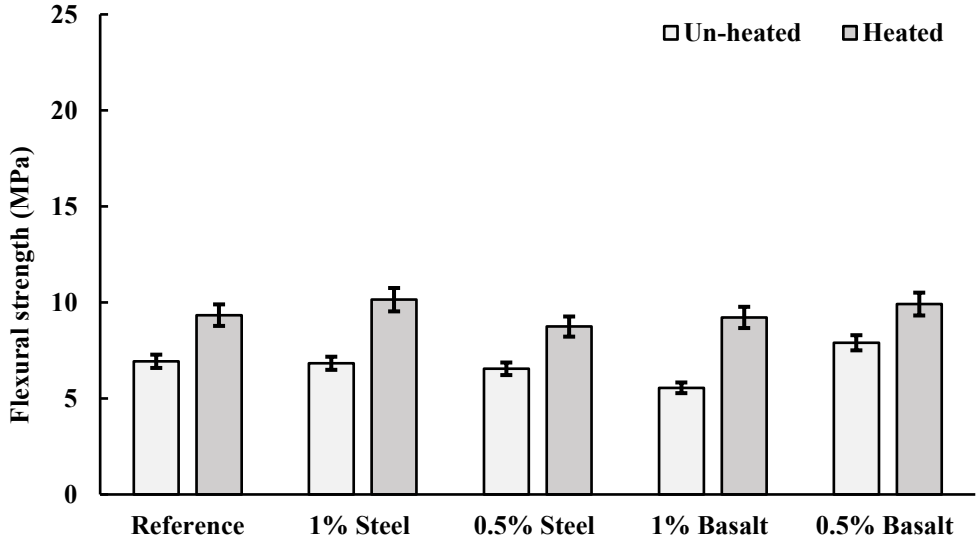

a)

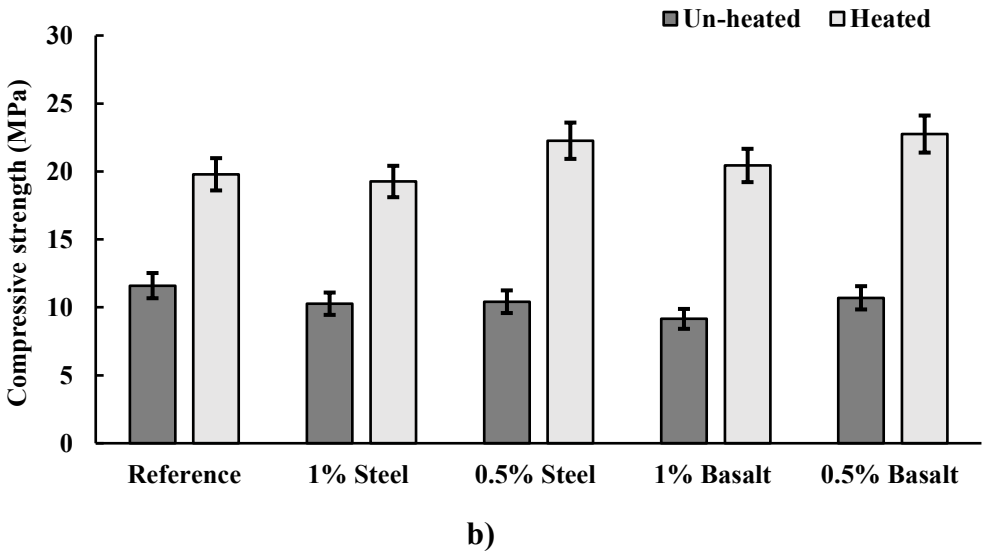

Fig 54. Effects of replacing 20% of soapstone with stone wool, using various type and dosage of fibers on the exposure to elevated temperature: **a)** Flexural strength; **b)** compressive strength after 3 h in 800 ^{o}C.

Fig. 55a, show the flexural strength of reinforced silica fume mixtures. The maximum and minimum flexural strength were recorded 10.6 MPa and 19.2 MPa for the plain mixture and mixture reinforced with 0.5% basalt fibers, respectively. According to the obtained results represented, the flexural strength were increased around 30% and 40% by adding 1% and 0.5 steel fibers, respectively. On the other hand, by employing 1% basalt fibers the flexural strength were decreased around 5%, while adding 0.5% basalt fibers increased the strength of 15% in compared to un-heated mixtures. Interestingly, it was found that using less amount of steel fibers could lead to better in terms of the resistance of the sample to high temperature. Fig. 55b, illustrates the effect of high temperature on the compressive of the reinforced silica mixtures. The maximum and minimum compressive strength were recorded around 10 MPa and 7 MPa for the mixtures reinforced with 1% basalt and 0.5% steel fibers mix compositions, respectively. The results showed that 1% of steel fibers increased the compressive strength by 12% compared to un-heated reinforced mixture, however, by adding 0.5% steel fibers, the strength were reduced around 25%. In addition, by adding 1% and 0.5% basalt fibers, compressive strength decreased by 1% and 17%, respectively.

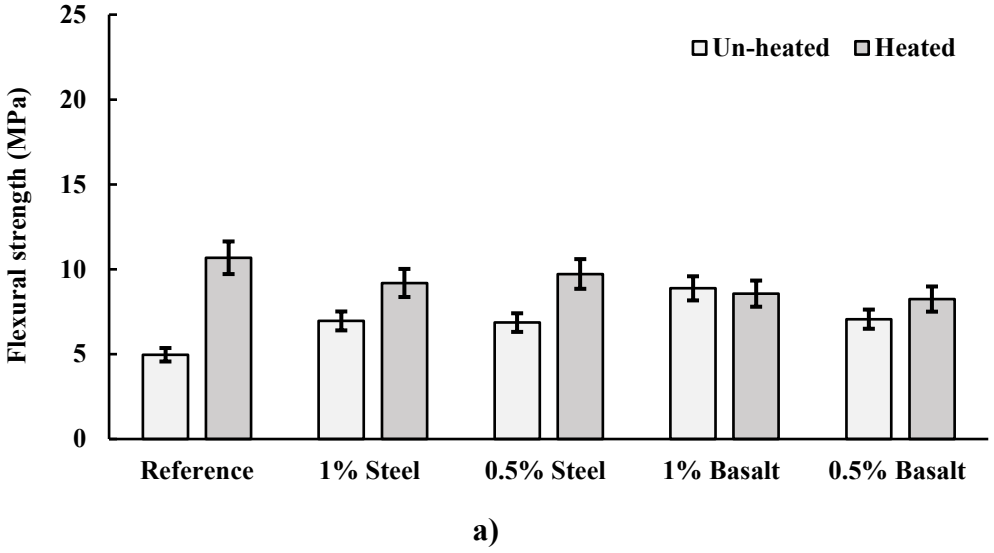

a)

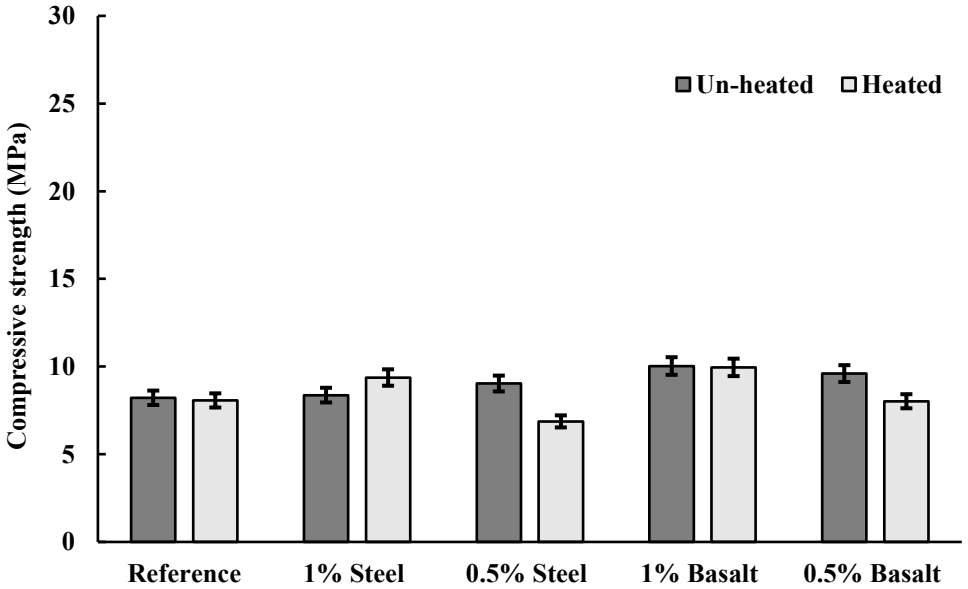

b)

Fig 55. Effects of replacing 20% of soapstone with silica fume, using various type and dosage of fibers on the exposure to elevated temperature: **a)** Flexural strength; **b)** compressive strength after 3 h in 800 ºC.

4.9 Carbonation

To evaluate the effects of carbonation on the flexural strength with different co-binders which were used as partial replaced of soapstone. Fig. 56a, shows the results of tested samples after exposing to carbonation chamber for 7 days which was compared with un-carbonized mixtures. The maximum and minimum flexural strength were recorded around 19 MPa and 2.5 MPa for the metakaolin and lime mixtures respectively. The metakaolin and lime plain mixtures, the flexural strengths were increased by around 70% higher in compared with un-carbonized mixture. Similarly, stone wool and silica fume

mix compositions, flexural strengths improved approximately by 80% and 100%, respectively compared to un-carbonized mixtures. Fig. 56b, shows the results of the carbonation effects on the compressive strength. The maximum and minimum compressive strength were recorded around 27.5 MPa and 7.5 MPa for the metakaolin and lime mixture, respectively. The achieved results showed that metakaolin mixture were recorded the highest compressive strength compared to other co-binders. Furthermore, In the silica fume mixture, compressive were increased by approximately 100%. By comparing the compressive strengths with un-carbonized and carbonized mixtures, lime and stone wool mixtures were improved by 40% and 60%, respectively.

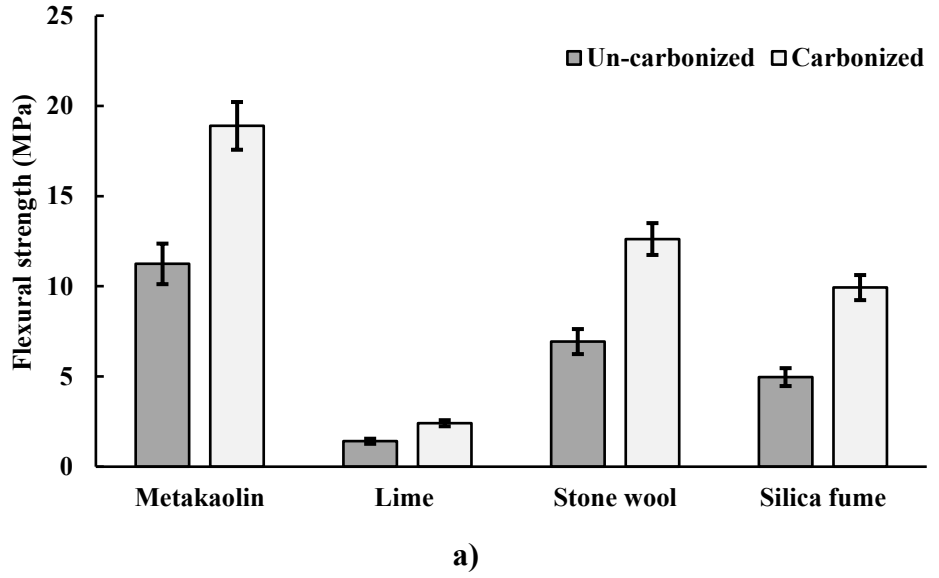

Fig 56. The effects of carbonation on using different co-binders: **a)** Flexural strength; **b)** Compressive strength.

Fig. 57a, illustrates the results of exposure of carbonation on the flexural strength of the reinforced metakaolin samples. The maximum and minimum flexural strength were recorded around 25 MPa and 18 MPa for the mixtures reinforced with 1% basalt fibers and 1% steel fibers, respectively. By adding 1% and 0.5% steel fibers, flexural strength were increased around 60% and 90%, respectively compared to un-carbonized mix compositions. Likewise, by using 1% and 0.5% basalt fibers flexural strength were increased by 230% and 90% respectively as compared to un-carbonized mix compositions. It was showed that by using higher amount of basalt fibers and lower amount of steel fibers could be influenced to get great improvement in strength.

Fig. 57b, illustrates the results of exposure to carbonation on the compressive strength of the reinforced metakaolin specimens. The maximum and minimum compressive strength were recorded around 31 MPa and 23 MPa for the mixture reinforced with 1% basalt and 0.5% steel fibers based mixtures, respectively. By using 1% and 0.5% steel fibers, the compressive strength were increased and decreased, respectively around 5% by comparison with un-carbonized mixtures. Moreover, by adding 1% and 0.5%, basalt fibers were increased the strength by 30% and 10% respectively. Remarkably, it was found that steel fibers dosages were not influenced to get higher strength. While basalt fibers were recorded highest strength, also dosages of fibers could be influenced to lead higher compressive strength.

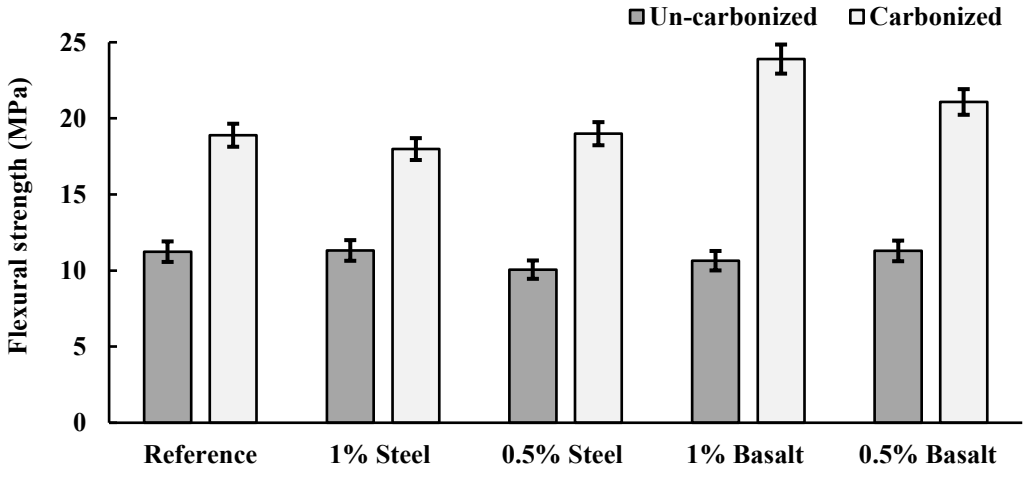

a)

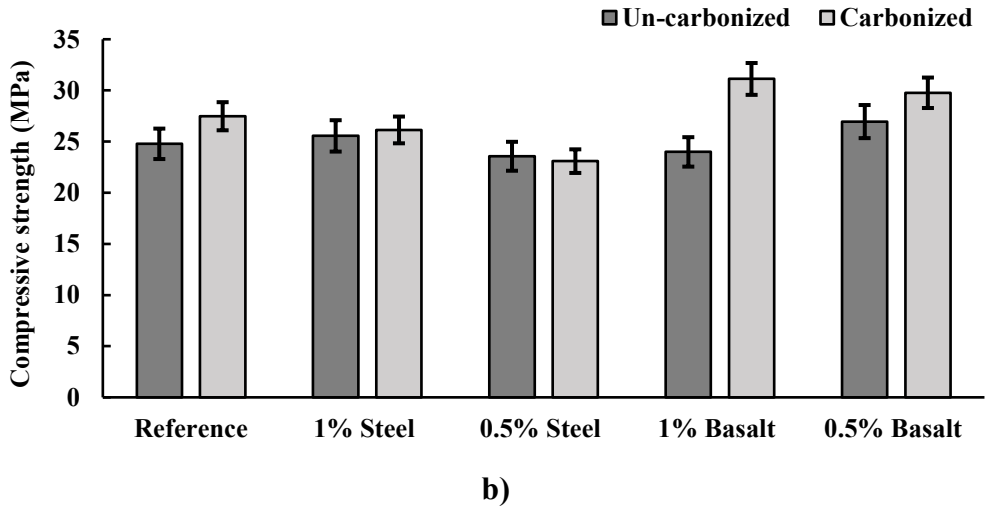

Fig 57. Effects of replacing 20% of soapstone with metakaolin, using various type and dosage of fibers on the carbonation: **a)** Flexural strength; **b)** compressive strength.

Fig. 58a, depicts the results of exposure to carbonation on the flexural strength of reinforced lime mixtures. The maximum and minimum flexural strength were recorded around 9.5 MPa and 2.5 MPa for the mixture reinforced with 1% basalt fibers and plain mix composition, respectively. According to the attained results showed, by adding 1% and 0.5% steel fibers the flexural strength were improved around 230% and 50%, respectively as compared to un-carbonized mixtures. Furthermore, by employing 1% and 0.5% basalt fibers, the strength were improved by 45% and 90%, respectively as compared to un-carbonized mix compositions. Moreover, it was interesting to find that a high amount of steel fibers were improved on their strengths due to high amount, while basalt had improved their strength due to less amount of fibers. Fig. 58b, illustrates the effects of carbonation on the compressive strength of the lime reinforced mixtures. The maximum and minimum compressive strength were recorded around 10.5 MPa and 7.5 MPa for the mixture reinforced with 1% basalt fibers and plain mixture respectively. Likewise, by employing 1% and 0.5% steel fibers the compressive strengths were increased by 35% compared to un-carbonized mixtures. On the other hand, by adding 1% and 0.5%, basalt fibers were improved the strength by 25%, respectively. It was found that fibers were influenced to get higher strength, however, dosages of fibers were low influenced on the compressive strength.

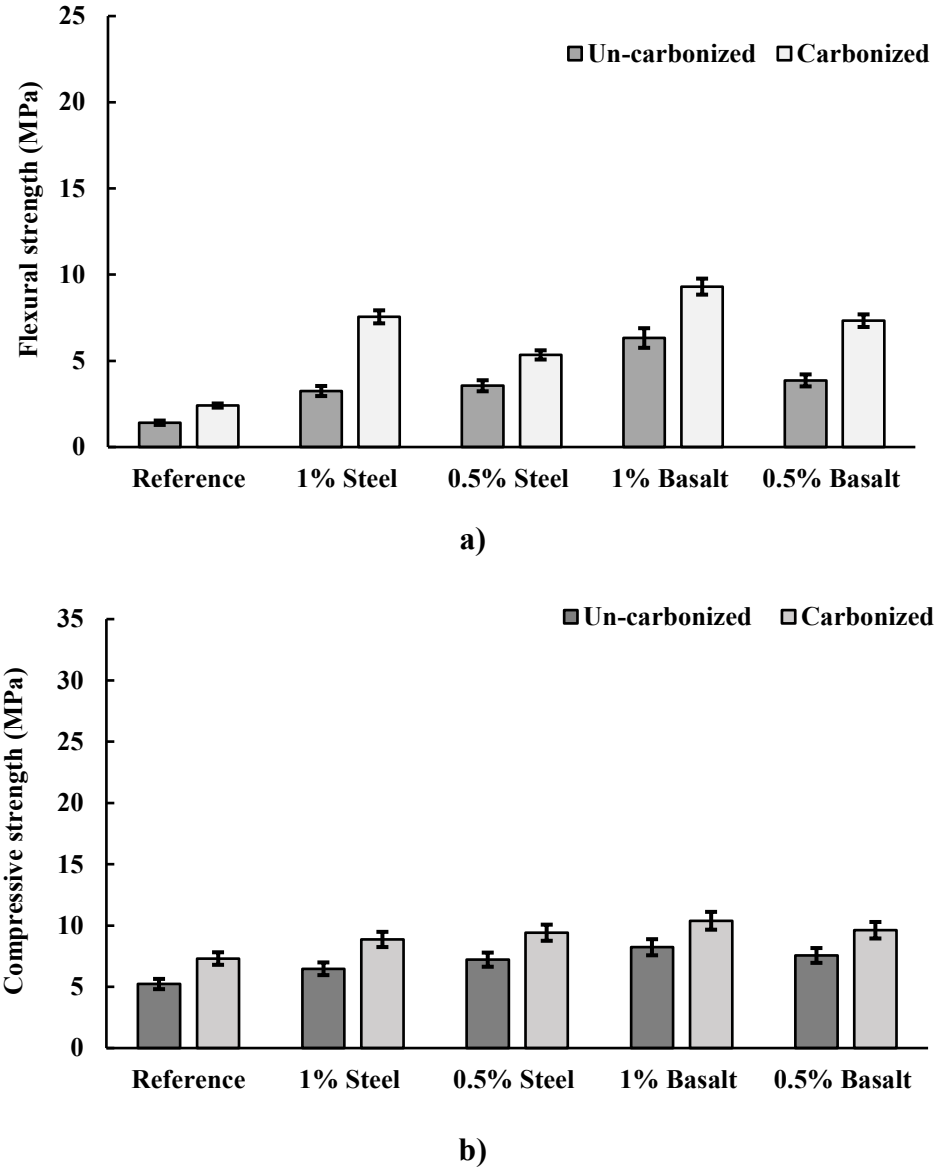

Fig 58. Effects of replacing 5% lime of soapstone with lime, using various type and dosage of fibers on the carbonation: **a)** Flexural strength; **b)** compressive strength.

Fig. 59a, depicts the results of exposure to carbonation effect on the flexural strength of reinforced stone wool mixtures. The maximum and minimum flexural strength were recorded around 16.5 MPa and 11 MPa for the mixtures reinforced with 0.5% basalt fibers and 0.5% steel fibers, respectively. The achieved results showed by adding 1%, and 0.5% of steel fibers, flexural strength were increased around 65% compared to un-carbonized mixtures. Likewise, 1% and 0.5% basalt fibers were improved by 230% and 200%, respectively compared to un-carbonized mixtures. Additionally, it was interesting to find that adding higher amount of basalt fibers were influenced to get higher strength, however, the amount of steel fibers was slightly influenced to enhance the strength. Fig. 59b, depicts the results of carbonation exposure on the compressive strength of reinforced

stone wool mixtures. The maximum and minimum compressive strength were recorded around 18.5 MPa and 14 MPa for the plain mix compositions and reinforced with 0.5% steel fibers. The achieved results showed by adding 1% and 0.5% steel fibers compressive strengths were improved around 55% and 35%, respectively compared to un-carbonized mixtures. On the Contrary, 1% and 0.5% basalts fibers were increased by 70% as compared to un-carbonized mix compositions. Additionally, it was interesting to find that by using either 1% or 0.5% basalt fibers, compressive strength were slightly improved, while higher amount of steel fibers could be led to higher strength after exposing to carbonation.

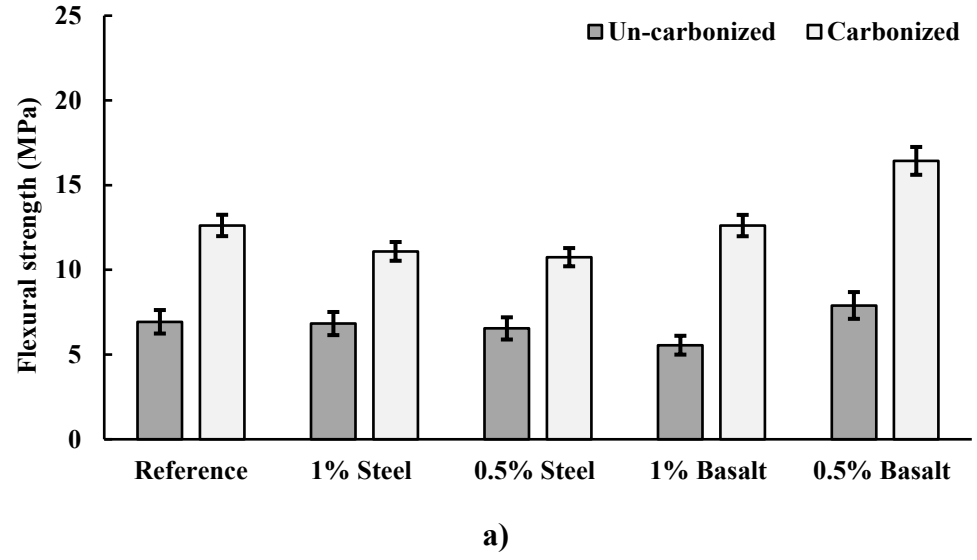

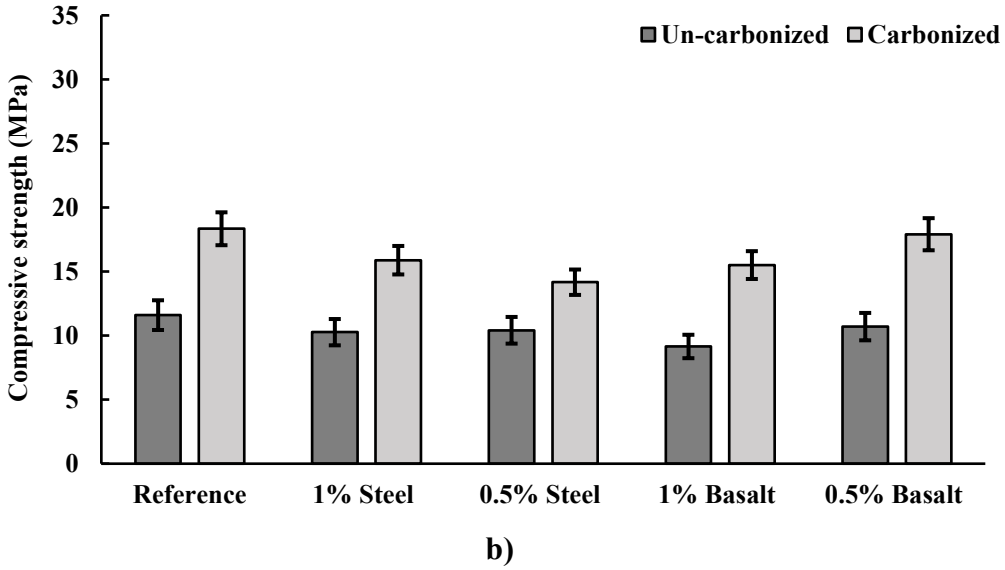

Fig 59. Effects of replacing 20% of soapstone with stone wool, using various type and dosage of fibers on the carbonation: **a)** Flexural strength; **b)** compressive strength.

Fig. 60a, shows the carbonation effects on the flexural strength for the reinforced silica fume mixtures. The obtained results showed great improvement when comparing with un-carbonized samples. The maximum and minimum flexural strength were recorded around 15 MPa and 10 MPa for the mixture reinforced with 1% steel fibers and plain mix composition. By using 0.5% and 1% steel fibers, flexural strength were improved around 70% and 200%, respectively in a compare to un-carbonized. Moreover, by adding 1% and 0.5% basalt fibers strength were improved around 55% to 75%, respectively. Interestingly, it was found that, by adding higher amount steel fibers could lead to great improvement. After exposing to carbonation. Fig. 60b, depicts the results the effects of carbonation on the compressive strength of reinforced silica fume mix compositions. The maximum and minimum compressive strength were recorded around 18 MPa and 17 MPa for the reinforced with 1% basalt fibers and plain mix compositions. The achieved results showed that by adding 1% and 0.5% steel fibers compressive strengths were improved around 100% and 90%, respectively compared to un-carbonized mixtures. Furthermore, by adding 1% and 0.5% basalts fibers, the compressive strength were increased by 75% and 90% as compared to un-carbonized mix compositions. Additionally, it was found that dosages of steel fibers did slightly effect on compressive strength.

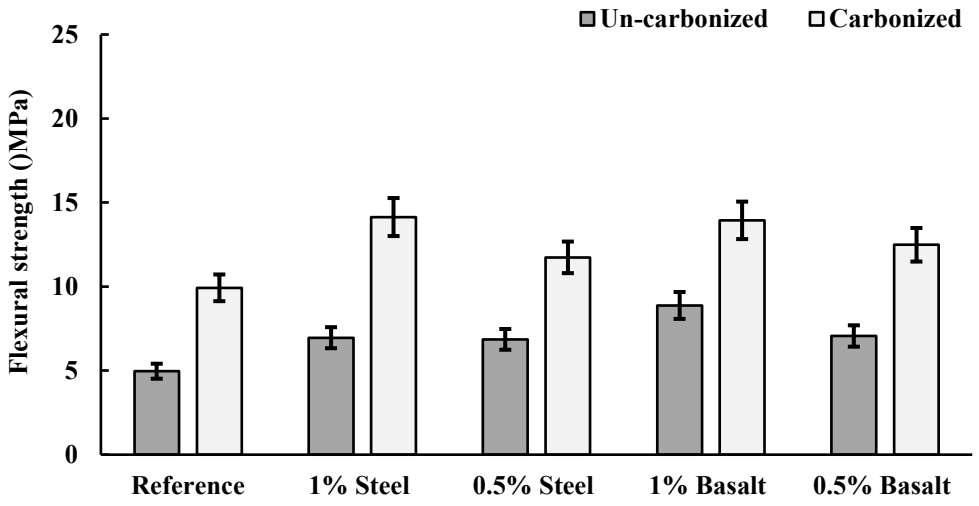

a)

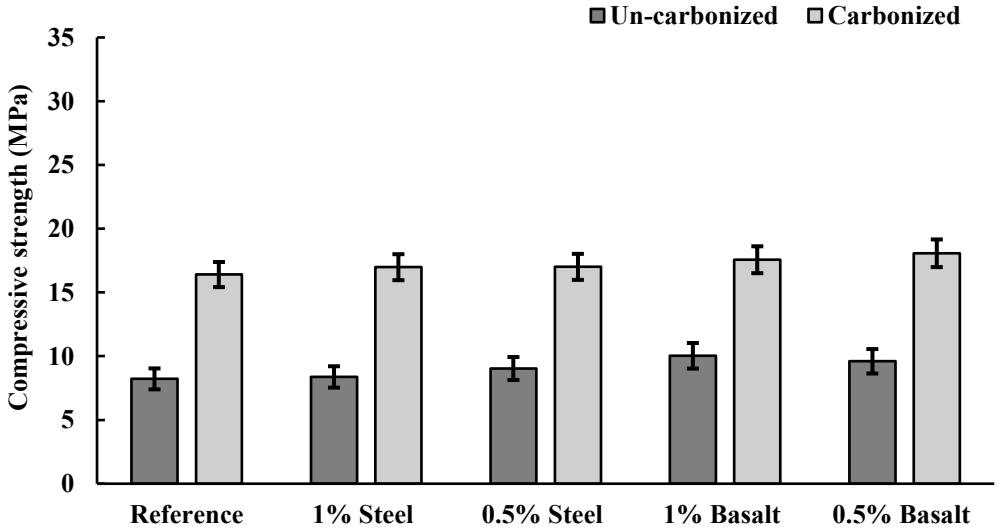

Fig 60. Effects of replacing 20% of soapstone with silica fume, using various type and dosage of fibers on the carbonation: **a)** Flexural strength; **b)** compressive strength.

4.10 Thermogravimetric analysis and differential thermogravimetry analysis

The TGA and DTG curves of the designed mix compositions of alkali-activated pastes at 28 days are illustrates in Fig. 61, the mass loss and noticeable DTG peaks of the co-binders which were partial replaced of soapstone. During TGA analysis, mass loss was observed at 100 ºC to 800 ºC (Luukkonen et al., 2019). Masse et al., 1993 reported that, the free water and structurally bond water which are existed in the mixture. The free water is vaporized at 100 ºC. However, the weight loss was examined at a temperature from 100 ºC to 800 ºC is recognized to the structural water. Moreover, the rate of mass loss becomes slowdown 250 ºC onwards due to chemically bonded and OH groups (Nath et al., 2016). The first destructive, second and third peak could be recognized to the C-S-H gel, portlandite and calcite, respectively.

According to the achieved curves shows three major endothermic peaks. The first, second and third peaks are destructed approximately 150 ºC, 580 ºC, and 730 ºC, respectively. The stone wool mixture lost its mass higher in compare to other co-binders. Whereas, metakaolin lost mass around 2% in compare to lime and silica fume. The maximum and minimum mass loss were recorded around 14% and 12% respectively.

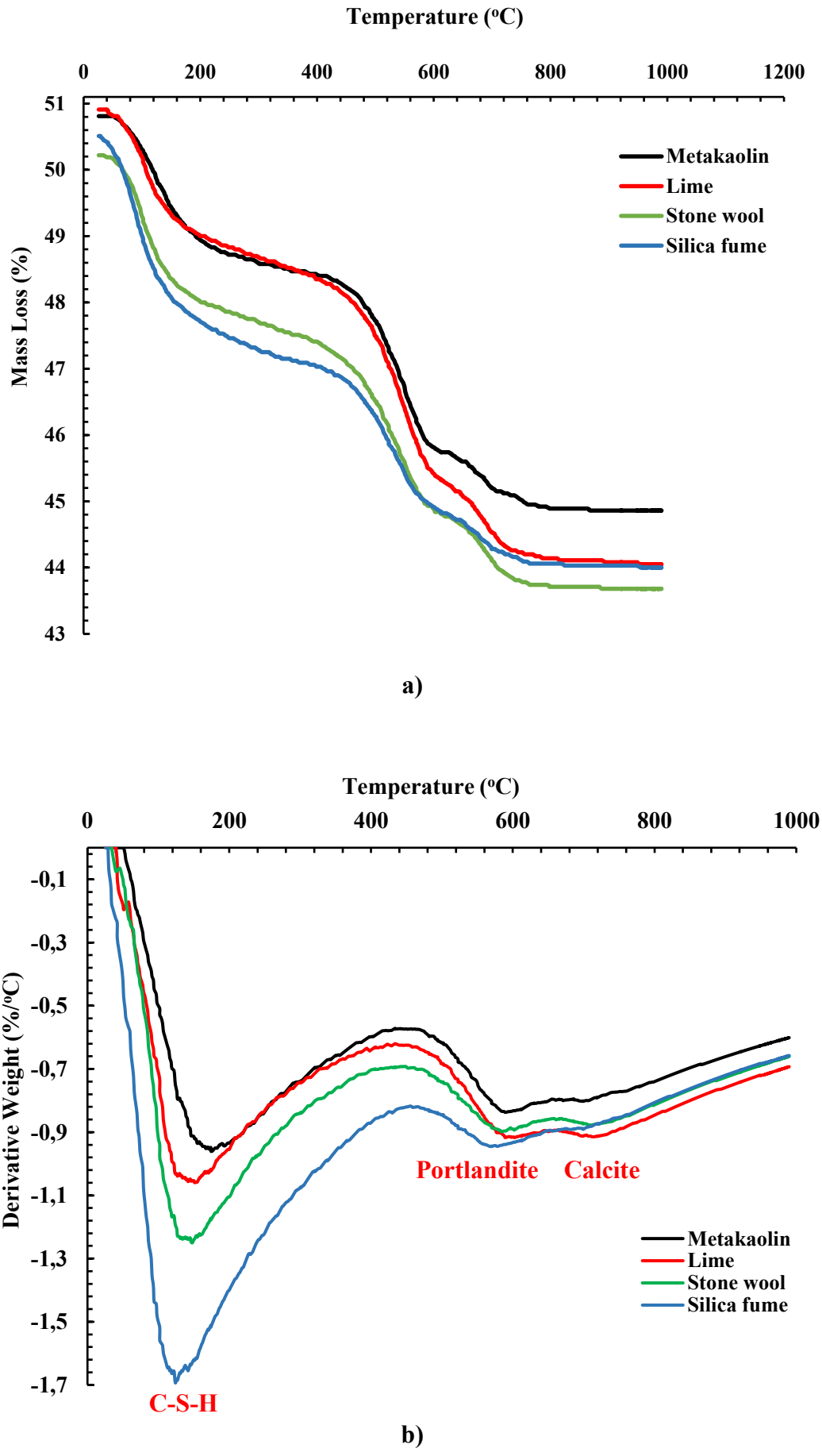

Fig 61. a) TGA analysis of replacing soapstone by four different co-binders; **b)** DTG analysis of replacing soapstone by four different co-binders

4.11 Efflorescence assessment

To visual monitoring of using different co binders on efflorescence with different fibers. Fig. 62, shows the designed mix compositions to observing the efflorescence. Rows are used to indicate types and dosages of fibers, while columns are represented the co-binders. According to Fig. 62a, it was not found any certain efflorescence while monitoring in the various mix compositions except stone wool mixtures. Furthermore, in Fig. 62b, the reinforced mixtures with 0.5% basalt fibers were high efflorescence compared to the reference mix composition.

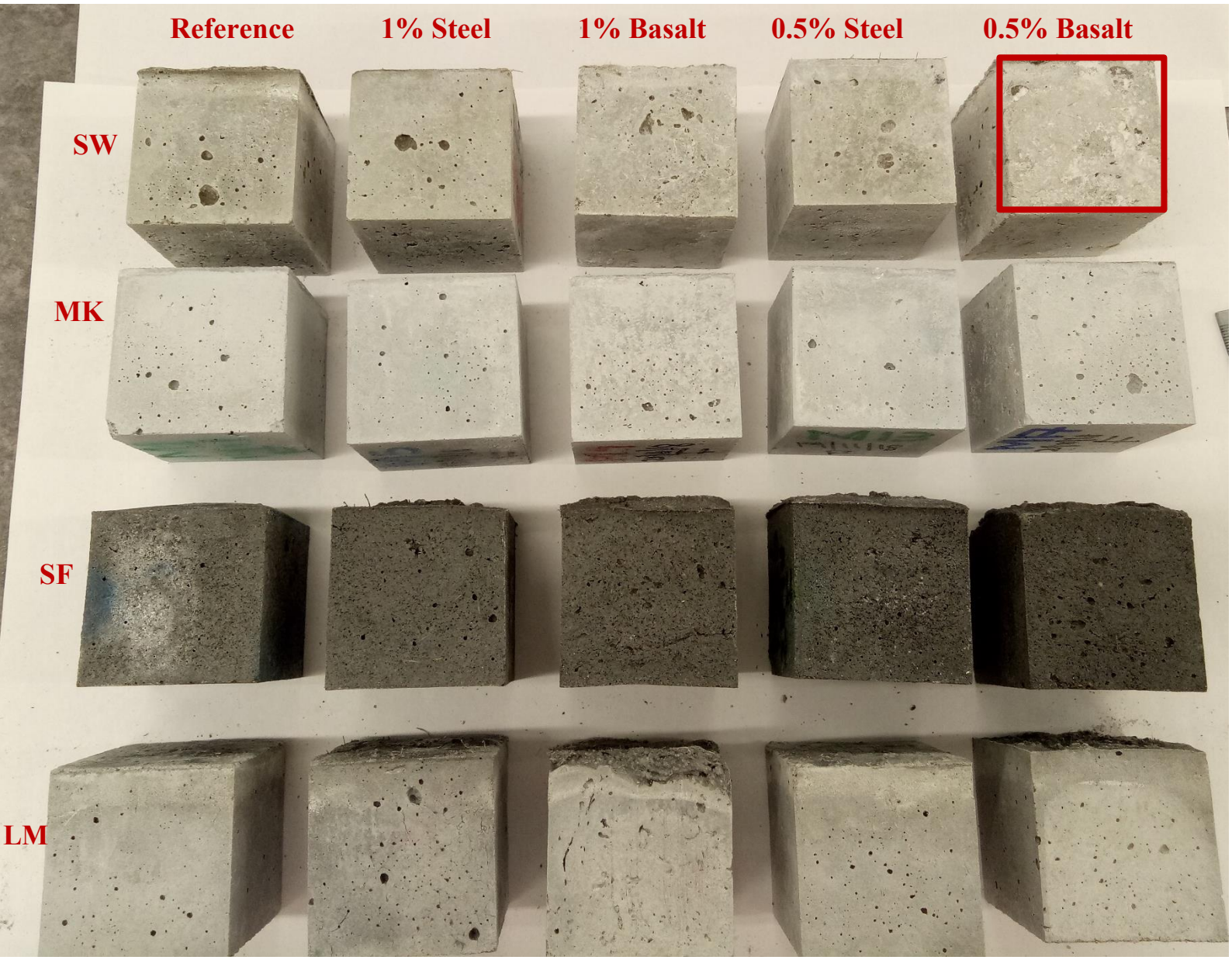

a)

MK* = Metakaolin
LM* = Lime
SW* = Stone wool
S F* = Silica fume

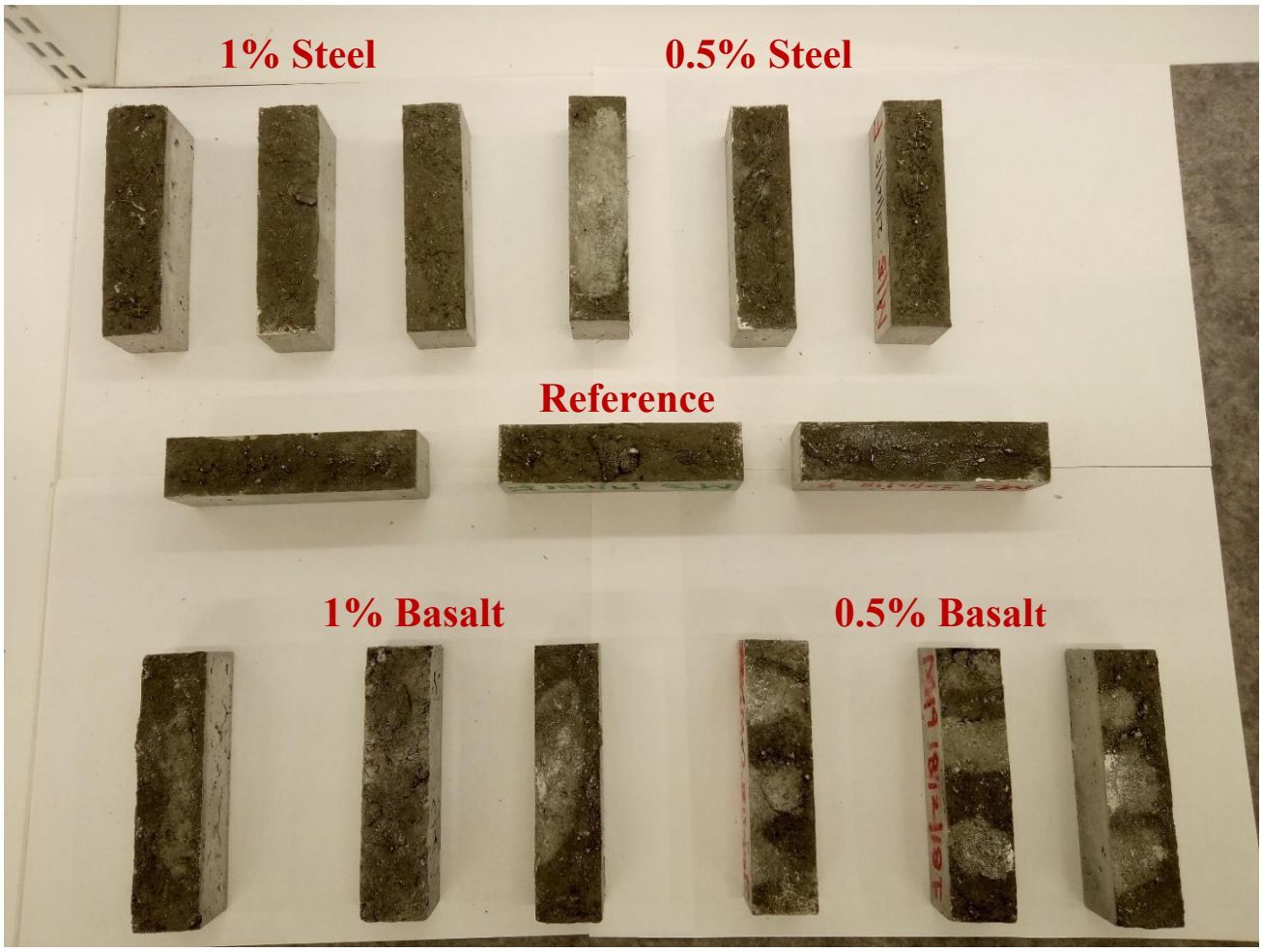

b)

Fig 62. a) Efflorescence observation between co-binders; **b)** By visual analyzing the efflorescence in the stone wool mix compositions.

5. CONCLUSIONS

This investigation reported on the effects of replacement of soapstone with different co-binders. In this study, there are four different co-binders (i.e., metakaolin, lime, stone wool and silica fume) which were partial replaced with soapstone. The effects were investigated through hardened properties at 28 days. The subsequent conclusions can be made:

— Regarding both flexural and compressive strength, metakaolin mixtures were registered the highest strength around 11.5 MPa and 25 MPa, respectively. Generally, addition of fibers had slightly effect on mechanical strength.

— In terms of shrinkage, with 20% metakaolin based mixtures recorded the best results. However, the addition of fibers shrinkage rates were reduced rates up to 80% as compared plain mixture.

— Relating to water absorption, silica fume based mix compositions were recorded lowest absorption amount about 5 times lower in compare to the metakaolin mixtures. By adding steel fibers did not effect on absorption rate, In addition, basalt fibers influenced to lead higher absorption around 38%.

— Concerning apparent porosity, the lowest apparent porosity were recorded around 6% for the silica fume mix composition. Furthermore, the effects of fibers were behaved similar as in water absorption.

— Capillary water absorption, replaced 20% of soapstone with silica fume mixture were recorded the lowest cumulative mass of water around 2.20 kg/m^2. Likewise, by adding less amount of steel fibers could be led to reduce cumulative mass about 15%.

— Relating to Acid resistance, replaced 20% of soapstone with stone wool mix composition recorded best results. Moreover, the addition of higher amount fibers were influenced to reduce mass loss.

— Concerning with UPV, silica fume mixtures were recorded highest around 3535 m/s. In addition, by adding fibers either steel or basalt fibers, UPV was reduced up to 4%.

— Effects of high temperature on the both flexural and compressive strengths after 3 h in 800 ^{o}C, both strengths of stone wool based mixtures were increased. Also, by using less amount of fibers had led to better improvement.

— After exposure of carbonation, the metakaolin based mixtures were improved both flexural and compressive strengths around 19 MPa and 27.5 MPa, respectively. Furthermore, by addition of higher amount of basalt fibers were influenced to great improvement.

— Regarding TGA analysis, the lowest mass loss was recorded in metakaolin mixtures, while rest of co-binders were lost around 2% to 3% higher than metakaolin.

— According to the efflorescence rate, in stone wool mixtures were found efflorescence. However, stone wool mixtures reinforced with basalt fibers were higher rate as compared to other stone wool based mix compositions.

6. FUTURE WORK

This thesis has apportioned with the development of Alkali-activated soapstone waste with partially replacing with different co-binders and using two different fibers in order to an analysis on the hardened properties, several problems might not be discussed due to time restraints. Consequently, the future wok must be carried out to gain a well understanding of the alkali activated magnesium aluminosilcate binders. The presented outcomes show the accomplishments of the performed study. However, additional studies still necessary; the following effort is brief as the recommendations for future work.

- Examine effects of different alkali activators ratios on the hardened properties

- Microstructural analysis has needed to be carried out to study their morphologies.

- While different tests were carried out in this thesis to observe the durability. Still, additional findings are needed to confirm the acid resistance to alkali-activated soapstone binder for an extended time.

- To the development of the soapstone binders with partial replacement of different industrial wastes (i.e., slags and fly ashes etc…) and various type of fibers.

Generally, the key aim of this thesis was to examine the use of waste soapstone to yield construction materials. However, there are still many open questions that need to be assessed before these materials can be commercially exploited.

7. REFERENCES

[1]. Abdollahnejad. Z, T. Luukkonen, M. Mastali, J. Yliniemi J, P. Kinnunen, M. Illikainen, (2018) 'Development Alkali-activated aluminosilicate binders from Soapstone magnesium', pp. 1–8

[2]. Abdollahnejad, Z., Mastali, M., Luukkonen, T., Kinnunen, P., Illikainen, M., (2018). Fiber-reinforced one-part alkali-activated slag/ceramic binders. Ceramics International.

[3]. Adam A. A. & X. X. X Horianto, (2014), 'Procedia engineering', vol. 95, pp. 410-414.

[4]. Al Bakria, A. M., Kamarudin, H., BinHussain, M., Nizar, I. K., Zarina, Y., & Rafiza, A. R. (2011). The effect of curing temperature on physical and chemical properties of geopolymers. Physics Procedia, 22, 286-291.

[5]. Alomayri, T., Shaikh, F.U.A. & Low, I.M. 2014a, "Synthesis and mechanical properties of cotton fabric reinforced geopolymer composites", Composites Part B: Engineering, vol. 60, pp. 36-42.

[6]. Araújo, M. De (2011) '1 - Natural and man-made fibers: Physical and mechanical properties', in Fangueiro, R. (ed.) Fibrous and Composite Materials for Civil Engineering Applications. Woodhead Publishing (Woodhead Publishing Series in Textiles), pp. 3–28. doi: https://doi.org/10.1533/9780857095583.1.3.

[7]. ASTM C116-90. Standard test method for compressive strength of concrete ASTM International, West Conshohocken, 2010.

[8]. ASTM C78. Standard test method for flexural strength of concrete (using simple beam with third-point loading). West Conshohocken, PA: ASTM International; 2010. USA. www.astm.org.

[9]. ASTM C157. Standard test method for drying shrinkage of concrete, ASTM International, West Conshohocken, 2015.

[10]. ASTM C1585, Standard Test Method for Measurement of Rate of Absorption of Water by Hydraulic Cement Concretes, ASTM International, West Conshohocken, PA, 2013.

[11]. Benhelal, E., Zahedi, G., Shamsaei, E., Bahadori, A., 2013. Global strategies and potentials to curb {CO}2 emissions in cement industry. J. Clean. Prod. 51 (0), 142e161. https://doi.org/10.1016/j.jclepro.2012.10.049.

[12]. BS EN 1015-18. Determination of water absorption coefficient due to capillary action of hardened mortar. UK: British Standards Institution; 2002.

[13]. Cervera, M., Faria, R., Oliver, J., & Prato, T. (2002). Numerical modelling of concrete curing, regarding hydration and temperature phenomena. Computers & structures, 80(18), 1511-1521.

[14]. Chen, C.H., Huang, R., Wu, J.K. and Yang, C.C. (2006), "Waste E-glass particles used in cementitious mixtures", Cement Concrete Res., 36(3), 449-456.

[15]. Chen, L. et al. (2016) 'Preparation and properties of alkali activated metakaolin-based geopolymer', Materials, 9(9), pp. 1–12. doi: 10.3390/ma9090767.

[16]. Cheng, H., Lin, K. L., Cui, R., Hwang, C. L., Cheng, T. W., & Chang, Y. M. (2015). Effect of solid-to-liquid ratios on the properties of waste catalyst–metakaolin based geopolymers. Construction and Building Materials, 88, 74-83.

[17]. Chindaprasirt, P., Chareerat, T., & Sirivivatnanon, V. (2007). Workability and strength of coarse high calcium fly ash geopolymer. Cement and Concrete Composites, 29(3), 224-229.

[18]. Concrete society, 2018, 'Metakaolin' available at http://www.concrete.org.uk/fingertips-document.asp?id=768 (Retrieved 12.11.2018)

[19]. Concrete countertop institute (2018) 'Pozzolanoic material', Availble at https://concretecountertopinstitute.com/free-training/the-use-of-pozzolans-in-concrete/ (Retrieved 10.11.2018)

[20]. Davidovits J. 1999, Chemistry of geopolymeric systems. Terminology. In: Proceedings of 99 geopolymer conference, vol. 1. 1999. p. 9–40. Available at http://books.google.fi/books?id=01_p1yZiL8C&pg=PA3&lpg=PA3&dq=geopolymer+99+proceedings&source=bl&ots=5FOXyBcMSX&sig=fJYN507bU4S3ZA9N_J7ai5kyfPw&hl=en&sa=X&ei=hMZ1VIfpK6KygP06IHQAg&ved=0CDkQ6AEwAw#v=onepage&q&f=false

[21]. Davidovits, P. J. (2002) '30 Years of Successes and Failures in Geopolymer Applications. Market Trends and Potential Breakthroughs .', pp. 1–16.

[22]. Duxson P., A. Fernández-Jiménez, J. L. Provis, G. C. Lukey, A. Palomo & J. S. J. van Deventer, (2007) Journal of materials and scince., vol. 42(9), pp. 917-933.

[23]. Dimas, D., Giannopoulou, I., & Panias, D. (2009). Polymerization in sodium silicate solutions: a fundamental process in geopolymerization technology. Journal of

materials science, 44(14), 3719-3730.

[24]. Fernández-Jiménez, A., Palomo, J.G. & Puertas, F. 1999, "Alkali-activated slag mortars: Mechanical strength behaviour", Cement and Concrete Research, vol. 29, no. 8, pp. 1313-1321.

[25]. Fernandez-Jimenez, A., Palomo, A., & Criado, M. (2005). Microstructure development of alkali-activated fly ash cement: a descriptive model. Cement and Concrete Research, 35(6), 1204-1209.

[26]. Gao, X., (2017). Alkali activated slag-fly ash binders: design, modelling and application. Department of Built Environment, Technische Universiteit Eindhoven.

[27]. Garcia-Lodeiro, I., Palomo, A. and Fernández-Jiménez, A. (2014) Crucial insights on the mix design of alkali-activated cement-based binders, Handbook of Alkali-Activated Cements, Mortars and Concretes. Woodhead Publishing Limited. doi: 10.1533/9781782422884.1.49.

[28]. Granizo, M. L. et al. (2004) 'Alkaline Activation of Metakaolin: Effect of Calcium Hydroxide in the Products of Reaction', Journal of the American Ceramic Society, 85(1), pp. 225–231. doi: 10.1111/j.1151-2916.2002.tb00070.x.

[29]. George, E. H. (2017) 'a Review on Silica Fume - an Additive in Concrete', (3), pp. 274–281.

[30]. Glukhovsky, V. D. (1959). Soil Silicates. Kiev, UKraine: Gastroi Publishers.

[31]. Glukhovsky V. (1994), 'Ancient, modern and future concretes', First Int. Conf. Alkaline Cements and Concretes, Kiev, Ukraine, 1, 1–8.Department of Built Environment, Technische Universiteit Eindhoven.

[32]. Glukhovsky V.D. (1967), Soil Silicate Articles and Structure (Gruntosilikatnye vyroby I konstruktsii), Ed. Budivelnyk Publisher, Kiev.

[33]. Hajimohammadi, A., Ngo, T. and Kashani, A. (2018) 'Glass waste versus sand as aggregates: The characteristics of the evolving geopolymer binders', Journal of Cleaner Production. Elsevier Ltd, 193, pp. 593–603. doi: 10.1016/j.jclepro.2018.05.086.

[34]. Hamid Behbahani and Behzad Nematollahi (2011) 'Steel Fiber Reinforced Concrete: A Review', Icsecm, (December 2011), pp. 1–13. Available at: https://www.researchgate.net/publication/266174465_Steel_Fiber_Reinforced_Concrete_A_Review

[35]. Hardjito, D., Wallah, S. E., Sumajouw, D. M., & Rangan, B. V. (2004). On the development of fly ash-based geopolymer concrete. ACI Materials Journal-American Concrete Institute, 101(6), 467-472.

[36]. Helmy, A. I. I. (2016). Intermittent curing of fly ash geopolymer mortar. Construction and Building Materials, 110, 54-64.

[36]. Holland, T. C. (2005) 'Silica fume user's manual', Federal Highway Administration, p. 194. doi: 10.1002/mds.23873. Available at www.silicafume.org/pdf/silicafume-users-manual.pdf (Retrieved 08.11.2018)

[38]. Imbabi, M.S., Carrigan, C., McKenna, S., 2012. Trends and developments in green cement and concrete technology. Int. J Sustain. Built Environ. 1 (2), 194e216. https://doi.org/10.1016/j.ijsbe.2013.05.001.

[39]. Indian Minerals Yearbook, Part III: Mineral Reviews 52nd Edition Talc, Soapstone and steatite, Government of India ministry of mines Indian bureau of mines, Indira Bhavan, Civil Lines, (2013) NAGPUR-440001. Available at http://ibm.nic.in/writereaddata/files/08172015173718Talc_Soapstone_Steatite.pdf

[40]. Ingham, J. P. (2013) '8 - Mortar, plaster, and render', in Ingham, J. P. (ed.) Geomaterials Under the Microscope. Boston: Academic Press, pp. 137–162. doi: https://doi.org/10.1016/B978-0-12-407230-5.50016-9.

[41]. Jeffrey C. Petermann, Michael I. Hammons and Athar Saeed (2012) Applied Research Associates, Inc. Panama City, FL 32401. Alkali-activated geopolymers: a literature review. Available at (http://www.dtic.mil/dtic/tr/fulltext/u2/a559113.pdf.

[42]. Jansen, M. S., & Christiansen, M. U. (2015). Effect of Water-Solids Ratio on the Compressive Strength and Morphology of Fly Ash-Waste Glass Geopolymer Mortars.

[43]. Kanuchova M., L. Kozakova, M. Drabova, M. Sisol, A. Estokova, J. Kanuch & J. Skvarla, (2015) Environmental progress & sustainable energy, vol. 34(3), pp. 841-849.

[44]. Khale, D., & Chaudhary, R. (2007). Mechanism of geopolymerization and factors influencing its development: a review. Journal of Materials Science, 42(3), 729-746.

[45]. Kirschner, A.V. & Harmuth, H. 2004, "Investigation of geopolymer binders with respect to their application for building materials", Ceramics - Silikaty, vol. 48, no. 3, pp. 117-120.

[46]. Kiisa, M., Lellep, K., Trossek, M., (2016). The effect of basalt fiber on the properties of normal-weight concrete. Professional Studies: Theory and Practice, Vol 1(16). P. 51 – 63.

[47]. Joshi, S. V. and Kadu, M. S. (2012) 'Role of Alkaline Activator in Development of Eco-friendly Fly Ash Based Geo Polymer Concrete', International Journal of Environmental Science and Development, 3(5), pp. 417–421. doi: 10.7763/IJESD.2012.V3.258.

[48]. Lemougna, P. N., Wang, K. T., Tang, Q., Melo, U. C., & Cui, X. M. (2016). Recent developments on inorganic polymers synthesis and applications. Ceramics International, 42(14), 15142-15159.

[49]. Lau, A. and Anson, M. (2006) 'Effect of high temperatures on high performance steel fiber reinforced concrete', Cement and Concrete Research, 36(9), pp. 1698–1707. doi: 10.1016/j.cemconres.2006.03.024.

[50]. Luukkonen, Z. A. T. et al. (2019) 'Microstructural Analysis and Strength Development of One-Part Alkali-Activated Slag / Ceramic Binders Under Different Curing Regimes', Waste and Biomass Valorization. Springer Netherlands, 0(0), p. 0. doi: 10.1007/s12649-019-00626-9.

[51]. Masse, S. et al. (1993) '29Si solid state NMR study of tricalcium silicate and cement hydration at high temperature', Cement and Concrete Research, 23(5), pp. 1169–1177. doi: https://doi.org/10.1016/0008-8846(93)90177-B.

[52]. Mastali, M. et al., 2019. A comparison of the effects of pozzolanic binders on the hardened-state properties of high-strength cementitious composites reinforced with waste tire fibers. Composites Part B: Engineering, Volume 134-153, p. 162.

[53]. Milena, J. and Robert, C. (2006), "Effect of hydrophilic admixtures on moisture and heat transport and storage parameters of mineral wool", Constr. Build. Mater, 20(6), 425-434.

[54]. Mo, B. H., Zhu, H., Cui, X. M., He, Y., & Gong, S. Y. (2014). Effect of curing temperature on geopolymerization of metakaolin-based geopolymers. Applied Clay Science, 99, 144-148.

[55]. Muñiz-Villarreal, M.S., Manzano-Ramírez, A., Sampieri-Bulbarela, S., Gasca-Tirado, J.R., Reyes-Araiza, J.L., Rubio-Ávalos, J.C., Pérez-Bueno, J.J., Apatiga, L.M., Zaldivar-Cadena, A. & Amigó-Borrás, V. 2011, "The effect of temperature on the geopolymerization process of a metakaolin-based geopolymer", Materials Letters,vol. 65, no. 6, pp. 995-998.

[56]. Ms. Nisha N. Jain, Prof. Hake S. L., Prof. Shirsath M. N., (2016) "geopolymer concrete with lime addition at normal room temperature", International Journal of Research Publications in Engineering and Technology [IJRPET] ISSN: 2454-7875, VOLUME 2, ISSUE 8, Aug. -2016.

[57]. National Center for Biotechnology Information, (2018) 'PubChem Compound Database', CID=14798, Available at: https://pubchem.ncbi.nlm.nih.gov/compound/14798 (Retrieved 08.11.2018)

[58]. Nath, S., Maitra, S., Mukherjee, S. & Kumar, S., (2016). Microstructural and morphological evolution of fly ash based geopolymers. Construction and Building Materials, Volume 111, pp. 758-765.

[59]. Natali, A., Manzi, S. & Bignozzi, M.C. (2011), "Novel fiber-reinforced composite materials based on sustainable geopolymer matrix", Procedia Engineering, pp. 1124.

[60]. Nazari, A., Maghsoudpour, A., Sanjayan, J.G., (2015). 'Flexural strength of plain and fibre-reinforced boroaluminosilicate geopolymer'. Construct. Build. Mater. 76,207e213

[61]. Normen sand, (2019), 'CEN-Standard Sand', Available at: https://www.normensand.de/en/products/cen-standard-sand-en-196-1/ (Retrieved 08.11.2018)

[62]. Panagiotopoulou, C., Kontori, E., Perraki, T. & Kakali, G. 2007, "Dissolution of aluminosilicate minerals and by-products in alkaline media", Journal of Materials Science, vol. 42, no. 9, pp. 2967-2973.

[63]. Phoo-ngernkham, T., Maegawa, A., Mishima, N., Hatanaka, S., & Chindaprasirt, P. (2015).Effects of sodium hydroxide and sodium silicate solutions on compressive and shear bondstrengths of FA–GBFS geopolymer. Construction and Building Materials, 91, 1-8.

[64]. Provis. J. L., (2006), 'Modelling the formation of geopolymers'. (PhD), University of Melbourne.

[65]. Provis. J. L., P. Duxson, E. Kavalerova, P. V. Krivenko, Z. Pan, F. Puertas & J. S. J. Van Deventer, (2014) Alkali activated materials, vol. 13, pp. 11-57.

[66]. Qian, C. X. and Stroeven, P., (2000) 'Development of hybrid polypropylene-steel fiber-reinforced concrete', Cement and Concrete Research, 30(1), pp. 63–69. doi: https://doi.org/10.1016/S0008-8846(99)00202-1.

[67]. Ramachandran, V.S. and Beaudoin, J.J. (2001), "Handbook of analytical techniques in concrete science and technology: principles, techniques and applications", 1st ed, William Andrew.

[68]. Rovnaník, P. 2010, "Effect of curing temperature on the development of hard structure of metakaolin-based geopolymer", Construction and Building Materials, vol. 24, no. 7, pp. 11761183.

[69]. Timakul P., W. Rattanaprasit, P. Aungkavattana, (2016), 'Improving compressive strength of fly ash-based geopolymer composites by basalt fibers addition',Ceram. Int. 42 (5) 6288–6295

[70]. Taylor, H. F., (1997). 'Cement chemistry'. Thomas Telford.

[71]. Torgal, F., Castro-Gomes, J. and Jalali, S., (2008) 'Alkali-activated binders: A review. Part 2.About materials and binders manufacture', Construction and Building Materials, 22(7), pp. 1315–1322. doi: 10.1016/j.conbuildmat.2007.03.019.

[72]. Sabouang, C. J. N. et al. (2014) 'Talc as raw material for cementitious products formulation', Journal of Asian Ceramic Societies, 2(3), pp. 263–267. doi: https://doi.org/10.1016/j.jascer.2014.05.007.

[73]. Samal S., N. Phan Thanh, I. Petríková, B. Marvalová, K.A.M. Vallons, S.V. Lomov, (2015), 'Correlation of microstructure and mechanical properties of various fabric reinforced geo-polymer composites after exposure to elevated temperature' ,Ceram.Int. 41 (9) 12115–12129

[74]. Schneider, M., Romer, M., Tschudin, M., Bolio, H., 2011. Sustainable cement production present and future. Cement Concr. Res. 41 (7), 642e650. https://doi.org/ 10.1016/j.cemconres.2011

[75]. Sivrikaya, O., Kiyildi, K. R. and Karaca, Z. (2014) 'Recycling waste from natural stone processing plants to stabilise clayey soil', Environmental Earth Sciences, 71(10), pp. 4397–4407. doi: 10.1007/s12665-013-2833-x.

[76]. Silva, F.J. & Thaumaturgo, C. 2003, "Fibre reinforcement and fracture response in geopolymeric mortars", Fatigue and Fracture of Engineering Materials and Structures, vol. 26, no. 2 SPEC., pp. 167-172.

[77]. Van Jaarsveld, J.G.S., Van Deventer, J.S.J. & Lukey, G.C. 2002, "The effect of composition and temperature on the properties of fly ash- and kaolinite-based geo-polymers", Chemical Engineering Journal, vol. 89, no. 1-3, pp. 63-73.

[78]. Vickers, L., van Riessen, A., & Rickard, W. D., (2015). Precursors and Additives for Geopolymer Synthesis. In Fire-Resistant Geopolymers (pp. 17-37). Springer Singapore.

[79]. Vijai, K., Kumutha, R. and G. Vishnuram, B. (2010) 'Effect of types of curing on strength ofgeopolymer concrete', International Journal of the Physical Sciences, 5, pp. 1419–1423.

[80]. Van Jaarsveld, J.G.S., Van Deventer, J.S.J. & Lukey, G.C. 2002, "The effect of composition and temperature on the properties of fly ash- and kaolinite-based geopolymers", Chemical Engineering Journal, vol. 89, no. 1-3, pp. 63-73.

[81]. Vu, M. H., Sulem, J., & Laudet, J. B. (2012). Effect of the curing temperature on the creep of hardened cement paste. Cement and Concrete Research, 42(9), 1233-1241.

[82]. Wickler, S., (2018) 'Soapstone in Northern Norway : Research status , production evidence and quarry survey results', pp. 117–128.

[83]. Yun-ming, L. *et al.* (2016) 'Progress in Materials Science Structure and properties of clay-based geopolymer cements : A review', *Progress in Materials Science*. Elsevier Ltd, 83, pp. 595–629. doi 10.1016/j.pmatsci.2016.08.002.

[84]. Xu, H. (2002). Geopolymerisation of Aluminosilicate Minerals. Ph.D Thesis, The University of Melbourne, Melbourne.

[85]. Xu, H., & Van Deventer, J. S. J. (2000). The geopolymerization of alumino-silicate minerals. International Journal of Mineral Processing, 59(3), 247-266.

[86]. Yao, X., Zhang, Z., Zhu, H., & Chen, Y. (2009). Geopolymerization process of alkali–metakaolinite characterized by isothermal calorimetry. Thermochimica Acta, 493(1), 49-54.

[87]. Y.M. Liew, H. Kamarudin , A.M. Mustafa Al Bakri, M. Bnhussain, M. Luqman. Khairul Nizar, C.M. Ruzaidi and C.Y. Heah, (2013), 'Effect of Curing Regimes on Metakaolin Geopolymer Pastes Produced from Geopolymer Powder'. doi: 10.4028/www.scientific.net/AMR.626.931.